CANCER BIOTHERAPY: TARGETING CANCER CELLS WITH A PLANT-EXPRESSED VIRUS-LIKE PARTICLE

by

MAMORAKE DONTY KOMANE

(5674-998-8)

submitted in accordance with the requirements

for the degree of

MASTER OF SCIENCE

in the subject

Agriculture (Animal Health)

at the

UNIVERSITY OF SOUTH AFRICA

SUPERVISOR: Prof Prudence Ngalula Kayoka-Kabongo

Co-SUPERVISOR: Dr Daria Anna Rutkowska

February 2026

DECLARATION

Name	MAMORAKE DONTY KOMANE
Student number	5674-998-8
Degree	Master of Science in Agriculture (Full dissertation)
Title	Cancer biotherapy: targeting cancer cells with a plant-expressed virus-like particle

I, Mamorake Donty Komane, declare that this dissertation is my own work and that all the sources used or quoted have been indicated and acknowledged by means of citation in the text and complete references in the reference list.

I further declare that the dissertation was submitted to originality checking software (Turn-it-in) and that it falls within the accepted similarity index by the University of South Africa. Current report is indicated 17% with single source below 1%. The published paper front page is included as an appendix

Finally, I declare that I have not previously submitted this work, or part of it, for examination at Unisa for another qualification or at any other higher education institution.

Signature: 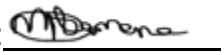 Date: 24-February- 2026

DEDICATION

This research is dedicated to everyone affected by cancer, patients, their families, and the researchers, who strive for breakthroughs. I also dedicate this study to my mentors, colleagues and loved ones, whose encouragement and unwavering support continue to inspire my research journey. May this research restore hope to those in need and contribute to the advancement of innovative cancer treatments.

ACKNOWLEDGEMENT

I wish to express my deep, humble gratitude to:

- My Supervisor, Professor Prudence Ngalula Kayoka-Kabongo from UNISA, for the invaluable guidance, mentorship, dedication, and unwavering support throughout this research journey.
- My co-supervisor, Doctor Daria Anna Rutkowska from CSIR, for the expert, critical insights, assistance during the experimental work, and encouragement. For being patient with me when things were tough and pushing me to the best I could do in the successful completion of my research.
- My family, including my parents, brothers and sisters and friends for their patience, love and encouragement during this demanding journey.
- CSIR research institution for providing the necessary facilities, resources, and a conducive research environment.
- The DSIT-CSIR inter-programme bursary scheme (IBS) and UNISA (Women in research funds) for funding my study.
- CSIR Laboratory team, including Dr Ilse du Preez, for her technical expertise in mammalian cell culture, Dr Asongwe Tantoh for this assistance in obtaining cell images with the Cytation3 imaging reader, fellow students/interns, Ms Galaletsang Hutang and Ms Pleasure Nzimande, as well as laboratory technicians Ms Sharon Kgasago and Mr Albert Mabetha, for their assistance with experiments, use of equipments, and technical troubleshooting.

ABSTRACT

Cancer continues to cause high mortality rates worldwide. Currently, treatments are limited by high cost, toxicity and poor specificity. Virus-like particles (VLPs), expressed in plants, are a promising platform for targeted cancer biotherapy due to their biocompatibility, uniform structure and capacity for surface modification. This study aimed to develop a plant-expressed Papaya mosaic virus (PapMV) virus-like particle as a vehicle for targeted cancer biotherapy and investigate its binding capability to a cancer cell line. PapMV VLPs were engineered and decorated with polygonatum cyrtonema lectin (PCL) via SpyTag/SpyCatcher technology to enable selective binding of VLP to tumor-associated glycans on cancer cells. The recombinant genes encoding chimeric PapMV coat protein (CP) and PCL fusion elements were co-expressed using a transient plant-based expression system in *Nicotiana benthamiana* DXT-FT plants to produce lectin-conjugated PapMV VLPs. Density gradient centrifugation, sodium dodecyl sulfate-polyacrylamide electrophoresis and western blotting verified protein expression and PCL-CP conjugation. Further structural analysis using transmission electron microscopy revealed uniform, assembled, rod-shaped VLPs. VLP tubules were purified via their 6-Histidine tag by using affinity beads and subsequently quantified and characterized. The results showed low expression levels of the chimeric PapMV VLPs and lectin-conjugated PapMV VLPs, ranging between ±0.042 to ±0.079 mg from 6.2 to 11.9 g harvested plant leaf biomass, respectively. These results indicated suboptimal expression of the recombinant genes. *In vitro* binding of the conjugated PCL-PapMV VLP to a HER2+ breast cancer cell line was assessed using a fluorophore-conjugated anti-His antibody, directed against the 6-His tag on the C-terminal of PapMV CP. However, no specific binding of the His-tagged PCL-PapMV VLPs to the target breast cancer cells was detected, indicating improper lectin orientation or steric hindrance affecting receptor accessibility. This highlights the importance of structural design in biological function. Although, chimeric PapMV VLPs were successfully expressed, assembled and conjugated to the co-expressed PCL lectin in plants via a SpyTag/SpyCatcher strategy, future studies should explore gene design strategies to optimise protein yield and enable VLP binding to target cancer cells.

Keywords: Cancer biotherapy, Plant-expressed VLPs, PapMV, PCL lectin, *Nicotiana Benthamiana*, agroinfiltration, SpyTag/SpyCatcher, pEAQ-HT expression vector.

TABLE OF CONTENTS

LIST OF TABLES

LIST OF FIGURES

ABBREVIATIONS

Ab	Antibody
ADC	Antibody-drug conjugates
BSA	Bovine serum albumin
bp	Base pair
CP	Coat Protein
CLP	Core-like particles
CPMV	Cowpea mosaic virus
CSIR	Council for Scientific and Industrial Research
ddH_2O	Double-distilled water
dH_2O	Distilled water
DNA	Deoxyribonucleic acid
d.p.i	Days post-infiltration
DSTI	Department of science technology and innovation
DOX	Doxorubicin
E. coli	*Escherichia coli*
GNA	Galanthus nivalis agglutinin
GPS	Geographical positioning system
HPV	Human papillomavirus
IMAC	Immobilized metal affinity chromatography
kDa	Kilodalton
LB	Luria Bertani
MS	Mass spectrophotometer
N. benthamiana	*Nicotiana benthamiana*
PBS	Phosphate-buffered saline

PapMV	Papaya mosaic virus
PCL	Polygonatum cyrtonema lectin
PCR	Polymerase chain reaction
PVX	Potato virus X
RNA	Ribonucleic acid
SDS-PAGE	Sodium dodecyl sulfate-polyacrylamide gel electrophoresis
SRM	Serum free medium
TEM	Transmission electron microscopy
TMV	Tobacco mosaic virus
TYMV	Turpin yellow mosaic virus
VLPs	Virus-like particles

SYMBOLS

°C	Degree Celsius
µg	Microgram
µL	Microlitres
mg	Milligram
mL	Millilitres
mM	Millimolar
®	Registered
™	Trademark
U	Units

PUBLICATIONS/ RESEARCH OUTPUT

1. Komane, M.D.; Kayoka-Kabongo, P.N.; Rutkowska, D.A. The Use of Plant Viral Nanoparticles in Cancer Biotherapy-A Review. *Viruses* 2025, 17, 218. https://doi.org/10.3390/v17020218

CHAPTER 1: GENERAL INTRODUCTION

1.1 Background of the study

Cancer continues to be the most researched non-communicable disease worldwide (Raza, 2025). Conventional treatment options include surgery, chemotherapy, and radiotherapy (Debela *et al*., 2021). These traditional cancer treatment approaches, although effective, have debilitating side effects due to their non-specific actions (Anand *et al*., 2023). In response, novel therapeutic approaches are required to improve the efficacy of cancer treatment while minimizing side effects. Recent emerging biotherapeutic strategies for this disease include the use of virus-based nanoparticles, such as virus-like particles, as delivery agents for the targeted delivery of chemotherapy drugs, enzymes and imaging agents to cancer cells (Chung *et al*., 2020; Zanganeh *et al*., 2023). Virus-like particles (VLPs) are highly ordered structures that self-assemble from viral structural proteins (Ludwig and Wagner, 2007; Mohsen and Bachmann, 2022) and resemble the three-dimensional structure of native viruses (Bruder and Aucoin, 2023).

Within this context, studies have focused on plant viral nanotechnology platforms such as Potato virus X (PVX) for medical purposes (Röder *et al*., 2019). Notably, filamentous or tubular VLPs are more desirable than spherical VLPs because their elongated shape allows tumor penetration, longer circulation times and increased surface availability to display targeting ligands (Peralta-Cuevas *et al*., 2025). Like PVX, the closely related Papaya mosaic virus (PapMV) has also been investigated as a delivery system for medical therapeutics (Lebel *et al*., 2016; Rioux, Babin, et al., 2012; Thérien *et al*., 2017). The potential of these VLP platforms is further supported by the increasing popularity of plant-based expression systems.

Transient expression of VLPs in plants offers several advantages over current mammalian, avian, insect cell, yeast, and prokaryotic expression systems including speed, ease of scale-up, post-translational eukaryotic protein modifications and safety due to a lack of contaminating mammalian pathogens (D'Aoust *et al*., 2010; Lomonossoff and D'aoust, 2016; Sainsbury *et al*., 2009). Evidence from several clinical trials have demonstrated the safety, quality and effectiveness of plant-based products (Fox, 2012; Ma *et al*., 2015; Pillet *et al*., 2016). Plants can also perform post-translational

modifications such as glycosylation, which can improve the immunogenicity of VLPs produced (Vo and Trinh, 2022), further supporting their application in cancer biotherapy.

In order to target VLPs to cancer cells for biotherapeutic applications, targeting ligands such as antibodies, peptides and lectins are used (Yan *et al*., 2024). Lectins from animals, plants and fungi are highly specific carbohydrate-binding proteins not having an immune origin and have great therapeutic potential for various pathological processes, including cancer (Fu *et al*., 2011). As cancer cells exhibit aberrant glycosylation patterns (Ho *et al*., 2016; Pinho and Reis, 2015), lectins that recognize such patterns may be used to direct VLPs to target cancer cells. Lectins have potential toxicity or immunogenicity (Liu *et al*., 2013) when compared to antibodies and their clinical use has so far been limited. Antibodies are large Y-shaped proteins called immunoglobulins which are produced by the immune system that recognize specific proteins foreign to the body named antigens on the cell surface (Chiu *et al*., 2019). Their large size limits penetration into solid tumor, slow clearance from the blood and high production cost (Chiu *et al*., 2019). Peptides are short chains of amino acids which recognize specific receptors or proteins overexpressed on cancer cells while they can penetrate deeper in tissue, they have a lower immunogenicity, shorter half-life and are easily modified by enzymes when compared to antibodies (Yan *et al*., 2024). However, the potential of lectin-mediated targeting of plant-expressed VLPs remains underexplored and is the focus of this study.

Here we aimed to develop plant-expressed PapMV VLPs as a means of delivering biotherapeutics to target cancer cells. The VLPs were specifically directed to the cancer cells by means of a Polygonatum cyrtonema lectin (PCL) protein conjugated to the VLP surface using the SpyCatcher/SpyTag technology (Brune *et al*., 2016, 2017; Reddington and Howarth, 2015). The binding of these lectin conjugated PapMV VLPs to target cancer cells was investigated *in vitro.* The data from this study will contribute to advancing knowledge on the application of plant-expressed VLPs for targeted cancer biotherapy.

1.2 Problem Statement

Cancer remains a major health concern globally and continues to be the leading cause of mortality in developed and developing countries (Mattiuzzi and Lippi, 2019). Recent studies have shown great improvement in the field of cancer treatment, with various therapeutic approaches being explored (Pucci *et al*., 2019). Despite the advancements, there are still inevitable adverse effects and reduced effectiveness when treating cancer

(Gavas *et al*., 2021) across different types and subtypes (Wang *et al*., 2021). Recent anticancer drugs are further constrained by toxicity, drug resistance and poor specificity against certain cancer types (Ioele *et al*., 2022). These limitations result in damage to healthy cells and reduce overall treatment efficacy. Collectively, these challenges contribute to the lack of specificity of current therapies, emphasizing the need to develop more novel targeted anticancer therapies that can offer specific and effective treatment. Hence, the overall aim of this research was to develop a plant-expressed, PapMV VLP-based delivery agent that would bind specifically to target cancer cells and deliver a therapeutic agent to these cells.

1.3 Aim and Objectives of the study

1.3.1 Aim

The aim of this study was to produce lectin-conjugated Papaya mosaic virus VLPs in *Nicotiana benthamiana* plants and assess their ability to bind to target breast cancer cells *in vitro*.

1.3.2 Objectives

The study objectives were as follows:

i. To transiently co-express chimeric PapMV coat protein (CP) and Polygonatum cyrtonema lectin (PCL) gene sequences, containing the SpyTag/SpyCatcher conjugation elements, in *Nicotiana benthamiana* plants and assess chimeric protein expression, VLP assembly and lectin-VLP conjugation.
ii. To investigate the binding capability of the plant-expressed, lectin-conjugated PapMV VLPs to HER2+ breast cancer cells *in vitro*.

1.4 Research questions

The study addressed the following research questions to achieve the above stated objectives:

i. Is it possible to transiently express and assemble lectin-conjugated PapMV VLPs in *Nicotiana benthamiana* plants?
ii. Are the plant-expressed, lectin-conjugated PapMV VLPs capable of binding target HER2+ breast cancer cells *in vitro*?

1.5 Hypothesis

i. Transient co-expression of the chimeric PapMV CP and PCL genes, containing the SpyTag/SpyCatcher elements, in *Nicotiana benthamiana* plants does enable the assembly of the chimeric PapMV VLPs and conjugation of the PCL lectin on the surface of these VLPs.
ii. Plant-expressed lectin-conjugated PapMV VLPs do exhibit specific binding to HER2+ breast cancer cells *in vitro.*

1.6 Scope of the study

This research focused on the development of the plant-expressed PapMV VLPs as a targeting delivery agent for the therapy of multiple cancer types, with breast cancer cells being used as a model. The study employed an experimental design. It explored the use of molecular farming techniques to create PapMV VLPs in *N. benthamiana* dXT-FT plants to develop affordable, scalable and biocompatible nanostructures that can target and bind to cancer cells. To achieve these goals, this study employed experimental methods including gene cloning, transient plant protein expression, protein purification and characterization using analytical methods and an *in vitro* target cell binding experiment. This is an initial proof of concept study and did not include clinical trials or *in vivo* testing. Rather, it established the foundation for additional research and emphasized how feasible plant-based platforms are for creating useful nanocarriers for cancer biotherapy. The study was restricted to laboratory-scale experiments in a controlled research environment, and it is interdisciplinary, drawing from plant biotechnology, nanotechnology, virology and cancer biology.

1.7 Significance of the study

The benefits of this study lie in its creative approach to cancer treatment by developing plant-expressed VLPs as a means of targeting cancer cells and delivering therapeutic agents exclusively to these cells. A targeted VLP-based biotherapeutic holds the promise of reducing side effects whilst improving the efficacy of the treatment. This research will not only open new horizons in the biotechnology field but also provide a safe, cost-effective and patient-friendly alternative to conventional cancer treatments for patients. This innovative approach promises to improve global health by lowering treatment costs and opening the door to customized therapies. This marks a major improvement in the battle against cancer and transforming the field of cancer therapy.

1.8 Dissemination of the research information

To achieve maximum impact, the findings of the research will be distributed to several key stakeholders. The main goal of the dissemination is to share important discoveries with the scientific community and the public, which adds to the expanding body of knowledge in plant-based pharmaceutical manufacturing and cancer nanobiotherapy. The findings will be published in a relevant peer-reviewed journal and showcased at local conferences for the presentation of the results to enable constructive feedback and open discussions with other fellows. Seminars hosted by universities, departments and research institutions will serve as platforms to interact with other researchers, relevant departments and students. Furthermore, the research highlights will be shared with the public through various platforms, including institutional websites. In conclusion, the research is hoping to boost the development of plant-based nanotechnology for cancer treatment by encouraging innovation.

1.9 Dissertation's organization

This thesis is presented in stand-alone chapters containing an introduction to the study (Chapter 1), a literature review (Chapter 2), materials and methods (Chapter 3), results (Chapter 4), discussion (Chapter 5), summary and conclusion (Chapter 6), references cited in this study and appendices.

CHAPTER 2: LITERATURE REVIEW

2.1 Introduction

Cancer continues to be one of the leading causes of human mortality, imposing a significant global economic and social burden (Wang *et al*., 2023). In 2022, the estimated number of new cancer cases were about 19.96 million with approximately 10 million cancer deaths globally (Bray *et al*., 2024). Thus, innovative approaches are urgently needed to combat this devastating disease. Cancer is characterized by an uncontrollable growth of cells that can spread to other parts of the body (Baskar *et al*., 2014). The cell division process becomes irregular resulting in abnormal cells growing uncontrollably (National cancer institute, 2021). Cancer is made up of trillions of cells and it can start almost anywhere in the human or animal body (NCI, 2021). Cancerous cells are heterogeneous in structure. They can infiltrate nearby tissues and spread to other parts of the body to produce new cancerous cells, a process known as metastasis (Lee *et al*., 2017). Modern cancer research has determined that gene mutations are responsible for the initiation and progression of cancer (Akash, 2021), with the discovery of oncogenes and tumor suppressor genes (Hanselmann and Welter, 2022).

Recent studies have revealed progress in the field of cancer biotherapy. Cancer biotherapy is a biological treatment that uses agents or compounds derived from living organisms to help the body immune system fight against cancerous cells (NCI, 2019). One notable innovative development includes precision medicine which selects treatment according to patient tumor specific genetic composition (Al Meslamani, 2023). This approach has allowed doctors to select more effective treatments. Immunotherapy has been a breakthrough due to its strategic employment of the immune system to target cancer cells (Koury *et al*., 2018). Among immunotherapy targets are immune checkpoint inhibitors (ICIs) (e.g., CTLA-4, PD-1 and PD-L1) which block proteins (Desai *et al*., 2024; Joshi *et al*., 2024) that allow the immune system to recognise and eliminate cancer cells (Mukherjee *et al*., 2022). Such drugs have proven to be effective in treating melanoma and lung cancers (Naimi *et al*., 2022). Another immunotherapy example includes chimeric antigen receptors (CAR) T-cells where patient's immune cells are extracted, genetically engineered to target cancer cells and infused back into the body (Desai *et al*., 2024; Garg *et al*., 2024; Grosser *et al*., 2019).

Research into the development of antibody-drug conjugates (ADCs) is ongoing (He *et al*., 2024). These current treatment strategies target cytotoxic drugs to cancer cells specifically and not healthy tissues (Yajaman *et al*., 2025). Bispecific antibodies provide molecular insights to immune modulation and antigen selection (Sun *et al*., 2023). These bispecific antibodies increasingly inform ADC design, making it much easier for the immune system to destroy cancer cells and reduce non-specific binding (Wang *et al*., 2025).

Despite such developments, cancer biotherapy faces many challenges. These include high financial cost or expensive novel therapies that might not be accessible to all individuals due to inequalities globally (Omotoso *et al*., 2023; Vaccarella *et al*., 2019). Additionally, it was notable that certain immune cancer therapies show effectiveness only on specific cancers or subgroups of cancer patients (Mc Neil and Lee, 2025; Peterson *et al*., 2022). These treatments further cause severe side effects including excessive immune reactions (Rahman *et al*., 2022). Cancer cells sometimes become resistant to treatment leading to disease recurrence (Damen *et al*., 2021). Furthermore, the tumor microenvironment tends to suppress the immune system and make it difficult for therapies to be effective (Labani-Motlagh *et al*., 2020).

Research is ongoing to find possible solutions to these challenges through combination of therapies or optimizing targeting strategies (Lopez and Banerji, 2017). In addition, the application of artificial intelligence (AI) to diagnose and customize cancer treatment is expanding (Bhinder *et al*., 2021). Within this promising landscape, plant-expressed virus-like particles (VLPs) provide a novel and innovative strategy to target cancer cells. Plant viral nanoparticles (PVNPs) can be engineered to deliver drugs directly to cancer cells. These PVNPs deliver chemotherapeutic drugs via encapsulation within particle hollow cores or attachment to the particle external surface (Sun *et al*., 2025). In addition, the structure of VLPs stimulates the immune system to fight cancer tumors, potentially alleviating some limitations of current treatments (Shahgolzari and Fiering, 2022).

2.2 Virus-Like Particles

2.2.1 Definition of VLPs and their structure

A significant amount of literature attests to the fact that virus-like particles (VLPs) are a rapidly emerging platform in the biotherapeutics field. Virus-like particles consist mostly of capsid proteins that spontaneously assemble into particles resembling native viruses

in structure and morphology (Nooraei *et al*., 2021; Flynn and Ramsey, 2015) but lack non-structural proteins, enzymes and the viral genome (Fuenmayor *et al*., 2017). This structural configuration underpins their biosafety advantage, as the absence of genetic material inside VLPs ensures that they do not replicate or cause disease (Tariq *et al*., 2022). Beyond safety, they possess high immunogenic properties which make them a safe and effective option for vaccine development, drug delivery and imaging (Kheirvari *et al*., 2023). Virus-like particle-based biotherapeutics can also be produced using various expression systems, enabling rapid and scalable manufacturing, which is particularly valuable during disease pandemics (Zeltins, 2013). Expression systems currently available include bacterial, yeast, insect, plant and mammalian cells (Arora *et al*., 2012; Kushnir *et al*., 2012; Yildiz *et al*., 2011).

2.2.2 VLPs as platform for the development of vaccines and biotherapeutics

Virus-like particles have emerged as a versatile platform for developing vaccines and biotherapeutics. In the field of vaccinology and immunotherapy, VLPs offer several distinct advantages. Unlike conventional viral vectors, VLPs can mimic the structure and antigenic properties of actual viruses without containing genetic material, making them safe and non-infectious, which is crucial for vaccine development (Bachmann and Jennings, 2010; Donaldson *et al*., 2018). According to López-Sagaseta *et al*. (2016), VLPs often induce a strong and targeted immune response due to their repetitive and ordered structures. They can efficiently stimulate both innate and adaptive immunity and enhance vaccine efficacy (Qian *et al*., 2020). These nanostructures have been employed in the development of vaccines against a range of infectious diseases, such as human papillomavirus (HPV) (Dai *et al*., 2018) and hepatitis B (Spice *et al*., 2020), as well as emerging pathogens such as SARS-CoV-2 (Ward *et al*., 2021). One example of VLPs that present heterologous antigen is hepatitis E VLPs that have been engineered to display human papillomavirus (HPV) antigens such as the HPV L1 protein (Kanekiyo and Buck, 2017; Meghana *et al*., 2025) resulting in a multivalent vaccine targeting both hepatitis E and HPV infections (Qian *et al*., 2020). VLPs also have the potential to be used as drug delivery carriers for targeted delivery to specific cells or tissues in biotherapeutics (Parodi *et al*., 2017).

2.2.3 VLPs used as delivery systems for chemotherapeutic agents

Virus-like particles, both plant-derived and expressed in mammalian, bacteria, yeast and insect systems, have been explored as delivery vehicles for chemotherapy. For example, Cowpea mosaic virus (CPMV) has been used for encapsulation of the chemotherapeutic drug doxorubicin (DOX), increasing tumor targeting and reducing toxicity (Aljabali *et al*., 2013; Beatty and Lewis, 2019; Liu *et al*., 2022). Meanwhile, Tobacco mosaic virus (TMV) has encapsulated and delivered anticancer drugs including cisplatin and phenanthriplatin, therefore enhance uptake in cancer cells (Czapar *et al*., 2016; Zhao *et al*., 2022). Bacteriophage MS2-based VLPs delivered cisplatin prodrugs for active cancer cells targeting modifications (Kim *et al*., 2023; Kolesanova *et al*., 2019). Insect cell-derived Newcastle disease virus (NDV) VLPs produced through baculovirus system delivered doxorubicin due to their eukaryotic post-translational modifications for enhanced targeting (Taghizadeh *et al*., 2024; Thong *et al*., 2019). Mammalian cells-derived HBc core-like particles (CLPs) with human-like glycosylation allow efficient drug delivery and immune evasion (Sakai *et al*., 2021). These chemotherapy delivery vehicles increase the effectiveness of drugs and reduce side effects, such as toxicity in healthy tissues (Paul *et al*., 2023).

2.3 Plant expression systems

Over the past thirty years, plants have been researched as expression systems (Formoso *et al*., 2022). Plant expression systems are useful tools in biotechnology for medical applications. Compared to other expression systems such as bacterial and mammalian, heterologous protein expression in plants has attracted interest due to its key advantages (Formoso *et al*., 2022). *Nicotiana benthamiana* is currently one of the main production host plants used by most companies in this field (Nosaki *et al*., 2021). This plant exhibits exceptional susceptibility to pathogens and is an excellent host for transient gene expression (Nosaki *et al*., 2021). *Nicotiana benthamiana's* susceptibility enables quick and effective screening of genes associated with pathogen defense mechanisms, facilitating the identification and characterization of pivotal genes related to plant immunity and disease resistance (Goodin *et al*., 2008; Koseoglou *et al*., 2022). Antigen and protein production in plants, known as biopharming, has been increasing and a variety of plant-produced products were reported in preclinical and clinical trials (Lomonossoff and D'aoust, 2016). However, challenges related to regulatory approval continue to limit widespread commercial adoption (Zahmanova *et al*., 2023).

2.3.1 Transient plant expression

Several methods of plant transformation have been developed over the years, with transient expression system among them, which occurs without gene recombination into the host genome (Formoso *et al*., 2022). Transient plant expression offers several advantages over current mammalian, insect and prokaryotic expression systems (Fischer et al., 2004; Kushnir *et al*., 2012) such as scalability, speed and eukaryotic post-translational protein modifications (Schütz *et al*., 2023). These make them suitable for vaccine production in epidemic/pandemic response situations or human biotherapeutic production. *Agrobacterium*-mediated transformation using a binary vector such as pEAQ have the capability of transporting T-DNA to plant cell nucleus (Hwang *et al*., 2017; Kaur *et al*., 2021; Nonaka *et al*., 2019). *A. tumefaciens* uses its natural ability to transfer DNA from the binary vector to plant cell nucleus (Cordeiro *et al*., 2023; Grace *et al*., 2024). Recombinant plant viral vectors can also introduce genetic material into plant cells leading to transient gene expression (Kole *et al*., 2024). Several studies have designed and established various plant viruses for expressing foreign proteins, such as the potato virus X (Wang *et al*., 2014), tobacco rattle virus (TRV) and TMV (Bamogo *et al*., 2019; Jin *et al*., 2015). These plant viral vectors were successfully developed and exploited for the industrial-scale expression of heterologous proteins, although they may present limitations in insert stability and cargo size which restrict their broader applicability (Hefferon, 2012; Jin *et al*., 2015).

2.3.2 Preclinical and clinical studies of plant-derived VLPs

2.3.2.1 Plant expressed VLPs against infectious diseases

Virus-like particles expressed in plants have shown immense potential as vaccine development platforms for various infectious diseases. These VLPs have been engineered to display antigens from pathogens such as influenza viruses, HPV and norovirus (Mejía-Méndez *et al*., 2022). Preclinical studies indicate that plant-expressed VLPs are significantly immunogenic, simulating strong humoral and cell-mediated immune responses (Chen and Lai, 2013). Research conducted on animals, specifically ferrets and mice, has demonstrated that VLP vaccines presenting influenza hemagglutinin (HA) generate protective antibodies (Thompson *et al*., 2013), mitigate pathology, and reduce viral load when exposed to various influenza strains (Balke and Zeltins, 2020; Landry *et al*., 2010; Makarkov *et al*., 2019; Peralta-Cuevas *et al*., 2025). Multiple plant-derived VLP vaccines have progressed to human clinical trials. A notable

example is the H5N1 influenza VLP vaccine, produced in the *N. Benthamiana* plant, which showed safety and immunogenicity during Phase I trial (D'Aoust *et al*., 2010; Landry *et al*., 2010). In this case, challenges resulted in effects that were mild-to-moderate and were resolved spontaneously. The vaccine was able to induce strong dose immunogenicity, with high rates of neutralizing antibody response (Landry *et al*., 2010). The quadrivalent influenza VLPs vaccine also exhibited good immunogenicity and safety during Phase II trials in diverse populations and various age groups (Pillet *et al*., 2019). Moreover, norovirus VLP-based vaccine candidates showed safety and mucosal immunity during preclinical trials on rabbits (Chen and Lai, 2013). The latest clinical Phase II trials of norovirus tested bivalent safety and immunogenicity, although Phase III trials to evaluate noroviral gastroenteritis effectiveness has been listed as protocol and not yet active on clinical trials (Sáez-Llorens *et al*., 2025). These results reinforce the advanced clinical development of plant-expressed VLP vaccines.

2.3.2. 1 Plant expressed VLPs vaccines against cancer

VLP-based cancer vaccines have been developed and produced using mammalian, yeast, or insect expression systems (Hemmati *et al*., 2022). In these strategies, tumor-associated antigens or epitopes are displayed on VLP platforms to stimulate immune response against cancerous cells (Bachmann *et al*., 2025). These promise to show effectiveness in inducing protective immunity and some tumor inhibition (Calvillo-Rodríguez *et al*., 2023). For example, HPV vaccine produced from baculovirus-insect cells have undergone clinical trials demonstrating efficacy in preventing HPV-related cervical cancer (Kurosawa *et al*., 2022; Palatty *et al*., 2024). Structural studies have confirmed VLP-based stability and effective interaction with antigen-presenting cells (Lindsay *et al*., 2018; Mardanova *et al*., 2024). Considering the structural and functional resemblances between plant-derived VLP-based and those generated from other expression systems, plant-derived VLPs can be engineered to present cancer-specific antigens (Balke and Zeltins, 2020; Mohsen *et al*., 2020; Ning *et al*., 2024). Currently, there are no approved plant-derived VLP-based vaccines to target cancer cells in clinical trials.

2.3.3 Filamentous plant virus VLPs as vaccines and delivery systems

Researchers have directed their attention towards plant viral nanotechnology platforms including Potato virus X (PVX), amongst others, for medical applications. PVX is a filamentous virus with a 500 nm capsid composed of 1300 copies of a single coat protein

(CP) surrounding a single RNA molecule (Grinzato *et al*., 2020). PVX belongs to the genus *Potexvirus* in the family *Alphflexiviridae* (Verchot, 2022). Potato virus X VLPs, lacking the nucleic acids (Pessione, 2020), have been produced (Shoeb *et al*., 2021). Moreover, particles derived from PVX have potential in multiple applications such as vaccine development and antigen presentation (Verdaguer *et al*., 2014). The filamentous Papaya mosaic virus (PapMV) is closely related to PVX, also belongs to the genus *Potexvirus* within *Alphaflexiviridae* family, but PapMV is less studied than PVX (Rioux, Babin, *et al*., 2012). Both PapMV and PVX filamentous viruses are known for their unique structures and immune stimulation features, making them suitable for cancer vaccine development (Lebel *et al*., 2015). Their flexible, elongated shape have a larger surface area that increases the number of tumour-associated antigens displayed thus enhancing immune activation (Ghosh *et al*., 2020; Lebel *et al*., 2016). Furthermore, filamentous VLPs can efficiently enter the lymphatic vessels and move to the lymph nodes more readily than spherical VLPs, making them a better chemotherapy delivery vehicle (Lee *et al*., 2023; Yang *et al*., 2022).

PVX particles can present proteins at the surface-expressed N-terminus of a proportion or all the coat protein subunits (Cañizares *et al*., 2005). Similarly, studies have also investigated PapMV as a delivery system with N-terminal of the CP displaying the M2e epitope (Carignan et al., 2015), the influenza HA11epitope (Rioux, Babin, *et al*., 2012) and an influenza NP CTL epitope (Babin *et al*., 2013). Additionally, the C-terminal of the CP has been used for the fusion of peptides (Yang *et al*., 2012). In this study, PapMV VLPs are investigated for the development of a targeted chemotherapy delivery system, a novel application.

2.4 Targeting cancer cells with lectins

Plant lectins are a diverse group of carbohydrate-binding proteins of non-immune origin with at least one-catalytic domain (Liu *et al*., 2013). Lectins selectively detect and reversibly bind to certain free sugars or glycans, present on glycoproteins and glycolipids, without modifying the structures of the carbohydrates (Tsaneva and Van Damme, 2020). This glycan-binding property is relevant to cancer biology as cancer cell surface antigens have aberrant glycosylation patterns (Tuccillo *et al*., 2014). In contrast, other targeting ligands, such as peptides and antibodies, rely on amino acid sequence recognition or antigen-antibody interactions, respectively (Yan *et al.,* 2024).

Among plant lectins, *Galanthus nivalis agglutinin* (GNA) is a family drawing attention due to its significant anti-tumor and antiviral activities (Wu and Bao, 2013). Polygonatum cyrtonema lectin (PCL), a member of this family, was initially isolated from Polygonatum cyrtonema Hua (An *et al*., 2006) and has been found to have anti-tumor effects towards HeLa, MCF-7, A375.0 and L929 cells but less toxicity to normal cells (Wang *et al*., 2011). These studies highlight selective activity that is mediated through lectin recognition of aberrantly glycosylated cancer cell surfaces.

2.5 SpyCatcher/ SpyTag- based protein conjugation

The SpyCatcher/SpyTag technology is a protein engineering approach that enables the site-specific covalent conjugation of proteins (Zakeri *et al*., 2012). This technology involves two components the SpyCatcher, a 12kDA protein, and the SpyTag, a 13 amino acid peptide sequence (Schoene *et al*., 2016). When SpyCatcher and SpyTag are brought together, they rapidly form an irreversible covalent bond through an isopeptide linkage (Brune *et al*., 2017; Zakeri *et al*., 2012). SpyCatcher/ SpyTag technology has been used to create covalently stable multiple proteins complexes, modular vaccine production (Hatlem *et al*., 2022), and protein labelling for applications such as microscopy (Hatlem et al., 2019). The PCL lectin may thus be conjugated to PapMV VLPs to enable targeted binding of the VLP-based biotherapeutic to a cancer cell. The SpyCatcher/SpyTag technology (Brune *et al*., 2016, 2017; Reddington and Howarth, 2015) was used to conjugate the PCL lectin to the surface of PapMV VLPs in this study.

CHAPTER 3: MATERIALS AND METHODS

3.1 Introduction

This chapter presents the methodology employed in this study to assemble lectin-conjugated PapMV VLPs in *Nicotiana Benthamiana* plants and assess the ability of these VLPs to bind to HER2+ breast cancer cells *in vitro*. It details experimental approaches and techniques used to produce, purify, characterize and evaluate binding of the plant-expressed lectin-conjugated VLPs to target cancer cells. Protocols described in this chapter include DNA cloning, bacterial transformation, agroinfiltration of whole *Nicotiana benthamiana* plants, transient plant protein expression, VLP harvesting, purification and characterization as well as the binding efficiency of PapMV VLPs to target cancer cells *in vitro.* These experimental designs were guided by the objectives set out in section 1.3.2. This methodological framework provides comprehensive experimental results and discussion in chapters 4 and 5, respectively.

3.2 Study area

The study was conducted in the Aquaculture and Animal Health Division of the Advanced Agriculture and Food (AAF) Cluster at the Council for Scientific and Industrial Research (CSIR). The CSIR is situated in the East of Pretoria (GPS coordinates S: 25° 45′ 31″ and E: 28° 16′ 60″), South Africa, within the research, academic and ambassadorial hub of Pretoria. It is known as a leading scientific and technology research organization that research, develops, localizes, and diffuses technologies to improve socioeconomic prosperity in South Africa. It was established in 1945 through an Act of Parliament and is partially funded by the South African government through the Department of Science Technology and Innovation (DSTI). CSIR is characterized by its multidisciplinary research, including but not limited to agriculture, health, aerospace, mining, energy and innovation technology. It allows collaborative research with various stakeholders such as universities, government departments, industry partners, and other research institutions, both within South Africa and internationally. Overall, the CSIR in South Africa plays a pivotal role in advancing the scientific and technological capabilities while contributing to the country's economic and social development. Its work is instrumental in addressing contemporary challenges and fostering innovation and competitiveness in South Africa's industries.

3.3 Transient plant-based expression and assembly of lectin-conjugated PapMV VLPs

3.3.1 Restriction enzyme digestion of insert and vector DNA

The genes of interest, encoding the Papaya mosaic virus (PapMV) coat protein (CP) and polygonatum cyrtonema lectin (PCL) with N-terminal or C-terminal SpyTag/SpyCatcher elements, were designed and codon-optimized for expression in *N. benthamiana* DXT/FT plant cells using bioinformatics tools (Dr. Rutkowska, personal communication) and synthesized by GeneArt (Thermo Fischer Scientific, Germany). Approximately 5 µg of lyophilized plasmid DNA containing a gene insert was resuspended into 50 µL double-distilled water (ddH_2O) to a final concentration of 0.1 ng/µL. The gene inserts ST-PapMV, SC-PapMV, PCL-ST, ST-PCL, PCL-SC and SC-PCL (Fig. 4.1) were subsequently cloned into the pEAQ-HT™ transient expression vector, available to the CSIR under a research licence agreement from Plant Bioscience Limited (PBL), as described hereunder.

The gene inserts and pEAQ-HT™ vector were digested using restriction enzymes AgeI (Thermo Fisher Scientific, USA) and XhoI (Thermo Fisher Scientific, USA), according to the manufacturer's instructions. Briefly, 1 µg of each plasmid DNA was mixed with 5 µL of 10X Buffer O, 5 U AgeI and 10 U XhoI restriction enzymes and ddH_2O to a total volume of 50 µL. Similarly, 1 µg of the pEAQ-HT™ vector was linearized using the same restriction enzymes to generate compatible cohesive ends. These restriction enzyme reactions were incubated for 2 hours inside a 37 °C water bath. Thereafter, the pEAQ-HT™ expression vector was dephosphorylated by adding 3 µL ddH_2O, 1 U alkaline phosphatase (Thermo Fisher Scientific, Rockford, USA) and 6 µL 10X Fast AF buffer in a total volume of 60 µL and incubated for a further 10 minutes in the 37 °C water bath. All the reactions were deactivated at 80 °C for 20 minutes using Eppendorf heating block equipment to eliminate the possibility of vector religation. Five microlitres of each reaction was mixed with 1 µL 6X DNA loading buffer (30% glycerol [v/v], 0.25% [w/v] bromophenol blue, 0.25%, xylene cyanol FF and dH_2O in 10 mL) and electrophorized on a 1% [w/v] agarose gel for 30 minutes at 100 V. The buffer used was 1X TAE buffer (40 mM [Tris (hydroxymethyl) aminomethane], 20 mM acetic acid, and 1 mM EDTA, pH 8) and the DNA stained with Pronosafe nucleic acid (4 µL/30 mL gel) (laboratories conda, S.A). Approximately 0.3-1 µg molecular weight marker (GeneRuler 1kb ladder, Thermo Fisher Scientific), depending on the size of the gel, was loaded into the first well of each gel to estimate the size of the restriction enzyme digested DNA fragments. Visualization of the

DNA fragments was achieved by viewing on wavelength ultraviolet (UV) illumination to confirm successful digestion. Images were captured using ChemiDoc™ MP Image System (Bio-Rad, Hercules, CA, USA).

3.3.2 DNA fragment purification

Following resolution of the restriction enzyme digested DNA fragments via agarose gel electrophoresis, the fragments were purified using QIAquick® Gel Extraction kit (Qiagen), following the manufacturer's instructions. Briefly, the desired DNA fragment and vector bands were excised from the 1% agarose gel with a clean sharp scalpel under UV light and weighed in a 2 mL Eppendorf tube using an analytical balance. Three volumes of Buffer QG were added per 1 volume gel. The mixture was incubated for 10 minutes at 50 °C using an Eppendorf heating block to melt the gel slices completely. Subsequently, 1 gel volume of isopropanol was added to the sample to facilitate DNA binding to the silica membrane spin column. Thereafter, samples were transferred to the QIAquick spin column, placed in a provided 2 mL collection tubes and centrifuged at 17 900 × g (13 000 rpm) (Eppendorf ® Centrifuge MiniSpin plus) for 1 minute to bind DNA. Flow-through was discarded and the QIAquick column placed back in the very same tube. As an extra wash step for optimal purity, 500 µL Buffer QG was added to the QIAquick column, centrifuged for 1 minute and placed the column again back in same tube after discarding the flow-through. Subsequently, the column was washed with 750 µL of Buffer PE, left to stand for 2-5 minutes and centrifuged again for 1 minute to remove the wash buffer. An additional centrifugation step of 13 000 rpm for 1min was performed to remove the residual wash buffer. The QIAquick column was then placed in a clean 1.5 mL microcentrifuge tube. DNA was eluted by adding 30 µL of the Buffer EB (10 mM Tris. HCL, pH 8.5) to the centre of the membrane, the column left standing at room temperature for 1 minute to increase DNA yield and then centrifuged for 1 minute. In this manner, the constructs were ready for ligation process.

3.3.3 Ligation of DNA fragments and pEAQ-HT expression vector

The purified insert DNA was ligated into the pEAQ-HT™ expression vector by using T4 DNA ligase following the manufacturer's protocol. Each ligation reaction mixture contained 1 U T4 DNA ligase (Invitrogen), 4 µL 5X ligase buffer,12 µL insert DNA and 3 µL pEAQ-HT™ vector for a vector : insert ratio of 1:4. The ligation reactions were incubated overnight at 4 °C and were ready for transformation into electrocompetent

DH10B cells the following day. These ligation reactions contained HT+PCL-ST, HT+ST-PCL, HT+SC-PapMV, HT+PCL-SC, HT+SC-PCL and HT+ST-PapMV

3.3.4 Transformation of ligations into electrocompetent DH10B Cells

Sixty microlitres aliquots of electrocompetent *Escherichia coli* (*E. coli)* DH10B cells (Invitrogen) were thawed on ice. Approximately 1 µL of each ligation reaction was added to a tube of 60 µL electrocompetent *E. coli* cells on ice. The bacterial cells containing the ligation mixture were pipetted into a 0.1 nm disposable cuvette (Sigma-Aldrich, USA) and subjected to electroporation at 1.6 kV, 25 µF and 200 Ω Gene Pulser™ instrument (Bio-Rad, USA). The transformed cells were recovered in 500 µL Super optimal broth catabolite repression medium (SOC) composed of 0.5 % yeast extract, 10 mM sodium chloride (NaCl), 2.5 mM potassium chloride (KCl), 10 mM magnesium chloride ($MgCl_2$), 10 mM magnesium sulfate ($MgSO_4$) (all from Sigma-Aldrich, Merck), 2% tryptone (Thermo Fisher Scientific) and 20 mM glucose (Associated Chemical Enterprises). These transformed cells were incubated for 1 hour and 30 minutes at 37 °C with rotational shaking at 200 rpm. Recovered cells were plated onto Luria Bertani (LB) agar (10 g NaCl, 5 g Yeast Extract, 15 g Agar powder [all from Sigma-Aldrich, Merck], 10 g Tryptone [Thermo Fisher Scientific, USA]; pH 7.4) plates (250 µL/plate) supplemented with 50 µg/mL Kanamycin (Sigma-Aldrich, Merck) and incubated at 37 °C overnight to allow growth of bacterial colonies.

3.3.5 Colony Polymerase Chain Reaction (PCR)

Successful transformations were verified by colony PCR using the pEAQ-HT vector-specific forward and reverse primers, pEAQ-HT-F and pEAQ-HT-R (Table 3.1). Each PCR reaction was set up using 0.4 µL (10 µM) pEAQ forward and 0.4 µL (10 µM) reverse primers, 5.7 µL ddH_2O, 1 µL $MgCl_2$ (25 mM), 7.5 µL Ampliqon master mix (Ampliqon A/S, Denmark) and the total volume of 15 µL inoculated with a single bacterial clone colony. The PCR master mix were prepared to test 16 colonies of each construct. Single colonies were picked from overnight LB agar plates and resuspended in a 15 µL volume of PCR master mix. PCR reactions were performed on the GeneAmp 2720 Thermocycler (Applied Biosystem). The thermocycler was programmed to perform PCR under the following conditions: 1 cycle of 95 °C for 5 min, 25 cycles of 95 °C for 20 sec, 56 °C for 20 sec and 72 °C for 1 min and 20 seconds, followed by 1 cycle of 72 °C for 5 min. Five microlitres of each PCR reaction was mixed with 2 µL 6X DNA loading buffer and

electrophorized a 1% agarose gel in 1X TAE buffer and the PCR products visualised as described in section 3.3.1. The bacterial clones validated as positive via PCR were inoculated into 5 mL LB broth supplemented with 5 µL kanamycin (Sigma-Aldrich, Merck) and incubated overnight at 37 °C with 200 rpm rotational shaking. About 1 mL of the overnight bacterial culture was frozen in 15% glycerol at -80 °C for long term storage and the remaining culture volume used to isolate recombinant plasmid DNA.

Table 3. 1. Primers used for colony PCR to confirm the presence of recombinant pEAQ-HT plasmid

Primers	5' – 3' sequence
pEAQ-HT-F	ACTTGTTACGATTCTGCTGACTTTCGGCGG
pEAQ-HT-R	CGACCTGCTAAACAGGAGCTCACAAAGA

***Note**: Primers were sourced from Inqaba Biotech (Pty) Ltd, South Africa and designed for colony PCR screening of transformed bacterial competent cells and target regions flanking the pEAQ-HT multiple cloning site. They do not encode amino acids.*

3.3.6 Plasmid DNA isolation

Plasmid DNA was extracted using the FavorPrep™ Plasmid Extraction Mini Kit (Favorgen® Biotech Corp), according to the manufacturer's instructions. Reagents in this kit are numbered and referred as "FAPD". Briefly, 2 mL of an overnight bacterial culture was aliquoted into 2 mL microcentrifuge tubes and centrifuged at 8000 × g for 3 minutes using an Eppendorf® mini spin centrifuge to pellet the cells. The supernatant was discarded after centrifugation. Subsequently, the bacterial pellet was completely resuspended with 250 µL of pre-chilled (4 °C) FAPD1 buffer. The cells were then lysed by adding 250 µL of room temperature FAPD2 buffer, facilitating membrane breakdown to release DNA. Following gentle inversion of tubes 2-5 times, the samples were incubated at room temperature for 2-5 minutes. Three hundred and fifty microlitres of FAPD3 buffer was added immediately after tube inversions to neutralize the bacterial cell lysates. By adding the neutralization buffer, cellular debris and chromosomal DNA were precipitated. These tubes were further re-inverted for 2-5 minutes, and the lysates were clarified by centrifugation at high speed (18 000 × g) for 10 minutes. While the lysates were being centrifuged, a FAPD column provided by the kit was placed in the collection tubes. The plasmid-containing supernatant was transferred into the FAPD column and centrifuged at 11 000 × g for 30 seconds. Following the discarding of the flow-through the FAPD columns were placed back in the collection tubes. Four hundred microlitres of WF

buffer to remove contaminants was added to the FAPD columns and they were centrifuged using the same conditions. Seven hundred microlitres of wash buffer was added to the FAPD column, the column centrifuged and the flow-through discarded. The FAPD column in the tubes were further centrifuged at full speed (18 000 × g) for an additional 3 minutes to remove any residual liquid. The FAPD columns were placed in new 1.5 mL microcentrifuge tubes. Approximately 50 µL of the elution buffer was added directly in the middle of the membrane of FAPD columns and incubated for 1 minute prior to centrifugation at 18 000 x g for 1 minute.

3.3.7 Plasmid DNA concentration, purity and sequencing

DNA concentration and purity of the isolated plasmids were determined using NanoDrop2000c spectrophotometer (Thermo Fisher Scientific). Prior to measurements, the spectrophotometer was blanked with dH_2O to calibrate the baseline. Approximately 1 µL aliquot of each DNA sample was pipetted directly on the measurement pedestal to record the absorbance spectra. The instrument automatically calculated DNA concentration based on absorbance at 260 nm (A260). An A260 of 1.0 absorbance value corresponds to 50 µg/mL double-stranded DNA. The plasmid DNA sample purity was assessed by evaluating the A260/280 and A260/230 ratios. The absorbance ratios of A260/280 between 1.8-2.2 indicate high DNA purity. A260/230 ratios above 2.0 were an indication of minimal contamination of either salt from chemicals or cell debris. The sequence of the inserts within the recombinant plasmid DNA were verified via dideoxy Sanger DNA sequencing using the pEAQ-HT-F and pEAQ-HT-R primers (Inqaba Biotechnical Industries (Pty) Ltd)

3.3.8 Transformation of electrocompetent *Agrobacterium tumefaciens* LBA4404

Once sequences of the inserts were verified, 1 µL of each recombinant plasmid was added to 60µL of electrocompetent LBA4404 *Agrobacterium tumefaciens* cells (Invitrogen, Waltham, MA, USA) on ice. The bacterial cells were transformed similarly to the way that the *E. coli* were transformed described in section 3.3.4, however, the voltage of the Gene Pulser (Bio-Rad) was 1.44 kV, 25 µF and 200 Ω. The electroporated cells were recovered in 500 µL SOC media and incubated at 28 °C for 3 hours with rotational shaking at 175 rpm. Thereafter, the recovered cells were plated onto two LB agar plates (250 µL/plate) supplemented with 50 µg/mL kanamycin, 100 µg/mL streptomycin and 30 µg/mL rifampicin (Sigma-Aldrich, Merck) and further incubated at 28 °C for 3 days. Single

colonies were picked from each plate and inoculated into 5 mL LB broth supplemented with 50 µg/mL kanamycin, 100 µg/mL streptomycin and 30 µg/mL rifampicin and incubated at 28 °C with rotational shaking at 175 rpm overnight (MRC incubator). The following day, recombinant *Agrobacterium* cultures were frozen in 32% glycerol at -80 °C freezer for long-term storage. The remaining volume of recombinant *Agrobacterium* cultures were streaked onto LB agar plates supplemented with the same antibiotics and incubated at 28 °C for 3 days.

The *Agrobacterium* cultures were collected/scrapped off the surface of a plate with a sterile disposable loop and inoculated into 50 mL YMB medium (0.1% yeast extract, 1.0% mannitol, 1.7 mM NaCL, 0.8 Mm $MgSO_4$. $7H_2O$ and K_2HPO_4 2.2 mM) (all from Sigma-Aldrich, Merck) supplemented with 50 µg/mL kanamycin, 100 µg/mL streptomycin and 30 µg/mL rifampicin. The *Agrobacterium* pellets were resuspended in the medium with a loop and the cultures incubated at 28 °C with rotational shaking at 175 rpm overnight.

3.3.9 *Agrobacterium*-mediated infiltration (Agroinfiltration) into the *Nicotiana Benthamiana* plant leaves

The recombinant *Agrobacterium* cultures grown overnight at 28 °C at 175 rpm were transferred into 50 mL falcon tubes and centrifuged at 7000 × g, 10 °C for 10 minutes. Following centrifugation, the harvested recombinant *Agrobacterium* pellets were resuspended thoroughly in 5 mL freshly prepared MMA infiltration buffer (pH 5.6, 10 mM MES hydrate, 10 mM $MgCl_2$, 100 µM 3,5 3,5-dimethoxy-4-hydroxy-acetophenone) (all from Sigma-Aldrich, Merck). This MMA buffer creates a conducive *Agrobacterium* environment for effective DNA transfer into plant cells. Because this experiment required co-expression of proteins, two different recombinant *Agrobacterium* cultures were combined at this stage to obtain a 1:1 ratio of bacterial density (Table 3.2). The *A. tumefaciens* combinations were diluted with MMA buffer to a final OD_{600} of between 2.0-2.3 in a final volume of 40 mL. Pots of *N. benthamiana* dXT-FT plants were prepared by CSIR plant technician Albert Mabetha. The dXT-FT mutant of *N. benthamiana* was used due to lack of plant-specific glycosylation enzymes and its ability to produce VLPs with human glycans (Jansing *et al*., 2019). The leaves of four to eight-week-old dXT-FT *N. benthamiana* plants were syringe infiltrated with the prepared *A. tumefaciens* suspensions. This process was accomplished manually by infiltrating the *Agrobacterium* suspensions into the abaxial side of the *N. benthamiana* DXT/FT leaves using needleless syringe. Agroinfiltrated leaves were marked with laboratory plastic tape. Following

infiltration, *N. benthamiana* plants were placed back into the growth room and grown at 28 °C under 16 hrs / 8 hours light/dark cycles and harvested at 8 days post-infiltration (d.p.i).

Table 3. 2. Summary of the agrobacterial suspensions used to agroinfiltrated *N. benthamiana* DXT/FT plants

Agrobacterial suspension	**Agrobacterial culture 1**	**Agrobacterial culture 2**	**Agrobacterial culture combination**
1	HT-ST-PapMV	-	HT-ST-PapMV
2	HT-SC-PapMV	-	HT-SC-PapMV
3	HT-SC-PapMV	HT-PCL-ST	HT-SC-PapMV+PCL-ST
4	HT-SC-PapMV	HT-ST-PCL	HT-SC-PapMV+ST-PCL
5	HT-ST-PapMV	HT-PCL-SC	HT-ST-PapMV+PCL-SC
6	HT-ST-PapMV	HT-SC-PCL	HT-ST-PapMV+SC-PCL

3.3.10 Harvesting of *N. Benthamiana* DXT/FT leaves, protein extraction and density gradient centrifugation

Agroinfiltrated *N. benthamiana* plant leaves were harvested and weighed 8 d.p.i and processed through a multipurpose juice extractor (MATSONE) with 2 volumes of 1X PBS buffer (137 mM NaCl, 2.7 m KCl, 10 mM Na_2HPO_4, 1.8 Mm KH_2PO_4, pH 7.4 = 10X PBS) (all from Sigma-Aldrich, Merck) supplemented with 0.2% Protease inhibitor cocktail P2714 (Sigma Life Science), according to manufacturer instructions. The lysates were incubated at 4°C with gentle agitation (Stovall belly dancer, Life Science Inc, USA) for 30 minutes and clarified by centrifugation at 7000 × g, 4 °C for 10 minutes to pellet the large debris using an Eppendorf centrifuge 5810 R. About 6 mL of each cell lysate, possibly containing proteins ST-PapMV, SC-PapMV, SC-PapMV-PCL-ST, SC-PapMV-ST-PCL, ST-PapMV-PCL-SC and ST-PapMV-ST-PCL were layered on 60%-20% Iodixanol (OptiPrep™) density gradients medium (Sigma-Aldrich, St. Louis, MO, USA) and centrifuged at 32 000 × g at 10 °C for 2 hours, with an acceleration rate of 5 and a

deceleration rate of 8 on Beckman Coulter Optima XE-100 Ultracentrifuge. Ten 500 µL fractions were collected from each gradient from the bottom of the ultracentrifuge tubes using a Minipuls2 peristaltic pump (Gilson, Madison, WI, USA).

3.3.11 Protein purification with MagResyn® NTA

The chimeric PapMV proteins were purified using the 6X Histidine-tag on their C-terminals. Plant cell lysates were prepared and clarified as described in section 3.3.10. MagResyn® NTA (Resyn Biosciences [Pty] Ltd) beads were used to capture the VLPs out of the clarified plant cell lysate (Fig. 3.1). According to the manufacturer's instructions, 20 µL MagResyn® NTA, sufficient to capture 20 µg of recombinant protein, was equilibrated by washing the beads three times with 200 µL binding buffer. Following the equilibration, 1 mL of each cell lysate was diluted 1:1 with 1 mL of 1X NTA binding buffer (80 mM sodium phosphate pH 7.4-8.0, 40 mM imidazole and 1.0 mM NaCl). This made up a total volume of 2 mL that was added into the 20 µL equilibrated MagResyn beads. After an incubation of 5 minutes at room temperature with inversion rotation, the tubes were placed on a magnetic separator and supernatant discarded. The binding step was repeated 3 times to ensure sufficient VLP binding to the magnetic beads from the cell lysate. The bound protein was washed three times with 200 µL 1X NTA buffer and the supernatant discarded. Each sample was eluted in 50 µL elution buffer (80 mM sodium phosphate pH 7.4-8.0, 500 mM NaCl, and 500 mM imidazole) three times, resulting in 150 µL sample volume for each purified protein. Five microlitres of each sample was electrophorized on a 12% SDS-PAGE gel to visualise the purified proteins, as described in the next section.

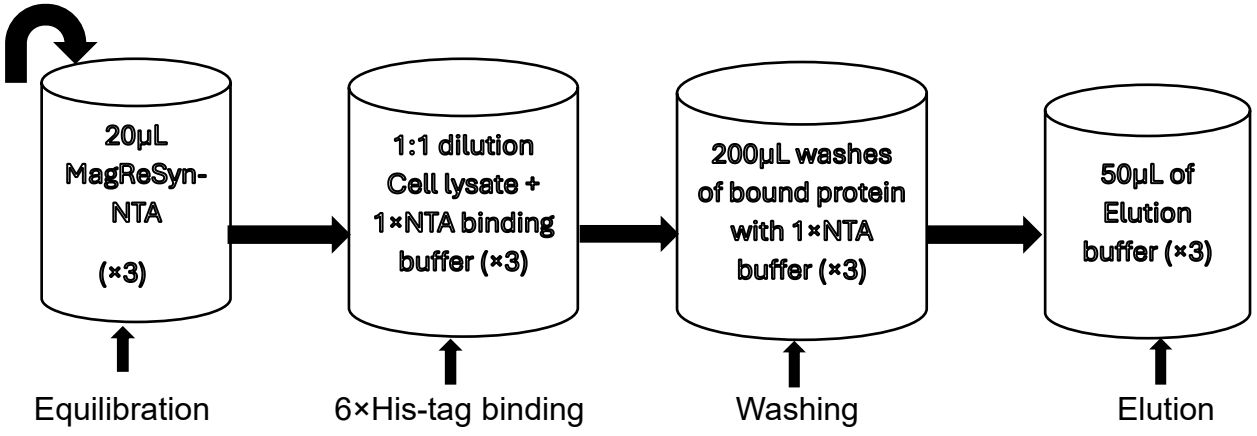

Figure 3. 1. Schematic representation of the His-tagged protein purification of chimeric PapMV VLPs using MagReSyn® NTA magnetic beads. The steps include equilibration of

the magnetic beads, binding of the 6X His-tagged proteins from *N. benthamiana* DXT/FT plant extracts, washing to remove non-specific proteins and elution of the VLP target protein.

3.3.12 Protein expression confirmation using SDS-PAGE

Protein content of samples was assessed by mixing 5-10 µL of sample with 1-2 µL of 6X protein loading dye (0.004% bromophenol blue, 10% 2-mercaptoethanol, 20% glycerol, 4% SDS and 0.125 M Tris-HCl) (all from Sigma-Aldrich, Merck). Samples were denatured at 95 °C for 2 minutes on an Eppendorf thermomixer R heating block and electrophoresed for 1hr 15 minutes at 130 V on a 12% Sodium Dodecyl Sulfate (SDS) Polyacrylamide Gel, prepared according to the manufacturer's instructions (Bio-Rad TGX™ FastCast™ Acrylamide Kit). Briefly, 12% SDS-PAGE gels comprise two layers namely, resolver gel which separates proteins based on size and stacking gel which concentrates proteins into narrow bands to improve resolution. These gels were polymerised by adding tetramethylethylene diamine (TEMED) (Sigma-Aldrich, Merck) and 10% (w/v) ammonium persulfate (APS) (Bio-Rad). The prepared gels were allowed to polymerize for 30 minutes at room temperature. Recombinant protein samples analysed on 12% SDS-PAGE gels included clarified plant cell lysate (5 µL), MagReSyn® NTA bead-purified proteins (5 µL) and iodixanol density gradient fractions (10 µL). Five microlitres of PageRuler™ Prestained Ladder (Thermo Fisher Scientific, Waltham, MA, USA) served as a molecular weight marker that was loaded into the first lane of each gel to estimate the size of the resolved protein bands. Non-infiltrated plant cell lysate (5 µL) served as a negative control.

Gel electrophoresis was carried out using Mini-PROTEAN® Tetra cell (Bio-Rad) filled with 1X TGS buffer (25 mM Tris, 192mM Glycine and 0.1% SDS) (Sigma-Aldrich, Merck). The 12% SDS-PAGE gels were electrophorized at 130V for 1 hour 15 minutes to resolve proteins. Following electrophoresis, gels was stained with Coomassie brilliant blue R-250 (0.25% Coomassie blue, 50% methanol,10% acetic acid [Sigma-Aldrich, Merck] and dH_2O) for 2 hours and subsequently destained with destain solution (30% methanol, 10% glacial acetic acid [Sigma-Aldrich, Merck] and 60% dH_2O) overnight at room temperature with gentle agitation (Stovall belly dancer, Life Sciences Inc, USA). The stained protein bands were visualized on the ChemiDoc™ MP Imaging System (Bio-Rad).

3.3.13 Protein identity confirmation via western blot

Western blotting was employed to confirm the identity of recombinant His-tagged proteins using anti-His-tag antibodies. After electrophoretic separation, proteins from a 12% SDS-PAGE gel were transferred onto a PVDF membrane within the Trans-blot Turbo Transfer Pack (Bio-Rad) using Trans-blot Turbo Transfer System (Bio-Rad) with a mixed MW application, following the manufacturer's instructions (25 V for 7 minutes). The membranes were immediately blocked with 5% blocking solution (5% skim milk with 1X PBS) and incubated overnight at 4 °C with gentle agitation or incubated for 2 hours at room temperature. Following 3 washes of 5 minutes each (1X PBS; 0.05% Tween®20) (Sigma-Aldrich, Merck), the membranes were incubated with a 1:2000 anti-His antibody solution (αHis-HRP mAb antibody [Sigma-Aldrich, Merck]; 5% skim milk with 1X PBS) for 1 hour at room temperature with gentle agitation (on rocker platform). After the detection antibody incubation, the membrane was washed three times (0.05% Tween®20 [Sigma-Aldrich, Merck]; 1X PBS). One millilitre of Tetramethylbenzidine (TMB) Liquid Substrate (Sigma-Aldrich, Merck) was added onto the membrane and the antibody bound proteins visualised with the ChemiDoc™ MP Image System (Bio-Rad) using a colorimetric assay application.

3.3.14 Protein quantification

3.3.14.1 Bicinchoninic Acid (BCA) assay

The quantity of chimeric PapMV VLPs produced from agroinfiltrated *N. benthamiana* plant leaves was determined using Pierce BCA Assay Kit (Thermo Fisher Scientific) according to the manufacturer's instructions, in a 96-well microplate (Thermo Fisher Scientific). The BSA standards were freshly prepared by serial dilution in ddH_2O assay buffer to generate standard curves (Table 3.3).

Table 3. 3. Bovine serum albumin (BSA) standard curve preparation

Stock	ddH_2O	Standard (µg/mL)
Solution A 750 µL (2 mg/mL BSA)	1425 µL	100
B 500 µL of A	125 µL	80
C 300 µL of A	200 µL	60
D 300 µL of B	300 µL	40

E 167 µL of C	333 µL	20
F 175 µL of D	525 µL	10
G 250 µL of F	250 µL	5
H 25 µL of E	475 µL	1

Iodixanol fractions 7 or 8 containing proteins ST-PapMV, SC-PapMV, SC-PapMV+PCL-ST, SC-PapMV+ST-PCL, ST-PapMV+PCL-SC and ST-PapMV+SC-PCL were diluted with Millipore water (ddH_2O) (1:20 dilution). Immediately before use, 25:24:1 Micro BCA Reagent A, B and C (Working solution) was freshly prepared. Approximately 150 µL of each standard and protein sample were pipetted into the 96-microplate wells as three replicates of each. Subsequent 150 µL of working reagent solution prepared was pipetted into the wells containing standards and samples. Three replicate wells contained 150 µL ddH_2O as a blank control to which 150 µL working reagent solution was added. The plate was gently mixed by hand shaking for 30 seconds, covered with parafilm to minimize evaporation and incubated at 37 °C for 2 hours in dark (Series 2000 Scientific incubator). The intensity of the colour development was then measured at 562 nm in a Hidex Spectrophotometer. A standard curve was compiled using the absorbance readings of the BSA standards and used to extrapolate the concentrations of the total protein content in the iodixanol fractions.

3.3.14.2 Gel densitometry

Gel densitometry was used to quantify the ST-PapMV, SC-PapMV, SC-PapMV-PCL-ST, SC-PapMV-ST-PCL, ST-PapMV-PCL-SC and ST-PapMV-SC-PCL proteins purified by means of the MagResyn® NTA bead protocol. Bovine serum albumin (BSA) (2 mg/mL) (Sigma-Aldrich, Roche) was diluted with dH_2O to concentrations of 100 µg/mL, 250 µg/mL, 500 µg/mL, 750 µg/mL, 1000 µg/mL, 1500 µg/mL and 2000 µg/mL. Twenty microlitres of the seven BSA standards and 20 µL of purified protein VLPs samples were each mixed with 3.2 µL 6X protein loading buffer and denatured on an Eppendorf heating block for 2 minutes at 95 °C. A total volume of 23.2 µL of standards and purified protein samples was loaded onto 12% SDS-PAGE gels and run under the conditions described in Section 3.3.12. Gels were stained with Coomassie blue brilliant and destained with solution described in section 3.3.12. A densitometry application on the ChemiDoc™ MP Image System was used to quantify the VLP samples by comparing them to the intensity of the BSA standard bands of known concentration.

3.3.15 Transmission electron microscopy (TEM)

Coated copper grids of about 200 mesh size were floated on 20 µL iodixanol fraction 8 sample for 5 minutes. Thereafter the grids were washed five times by floating the copper grid on five 10 µL drops of sterile milli-Q water and stained for 15 seconds with 2% uranyl acetate. The grids were air dried and samples viewed using the JEOL-1400 Flash Electron Microscope at the University of Pretoria, Onderstepoort Veterinary Campus.

3.4 *In vitro* binding of lectin-conjugated PapMV VLPs to breast cancer cells

The binding of the His-tag purified lectin-conjugated PapMV VLPs to target breast cancer cells was evaluated *in vitro*. AU565 (ATCC CRL-2351™), a HER2+ breast cancer cell line available in the CSIR host laboratory, was seeded in a 24 well plate (Nunc) at a density of 50 000 cells per well (Gross et al., 2023) using RPMI-1640 Medium (Gibco) with 10% Foetal calf serum (FCS) (Gibco). The cells were incubated at 37 °C in a Thermo Scientific (Sep Sci) incubator with humidified atmosphere containing 5% CO_2 for 48 hours (Dr Ilse Du Preez, personal communication). After the 48 hours incubation, the medium was discarded and cells were washed three times with filter-sterilized Dulbecco's Phosphate Buffered Saline (DPBS; 1% BSA pH=7.2) (2 mL per well). After the third wash, the plate was placed at 4 °C for 30 minutes. The DPBS; 1% BSA wash solution was subsequently discarded and 200 µL of a 4% (w/v) paraformaldehyde (PFA) solution added to fix the cells and the plates incubated for 10 minutes at room temperature. The PFA solution was then removed and discarded. Subsequently, cells were washed three times (3 minutes each wash) with 1 mL of 1X PBS buffer. Approximately 0.253 µg purified ST-PapMV, SC-PapMV, SC-PapMV-PCL-ST, SC-PapMV-ST-PCL, ST-PapMV-PCL-SC and ST-PapMV-SC-PCL VLPs were added to each well with serum-free medium (SFM)/1% BSA to a final volume of 200 µL/well (Table 3.4). The volume of the purified proteins added varied between proteins depending on protein concentration however the final volume remained 200 µL for each well. One hundred microlitres SFM/1% BSA and 100 µL glycerol was added to each of the negative control wells. Each reaction was performed in triplicate as indicated by same colour in Table 3.4. The plate was incubated for 1.5 hours at 4 °C with gentle agitation on a bench-top rocker platform to allow VLP binding. After incubation, the cells were washed three times with cold 1X DPBS/0.1 % BSA buffer to remove any unbound VLPs (1 mL/well). Thereafter, 200 µL of anti-His Alexa Fluor 488-conjugated antibody (Ab) (Invitrogen), diluted 1:1000 in 1X DPBS/0.1% BSA, was added per well, the plate covered with a layer of tinfoil and incubated for 1 hour at room temperature in

darkness. The wells were washed again three times with 1X DPBS/0.1%BSA for 3 minutes with gentle agitation at 4°C (1 mL/well). Two hundred microlitres of 1X DPBS were added per well and the fluorescence intensity readings measured using the Hidex plate reader. The Cytation™ cell imaging multi-mode reader (Biotek) allowed for visualisation of fluorescing cells.

Table 3. 4. Content of the 24-well cell culture plate used *in vitro* binding experiment.

Cells + SC-PapMV VLPs	Cells + SC-PapMV VLPs	Cells+ SC-PapMV VLPs	Cells+ ST-PapMV VLPs	Cells+ ST-PapMV VLPs	Cells + ST-PapMV VLPs
Cells + SC-PapMV + PCL-ST VLPs	Cells + SC-PapMV + PCL-ST VLPs	Cells + SC-PapMV + PCL-ST VLPs	Cells + ST-PapMV + PCL-SC VLPs	Cells + ST-PapMV + PCL-SC VLPs	Cells + Cells+ ST-PapMV + PCL-SC VLPs
Cells + SC-PapMV + ST-PCL VLPs	Cells + SC-PapMV + ST-PCL VLPs	Cells + SC-PapMV + ST-PCL VLPs	Cells + ST-PapMV + SC-PCL VLPs	Cells + ST-PapMV + SC-PCL VLPs	Cells + ST-PapMV + SC-PCL VLPs
Negative Control-Cells +Ab (No VLPs) SFM + Glycerol	Negative Control-Cells +Ab (No VLPs) SFM + Glycerol	Negative Control-Cells +Ab (No VLPs) SFM (no Glycerol)	Negative Control-Only cells (No VLPs; no Ab) SFM + Glycerol	Negative Control-Only cells (No VLPs; no Ab) SFM+ Glycerol	Negative Control-Only cells (No VLPs; no Ab) SFM (No Glycerol)

3.5 Statistical analysis

All quantitative data obtained from recombinant protein expression, VLPs and assembly, and *in vitro* binding assays were statistically analysed with IBM SPSS Statistics software

(Version 30.0.0). Each experiment was performed in triplicate. Therefore, results were expressed as mean ± standard deviation. Gel densitometric values from SDS-PAGE and Western corresponding band sizes were quantified to assess protein levels. The results were analysed to verify consistency among replicates.

All HER2+ cancer cells were treated with the same buffer conditions for the fluorescence *in vitro* binding assays to maintain uniformity across the experiment. Negative controls were included in the assay. The mean fluorescence intensity emitted served as a measure of VLP binding efficiency to HER2+ cancer cells. A two-way analysis of variance was used to assess the impact of treatment type and recombinant protein expression/VLP variation and fluorescence intensity. Statistical significance threshold was established at (p value) of 5% ($p < 0.05$). Data were presented in column clusters and tables.

3.6 Ethical considerations

It was mandatory to ensure that research is conducted with integrity, honesty and commitment to the well-being of individuals and society. This study obtained necessary approvals before commencement. The study was granted ethical approval from the CSIR research ethics committee with the CSIR research reference number 470/2024. This CSIR research approval granted permission to work with protocols involving GMO microorganisms, available cancer cell lines (ATCC CRL-2351™), and any *in vitro* experimental procedures to ensure environmental safety and scientific integrity. Additionally, the University of South Africa (UNISA) granted ethical clearance from the College of Agriculture and Environmental Sciences, Health REC with reference number 2024/CAES_HREC/3343. By adhering to ethical considerations, this project ensured all research was conducted responsibly, safeguarding the welfare of biological systems and maintaining compliance with institutional and regulatory standards.

CHAPTER 4: RESULTS

4.1 Design of the PapMV CP and PCL lectin proteins containing the SpyTag/SpyCatcher elements

The PapMV CP and PCL lectin proteins used in this study were designed as described in section 3.3.1 by Dr Rutkowska (personal communication) prior to commencement of the experimental work. These proteins had SpyTag (ST) and SpyCatcher (SC) peptide elements positioned at either N-terminal or C-terminal ends of the above mentioned proteins. The constructs formed the basis for gene cloning, expression and protein characterization experiments. A schematic representation of all six chimeric protein constructs designed are indicated in Fig. 4. 1.

Papaya mosaic virus (PapMV) CP was engineered to contain either a SpyTag or SpyCatcher element positioned at N-terminal end of CP, resulting in ST-PapMV (Fig. 4 .1 (1)) and SC-PapMV (Fig. 4 .1 (2)). It was unknown how these N-terminal insertions would affect protein folding and VLP assembly and whether the elements would be accessible to the exterior following VLP assembly and needed to be investigated. The C-terminal was not used for PapMV CP to present ST/SC elements to avoid instability and aggregation (Babin *et al*., 2013).

SpyTag and SpyCatcher elements were positioned at N-terminal or C-terminal ends of the Polygonatum crytonema lectin (PCL) protein, generating four distinct constructs. These included ST-PCL (Fig. 4 .1 (3)) and SC-PCL (Fig. 4 .1 (4)), where the SpyTag or SpyCatcher elements were fused to the N-terminal end of PCL. Similarly, the SpyTag or SpyCatcher elements were fused to the C-terminal end of the PCL protein generating the PCL-ST (Fig. 4 .1 (5)) and PCL-SC (Fig. 4.1 (6)) chimeric proteins, respectively. Different constructs were designed as it was not known which chimeric proteins would fold correctly and be soluble. The constructs were paired to allow for controlled assembly of the SpyTag and SpyCatcher elements (Hatlem *et al*., 2019).

ST-PapMV (N-terminal fusion)

1. 

SC-PapMV (N-terminal fusion)

2. 

ST-PCL (N-terminal fusion)

3. 

SC-PCL (N-terminal Fusion)

4. 

PCL-ST (C-terminal fusion)

5. 

PCL-SC (C-terminal fusion)

6. 

Figure 4. 1. Schematic diagram showing the designed gene constructs of PapMV CP and PCL lectin linked with SpyTag/SpyCatcher elements. Gene tags fusions are indicated, 1. ST-PapMV (N-term fusion), 2. SC-PapMV (N-term fusion), 3. ST-PCL (N-term fusion), 4. SC-PCL (N-term fusion), 5. PCL-ST (C-term fusion) and 6. PCL-SC (C-terminal fusion), respectively.

4.2 Gene cloning into pEAQ-HT plant expression vector

The genes of interest in this study, SC-PCL, PLC-SC, SC-PapMV, ST-PapMV, PCL-ST and ST-PCL, originating from the recombinant pUC-57 plasmids synthesized by GeneArt,

were individually cloned into the pEAQ-HT™ transient plant expression vector using directional restriction enzyme-based cloning. Restriction enzyme sites *AgeI*, located on the 5'end of each gene, and *XhoI*, located on the 3'end of the gene, were used to excise the gene of interest from the pUC-57 vector and insert it into the corresponding restriction enzymes sites within the pEAQ-HT vector. Restriction enzyme reactions were performed using the reaction conditions recommended by the manufacturer and detailed in section 3.3.1, ensuring complete digestion while minimizing non-specific cleavage. The success of the digestion was assessed by electrophoresis of the reaction contents on a 1% agarose gel (Fig. 4.2; Table 4.1). Plasmids bands corresponding in size to the SC-PCL (1114bp) (a; lane 1), ST-PapMV (781bp) (b;lane-1), PCL-SC (1114bp) (c;lane-1), ST-PCL (795bp) (d; lane-1), SC-PapMV (1065bp) (d; lane-3) and PCL-ST (801bp) (d; lane-5) DNA fragments were observed on 1% agarose gel (Fig. 4.2 (a)-(d)). The digested pEAQ-HT vector, 10003bp in size, was observed in the last lane of each agarose gel (Fig. 4.2 (a)-(d)).

Table 4. 1. Sizes of the DNA inserts in the recombinant pUC-57 vectors

Insert DNA	**Expected DNA fragment size (bp)**
SC-PCL	1114 bp
ST-PapMV	781 bp
PCL-SC	1114 bp
ST-PCL	795 bp
SC-PapMV	1065 bp
PCL-ST	801 bp

DNA bands corresponding in size to the expected pEAQ-HT vector and the SC-PCL, ST-PapMV, PCL-SC, ST-PCL, SC-PapMV PCL-ST insert DNA sized fragments (Table 4.1) were excised from the 1% agarose gel and purified using Qiagen DNA extraction kit, as described in section 3.3.2, and according to the manufacturer's instructions. The aim was to remove contaminating agarose, enzymes and buffer salts that may interfere with the ligation process. The DNA fragments were individually covalently ligated to the linearized pEAQ-HT vector using T4 DNA ligase. This ligation reaction, performed overnight (approximately 16 hours) at 4°C, allowed for the annealing of the cohesive ends. Although

it was not possible to directly visualize the outcomes of the ligation, *E. coli* transformation served as proxy.

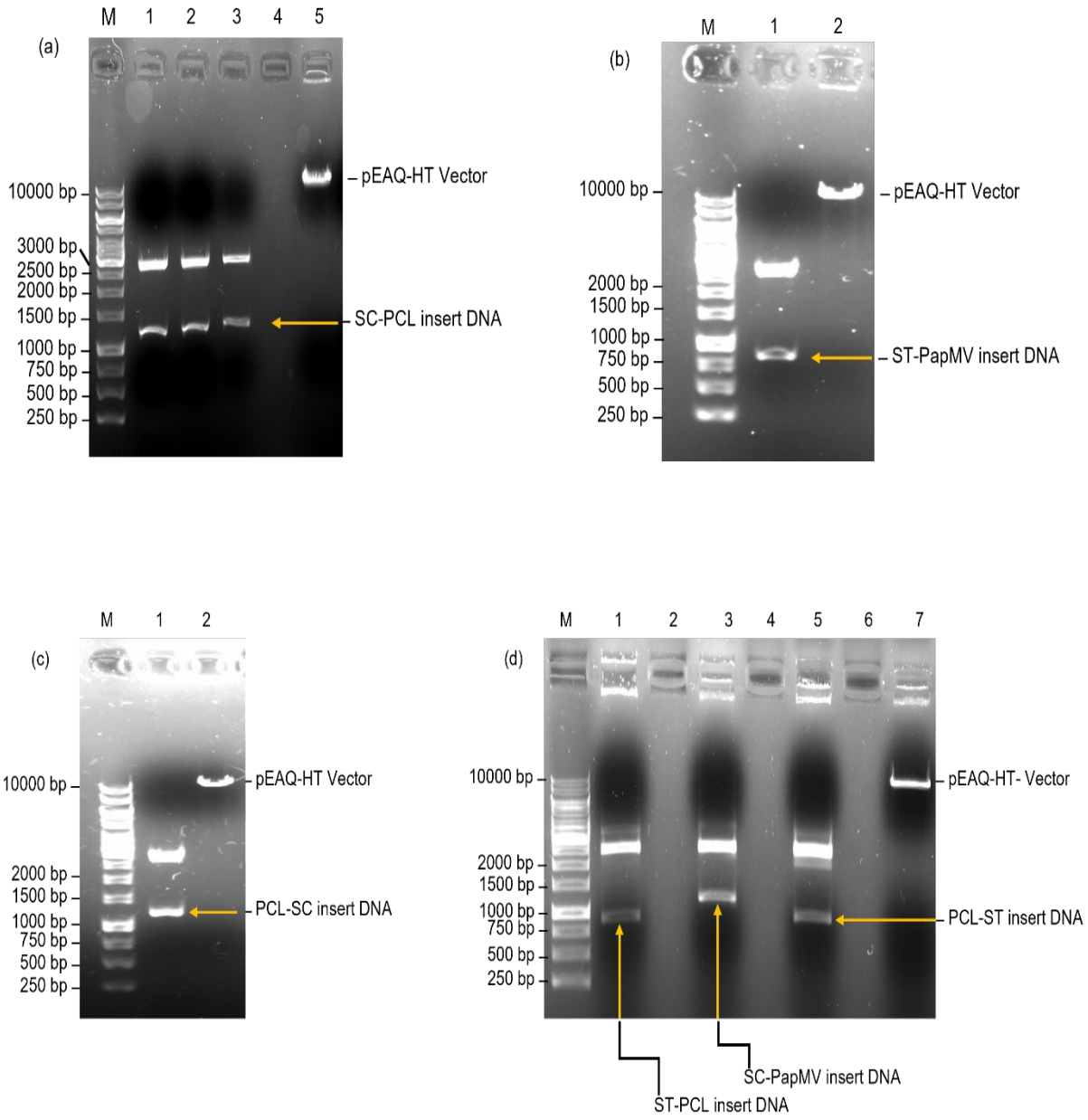

Figure 4. 2. 1% agarose gel electrophoresis analysis of the contents of recombinant pUC-57 plasmid and pEAQ-HT vector restriction enzyme reactions. Plasmids pUC-57-SC-PCL (a), pUC-57-ST-PapMV (b), pUC-57-PCL-SC (c), pUC-57-ST-PCL (d), pUC-57-SC-PapMV (d) and pUC-57-PCL-ST (d) were digested with restriction enzymes *AgeI* and *XhoI* and samples of the reactions loaded into lanes of their respective gels as indicated. The first lane in each gel designated 'M' contains the DNA molecular weight marker

GeneRuler 1kb Ladder (Thermo Fisher Scientific) and the relevant band sizes are indicated in base pairs (bp). Yellow arrows indicate the position of the inserts (a) SC-PCL(1114bp) (lane 1), (b) ST-PapMV (781bp) (lane 1), (c) PCL-SC (1114bp) (lane 1), (d) ST-PCL (795bp) (lane 1), (d) SC-PapMV (1065bp) (lane 3) and (d) PCL-ST (801bp) (Lane 5). The last lane in all 1% agarose gels from (a)-(d) contain the linearised pEAQ-HT vector (10003bp).

4.3 Transformation into competent *E. coli* bacterial cells

Each ligation reaction was transformed into electrocompetent *E. coli* DH10B cells using a Gene Pulser electroporator, according to the manufacturer's instructions, followed by recovery in SOC medium and plating on LB agar supplemented with kanamycin antibiotic. The plasmids enabled the transformed bacteria to form colonies on the agar plates because pEAQ-HT vector is known to carry a kanamycin resistance gene. Sixteen colonies from each transformation were streaked onto a replica plate, examples of which are shown in Fig 4.3 (a)-(c), and the candidate bacterial clones tested for the presence of recombinant plasmids via PCR.

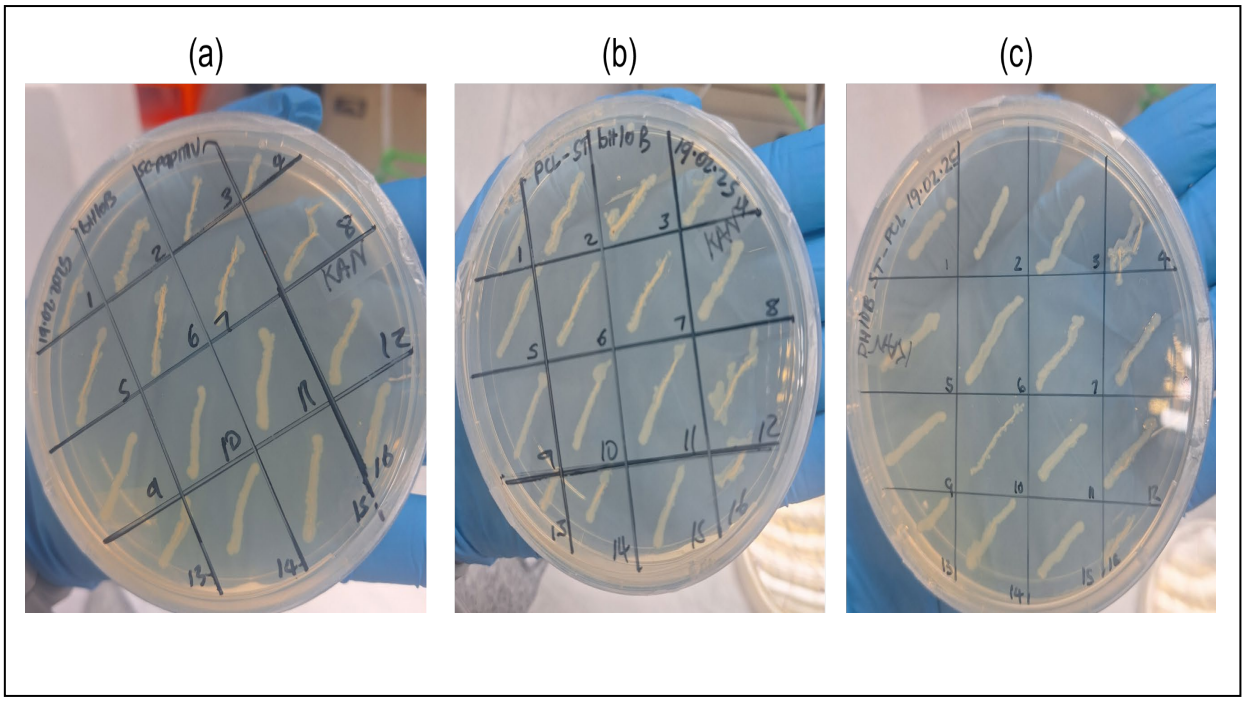

Figure 4. 3. LB replica agar plates containing transformed bacterial colonies. DH10B bacterial cells transformed with ligation reactions pEAQ-HT+SC-PapMV, pEAQ-HT+PCL-ST, and pEAQ-HT+ST-PCL were grown on LB plates (Kan+) and 16 colonies from each plate streaked onto LB replica plates (Kan+) shown in (a)-(c), respectively.

4.4 Validation of recombinant clones via PCR

Colony PCR was performed to confirm the presence of recombinant plasmid in the candidate *E. coli* DH10B colonies. Candidate bacterial clones were inoculated directly into PCR reactions containing the pEAQ-HT-F and pEAQ-HT-R primers (Table 3.1). The forward primer, pEAQ-HT-F, bound to the 5' region upstream of *Age*I site and reverse primer, pEAQ-HT-R, bound to the 3' region downstream of *XhoI* site in the pEAQ-HT vector. Because these primers flank the insertion site region, the size of the PCR product that they amplify is an indication of the presence of insert DNA in the pEAQ-HT vector. Sixteen colonies of each of the five constructs, and 8 colonies of the pEAQ-HT-ST-PapMV construct, were tested using colony PCR, as described in section 3.3.5.

The contents of the PCR reactions were resolved by 1% agarose gel electrophoresis. DNA bands were observed in the majority of the lanes into which the contents of the PCR reactions had been loaded (Fig. 4.4 (a)-(f)). The additional base pairs added during PCR due to position of the pEAQ-HT-F and pEAQ-HT-R primer binding sites on either side of the insertion site resulted in the sizes of the PCR products being slightly larger than the expected insert sizes in Table 4.1. DNA bands of approximately expected 1114bp (a), 781bp (b), 1114bp (c), 1065 (d), 801 (e) and 795 (f), corresponding to the sizes of the PCL-SC, ST-PapMV, SC-PCL, SC-PapMV, PCL-ST and ST-PCL PCR products, respectively, were visualised on the 1% agarose gels.

These PCR product sizes indicated that the pEAQ-HT vector was recombinant and contained insert DNA in the AgeI/XhoI insertion site. No DNA bands were observed in the lanes where the negative control reactions were loaded indicating no contaminating DNA in the PCR master mix. The presence of DNA bands of specific sizes in the positive control lanes indicated that the PCR reactions were successfully performed. The sizes of these DNA correlated with the recombinant pEAQ-HT plasmid template that was used.

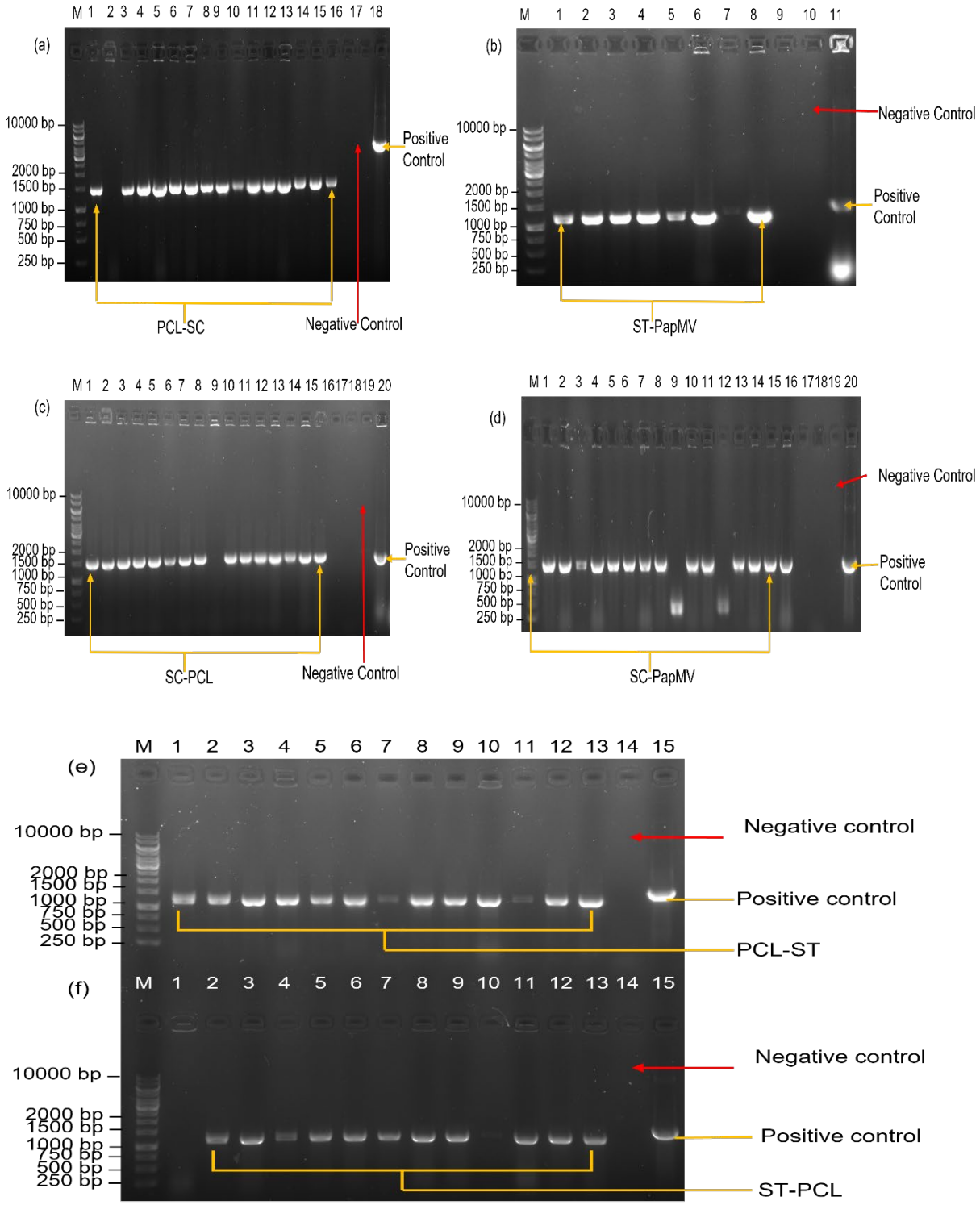

Figure 4. 4. 1% Agarose gel electrophoresis of the PCR products amplified from candidate bacterial clones. The PCR reactions were performed with pEAQ-HT-F and pEAQ-HT-R primers and contained candidate recombinant clones transformed with the pEAQ-HT+PCL-SC (a), pEAQ-HT+ST-PapMV (b), pEAQ-HT+SC-PCL (c), pEAQ-HT+SC-PapMV (d), pEAQ-HT+PCL-ST (e) and pEAQ-HT+ST-PCL (f) ligation reactions.

The first lane in each gel designated ‘M’ contains the DNA molecular weight marker (GeneRuler 1kb Ladder, Thermo Fisher Scientific) and the relevant band sizes are indicated in base pairs (bp). The second last lane (red arrows) in each gel contains the contents of the negative control PCR reaction with no template DNA while the last lane of each gel contains the contents of the positive control PCR reaction, performed with different validated recombinant pEAQ-HT template DNA.

4.5 Recombinant plasmid purification and quantification

From each replica agar plate, two bacterial clones, both PCR-verified to contain recombinant plasmid, were randomly selected and inoculated into 5 mL LB broth with kanamycin, as described in section 3.3.5. The cultures grown overnight at 37°C were subsequently frozen away in 15% glycerol at -80°C for long term storage. The remaining culture was used to isolate recombinant plasmid DNA using FavorPrep™ plasmid extraction mini kit, as described in section 3.3.6. After isolation, plasmid DNA purity and concentration was determined with the Nanodrop microvolume Spectrophotometer (Table 4.2).

Table 4. 2. Recombinant plasmid concentration and purity measured using the Nanodrop spectrophotometer

Isolated plasmid DNA	**Concentrations (ng/µL) of clones**	**Absorbance ratio 260 / 280**	**Absorbance ratio 260 / 230**
pEAQ-HT-SC-PCL	Clone 3= 19.7 ng/µL Clone 16= 56.8 ng/µL	1.88 1.80	0.94 1.29
pEAQ-HT-ST-PapMV	Clone 3= 19.6 ng/µL Clone 5= 17.0 ng/ µL	2.11 1.73	2.08 0.81
pEAQ-HT-PCL-SC	Clone 1= 26.1 ng/µL Clone 12= 44. 8 ng/µL	1.97 2.50	1.58 2.32
pEAQ-HT-SC-PapMV	Clone 2= 50.0 ng/µL Clone15= 41.0 ng/µL	2.14 2.08	2.25 2.33
pEAQ-HT-PCL-ST	Clone 3= 239 ng/µL Clone 12= 219 ng/µL	2.03 2.11	2.38 2.36
pEAQ-HT-ST-PCL	Clone 3= 39 ng/µL Clone 4= 40.3 ng/µL	2.10 1.96	2.50 1.58

The concentrations of plasmid DNA measured were between 17-239 ng/µL and provided ample template for the sequencing and *Agrobacterium* transformation steps. The plasmids DNA were further assessed by measuring the absorbance ratios A260/280 where the ratios ranged from 1.73-2.50. The absorbance A260/280 ratios of about 1.8 are considered pure, while lower or higher ratios values indicate either protein contamination or nucleic acid degradation. No residual salts or any other organic compounds were present in the samples with A260/230 ratios between 2.0-2.2. However, samples which had A260/230 ratios lower than 2.0-2.2 indicated residual contamination due to poor purification, while higher values suggest spectrophotometer blanking error. Recombinant plasmids with a high concentration and high purity were selected for sequencing analysis by a commercial company (Inqaba Biotech (Ltd)), their insert sequences verified by sequencing and subsequently used for LBA4404 *Agrobacterium* transformation.

4.6 Transformation of *Agrobacterium tumefaciens* strain LBA4404

After confirmation of successful cloning and validation of all six recombinant pEAQ-HT constructs via colony PCR and plasmid sequencing, the next step entailed transforming these constructs into *Agrobacterium tumefaciens* strain LBA4404. High-purity recombinant plasmid DNA was electroporated into electrocompetent LBA4404 *Agrobacterium*, as described in 3.3.8. Following electroporation, *Agrobacterium* cells, transformed with the recombinant pEAQ-HT constructs, were recovered in SOC medium and all the medium plated on LB agar plates supplemented with the kanamycin, streptomycin and rifampicin antibiotics. These antibiotics of choice were used to recover rifampicin-resistant *Agrobacterium* strain LBA4404 carrying kanamycin-resistant plasmids and streptomycin-resistant gene within the genome of the LBA4404 bacteria.

Following a 28 °C incubation for 72 hours, all six plates showed visible single colonies indicating successful transformation of the agrobacterial cells. Individual colonies were picked and inoculated into LB broth with kanamycin, streptomycin and rifampicin antibiotics (section 3.3.8) and grown in order to freeze the recombinant agrobacterial clones away in 32% glycerol for long-term storage. This process enabled successful transformation of the recombinant plasmid into *Agrobacterium* for agroinfiltration into *N. benthamiana* DXT/FT plant leaves.

4.7 Agroinfiltration of *Nicotiana benthamiana* plants

Transient expression of the chimeric proteins and assembly of lectin-conjugated PapMV VLPs in *N. benthamiana* DXT/FT plants was facilitated through *Agrobacterium*-mediated infiltration of these plants (described in section 3.3.9). Four agrobacterial suspension combinations pEAQ-HT-SC-PapMV+pEAQ-HT-PCL-ST, pEAQ-HT-SC-PapMV+pEAQ-HT-ST-PCL, pEAQ-HT-ST-PapMV+pEAQ-HT-PCL-SC and pEAQ-HT-ST-PapMV+pEAQ-HT-SC-PCL were infiltrated into *N. benthamiana* dXT-FT plant leaves, allowing co-expression of the paired proteins required for VLP assembly and lectin-VLP conjugation. Agrobacterial suspensions containing pEAQ-HT-ST-PapMV and pEAQ-HT-SC-PapMV were infiltrated individually into the *N. benthamiana* dXT- FT plant leaves to assess VLP self-assembly and provide a comparative control to co-expressed constructs.

Eight days post-infiltration (dpi) visual inspection of the *N. benthamiana* plant leaves revealed distinct construct-dependent phenotypes. Specifically, leaves agroinfiltrated with pEAQ-HT-ST-PapMV (Fig.4.5 (A)) showed yellowish colour or chlorosis indicating stress triggered by foreign protein expression. Leaves agroinfiltrated with pEAQ-HT-SC-PapMV, however, showed a pronounced cytopathic effect distinguished by local leaf tissue degradation and slight necrosis in Fig.4.5 (B). Fusion of the SpyCatcher (SC) peptide to the PapMV CP may have caused misfolding of the chimeric protein and triggered endoplasmic reticulum stress in the plant cells.

In contrast, leaves agroinfiltrated with the pEAQ-HT-SC-PapMV+pEAQ-HT-PCL-ST combination (Fig.4.5 (C)) appeared healthy, suggesting correct protein folding and VLP assembly possibly assisted by the co-expression of the PCL lectin. Leaves agroinfiltrated with the pEAQ-HT-SC-PapMV+pEAQ-HT-ST-PCL (Fig.4.5 (D)) and pEAQ-HT-ST-PapMV+pEAQ-HT-PCL-SC (Fig.4.5 (E)) combinations demonstrated noticeable yellowish leaf colour possibly due to increased target protein expression and greater protein folding and VLP assembly demands. Leaves agroinfiltrated with the pEAQ-HT-ST-PapMV+pEAQ-HT-SC-PCL combination (Fig.4.5 (F)) showed a slight change in leaf colour that may have been due to lower protein expression and VLP assembly demands. Non-infiltrated healthy *N. benthamiana* DXT/FT plant leaves in Fig.4.5 (G) served as negative control.

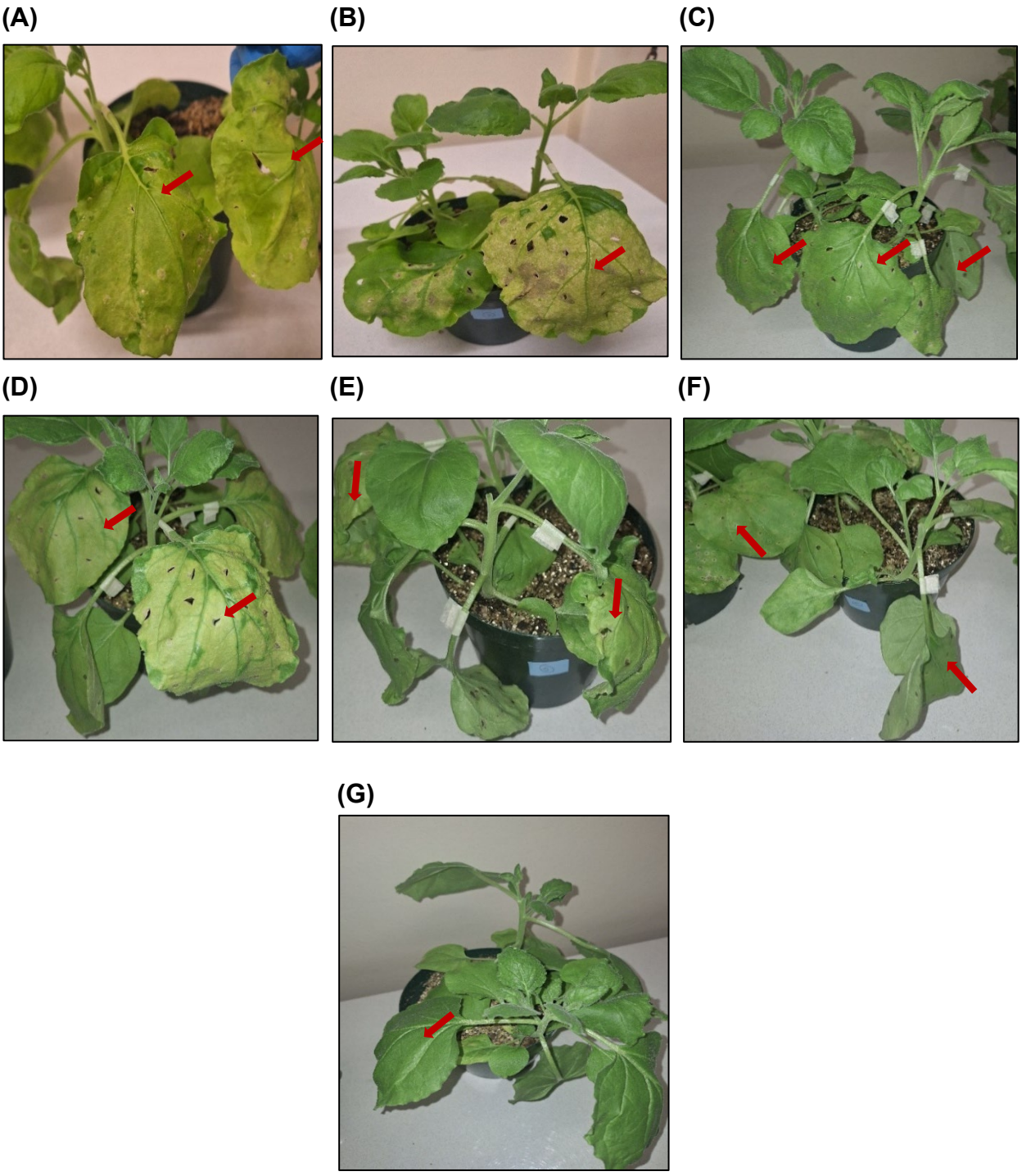

Figure 4. 5. *Nicotiana Benthamiana* plant leaves agroinfiltrated with LBA4404 agrobacterial suspensions containing pEAQ-HT-ST-PapMV (A); pEAQ-HT-SC-PapMV (B); pEAQ-HT-SC-PapMV +pEAQ-HT-PCL-ST (C); pEAQ-HT-SC-PapMV +pEAQ-HT-ST-PCL (D); pEAQ-HT-ST-PapMV+pEAQ-HT-PCL-SC (E) and pEAQ-HT-ST-PapMV+pEAQ-HT-SC-PCL (F). Non-infiltrated *N. benthamiana* DXT/FT leaves are depicted in (G).

4.8 Assessment of VLP assembly via density gradient ultracentrifugation

Agroinfiltrated leaves were harvested and the expressed proteins extracted as described in 3.3.10. Clarified plant extracts were loaded onto discontinuous iodixanol gradients (Fig. 4.6 (a)) and ultracentrifuged to concentrate the assembled VLPs within a specific region of the gradient. After ultracentrifugation, a green band was observed in the 20% to 30% region of the iodixanol gradient (Fig. 4.6 (b-c)). Previous studies have shown that PapMV VLPs are located in the vicinity of this green band (Dr. Rutkowska, personal communication). Fractions were collected from the bottom of the ultracentrifuged gradients and protein content of gradient fractions assessed using SDS polyacrylamide electrophoresis and Western blot analysis.

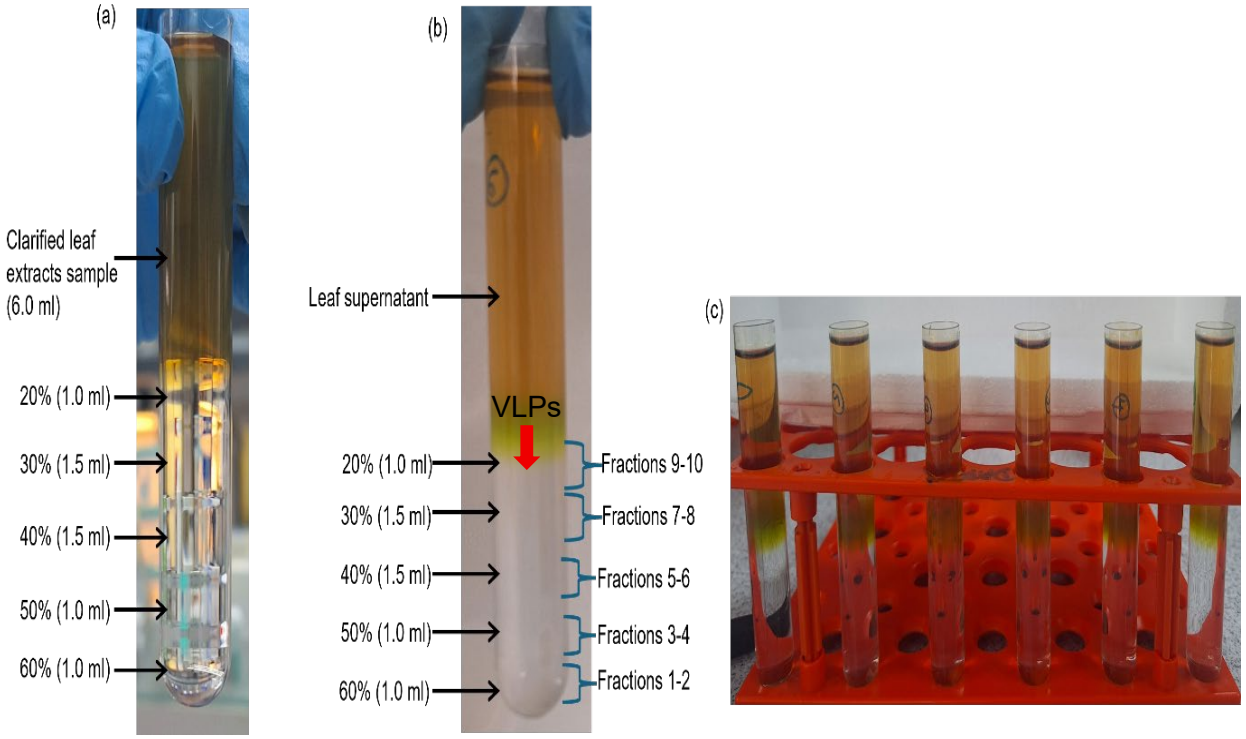

Figure 4. 6. Iodixanol density gradient centrifugation of the crude lysates extracted from agroinfiltrated *N. benthamiana* plants 8 d.p.i. Six millilitres of plant lysate was loaded onto 60% -20% iodixanol density gradient (a). After centrifugation at 32 000 x g for 2 hours, fractions 1-10 were collected from the bottom of the gradients (b). Iodixanol density gradients after ultracentrifugation containing the lysates of plants infiltrated with the single and combination agrobacterial suspensions.

4.9 Detection of plant-expressed protein in density gradient fractions

4.9.1 SDS-PAGE and Western blotting

The protein content of fractions 9 and 10 of each iodixanol density gradient was assessed by SDS-PAGE analysis (Fig. 4.7 (a)) and Western blotting (Fig. 4.7 (b)), as described in sections 3.3.12 and 3.3.13, respectively. These 20-35% fractions were associated with the green bands observed in the gradients (Fig. 4.6 (c)). Protein bands of 27kDa (ST-PapMV), 37.6kDa (SC-PapMV), 65.3kDa (SC-PapMV-PCL-ST), 64.9kDa (ST-PapMV-PCL-SC), 65.2kDa (SC-PapMV-ST-PCL), and 65kDa (ST-PapMV-SC-PCL) were expected to be visualised in lanes 1-2, 3-4, 5-6, 7-8, 9-10 and 11-12, respectively (Fig. 4.7 (a)). Although faint protein bands of some of these expected sizes were visualised and are indicated with arrows, it was decided to perform a Western blot with an α-His-HRP monoclonal antibody in order to confirm the presence of the PapMV CP protein with a 6x Histidine tag on its C-terminal.

The anti-His antibody bound to protein bands in the 20%-35% iodixanol fractions (Fig. 4.7 (b)) in lanes 2 (20 kDA), 4 (45 kDA), 8 (44 kDA), 11 (19 kDA) and 12 (19 kDA). These bands were not visible in lanes 1, 3, 5, 6, 7, 9 and 10 (Fig. 4.7 (b)). The presence of His-tagged PapMV protein in these density gradient fractions confirmed the presence of assembled PapMV VLPs in these gradient fractions. Although visibly smaller than the expected size of 27kDa, the approximately 20kDa ST-PapMV protein in lane 2 of Fig. 4.7 (b) indicated that the chimeric ST-PapMV protein was able to fold correctly and assemble into VLPs found in 20% iodixanol fraction 10. The smaller than expected protein may have been as a result of whole or partial cleavage/truncation of the ST element (12kDa) from the PapMV CP protein. The same sized protein was also observed in lanes 11 and 12 (Fig. 4.7 (b)) containing the co-expressed ST-PapMV and SC-PCL proteins indicating the assembly of ST-PapMV VLPs in this plant lysate. The lack of a 65kDa protein band in these lanes indicates that no conjugation occurred between the assembled ST-PapMV VLPs and the co-expressed SC-PCL protein. However, a protein band of approximately 44kDa was observed in lane 8 (Fig. 4.7 (b)) containing the co-expressed ST-PapMV and PCL-SC proteins indicating the assembly of conjugated ST-PapMV VLPs in this plant lysate. This highlights the importance of where the SC element is located on the PCL lectin. When on the N-terminal, the SC-PCL protein does not enable conjugation to ST-PapMV VLPs (Fig. 4 .7 (b), lanes 11-12). However, a 44 kDa protein band is observed in lane 8 of Fig. 4.7 (b) indicating that when the SC element is on the C-terminal of the PCL

lectin, this allows for assembly of conjugated ST-PapMV VLPs. The conjugated ST-PapMV-PCL-SC protein is not the expected size of 64.9kDa and this could be explained by possible cleavage or truncation of the conjugated protein.

The approximately 45kDa SC-PapMV protein observed in lane 4 of Fig. 4.7 (b) was larger than the 37.6kDa protein expected. This may indicate the presence of additional post-translational modifications that may increase the molecular size. Although larger than expected, the chimeric SC-PapMV protein was able to fold correctly and assemble into VLPs found in 20% iodixanol fraction 10. However, when co-expressed with either PCL-ST or ST-PCL, there are no His-tag specific protein bands in lanes 5-6 or 9-10 (Fig 4.7 (b)), respectively. This indicates that any conjugation between these constructs interferes with PapMV VLP assembly. These results show that only one out of the four protein combinations tested, ST-PapMV-PCL-SC, was able to assemble into conjugated PCL-PapMV VLP. This highlights the importance of designing and experimentally testing different construct designs and combinations.

(a) SDS-Page gel of fractions

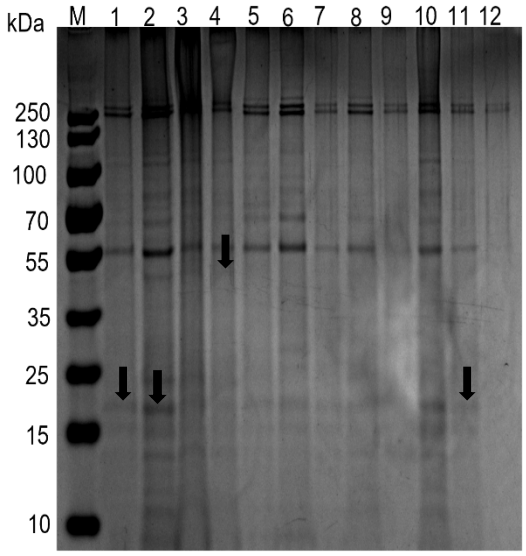

(b) Western Blot of fractions

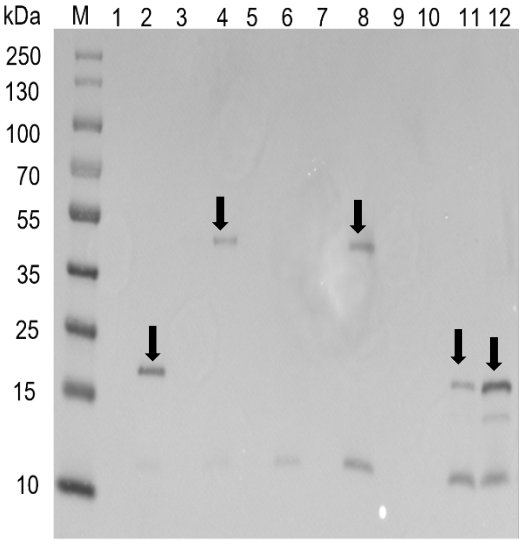

Figure 4. 7. 12% SDS-PAGE gel and western blot analyses of protein content of the density gradient fractions. (a) Coomassie stained SDS-PAGE gel containing fractions 9 and 10 of density gradients with lysates ST-PapMV, SC-PapMV, SC-PapMV+PCL-ST, ST-PapMV+PCL-SC, SC-PapMV+ST-PCL, and ST-PapMV+SC-PCL in lanes 1-2, 3-4, 5-6, 7-8, 9-10 and 11-12, respectively. (b) Western blot analysis of the same fractions, probed with αHis-HRP monoclonal antibody (Sigma, Aldrich). The first lane in each gel

designated ‘M’ contains the PageRuler Prestained Protein ladder (Thermo Fisher Scientific) and the relevant band sizes are indicated in base pairs (kDa).

4.9.2 Transmission electron microscopy (TEM)

To investigate the structural integrity of the particles detected in the density gradient fractions via Western blotting (Fig. 4.7 (b)), these selected fractions were absorbed onto coated copper grids, stained with uranyl acetate (described in section 3.3.15) and visualized under the transmission electron microscope (TEM) (Figure 4.8 (A)-(F)). Wild type PapMV CP is reported to assemble into tubules between 13-15 nm in diameter and 500-530 nm in length (Rioux, Majeau *et al*., 2012). Recombinant PapMV proteins assemble into shorter VLPs (60-15 nm length) but retain their 15 nm diameter (Yang *et al*., 2012). Transmission electron microscopy (TEM) analysis here demonstrated slight variation in tubule morphology and yield amongst the chimeric PapMV CP VLPs. Tubule lengths and diameters across multiple TEM images of distinct constructs were measured using ImageJ software, and the average mean calculated.

Chimeric ST-PapMV formed elongated rod-shaped tubules of 717-767 nm length and 16.94 nm in diameter (Fig. 4.8 (A)), while chimeric SC-PapMV assembled into shorter rods measuring 575 nm length and 16.09 nm diameter (Fig. 4 .8 (B)). VLPs with slightly larger diameters were observed in the lysates containing the SC-PapMV and PCL-ST proteins, 714.04 nm in length and 18.33 nm diameter (Fig. 4.8 (C)), SC-PapMV and ST-PCL proteins, 814.01 nm in length and 18.97 nm diameter (Fig. 4.8 (D)), ST-PapMV and PCL-SC proteins, 523.47 nm in length and 23.43 nm diameter (Fig. 4.8 (E)). The ST-PapMV and SC-PCL proteins produced the longest rod-shaped tubule 1.14 µm in length and 19.22 nm in diameter (Fig. 4.8 (F)). Constructs SC-PapMV with PCL-ST protein yield was too low to be detected in SDS-PAGE gel (Fig. 4.7 (a)) and Western blot (Fig. 4.7 (b)) but a few VLPs were visible in TEM. Moreover, TEM images showed that ST-PapMV with SC-PCL protein gives a larger tubule size than ST-PapMV, indicating that SC-PCL fusion influenced VLPs morphology. From these results, it is clear that the PapMV CP protein with a SpyCatcher of SpyTag element linked to its N-terminal is able to fold correctly and assemble into filamentous VLPs very similar to wild type PapMV VLPs in size and morphology. Although, not visible on an SDS-PAGE gel, the increased diameter of the VLPs observed when the chimeric ST-PapMV VLPs are expressed with the chimeric

PCL-SC protein may be as a result of multiple copies of this protein conjugating to the exterior surface of the PapMV VLP.

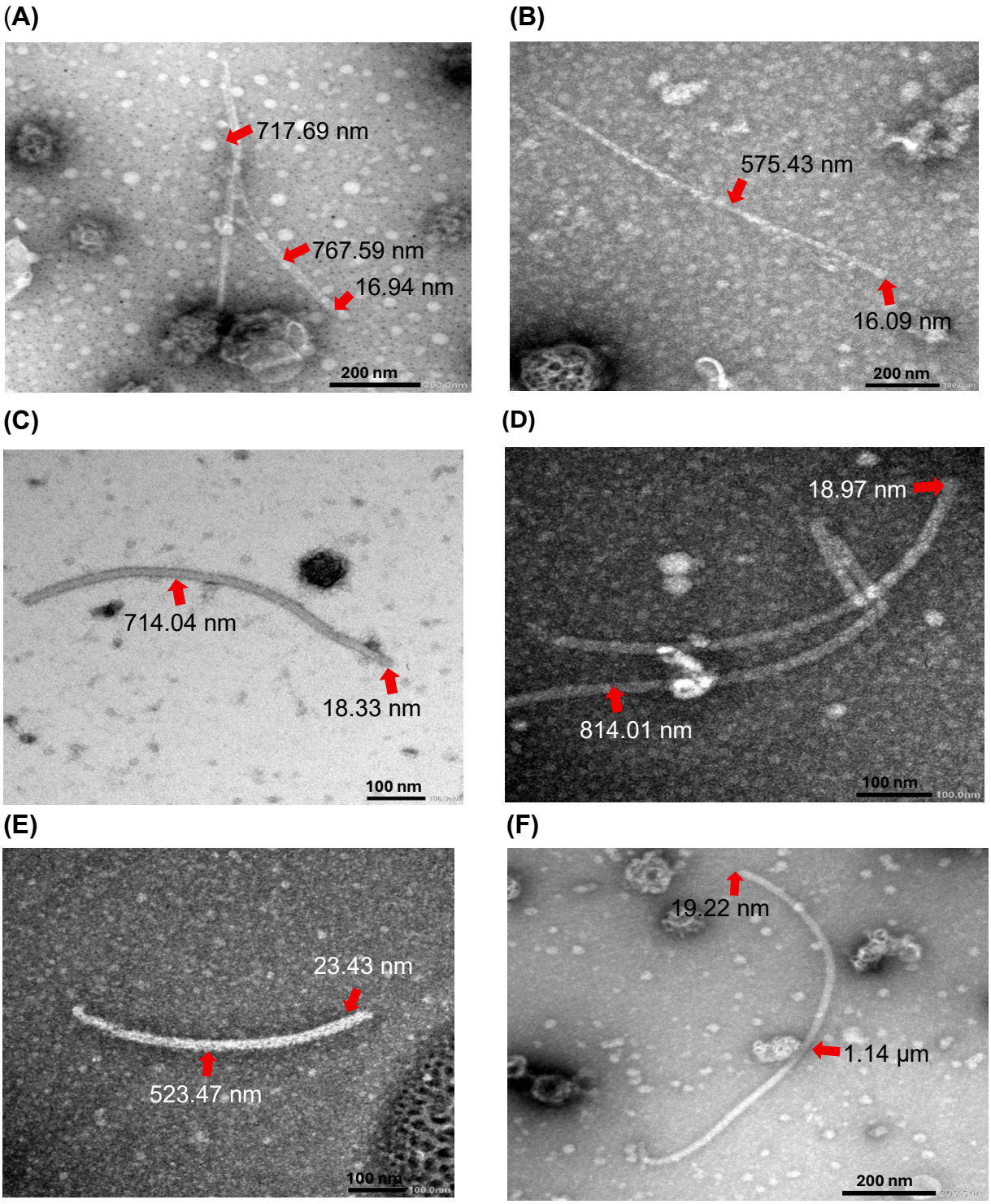

Figure 4. 8. Transmission electron microscopy (TEM) of iodixanol gradient fractions containing (a) ST-PapMV, (b) SC-PapMV, (c) SC-PapMV-PCL-ST, (d) SC-PapMV-ST-PCL, (e) ST-PapMV-PCL-SC and (f) ST-PapMV-SC-PCL proteins. Fractions 9 of each

gradient were adsorbed onto coated copper grids and stained with uranyl acetate stain. The length and diameter (nm) of the PapMV and lectin-conjugated PapMV VLPs are indicated with red arrows. Scale bar in 200nm and 100nm.

4.10 His-tag purification of chimeric and lectin-conjugated PapMV VLPs

4.10.1 MagResyn NTA purification

His-tag purification is a well-established method for purifying proteins that utilises immobilized metal affinity chromatography (IMAC) with resins (Spriestersbach *et al*., 2015). The PapMV core protein (CP) in this study has a 6 Histidine residue tag inserted at its C-terminal to facilitate easy purification of PapMV VLPs assembled from the CP protein. Here we used MagResyn® NTA bead-mediated purification to bind and purify the polyhistidine-tagged PapMV VLP proteins. This method was used to enhance protein yield and purity to confirm the results obtained in 4.9.1 and accomplish objective two of this study. Purification was done according to the manufacturer's instructions and by following the protocol described in section 3.3.11. After the last three washes to remove unbound proteins, the chimeric VLPs were eluted with elution buffer. The purified proteins were further analysed on SDS-Page gel and Western blot in the subsequent sub-section 4.10.2.

4.10.2 SDS-PAGE gel and Western blot

The presence of the PapMV capsid proteins within the MagReSyn® NTA eluant was assessed by SDS-PAGE analysis (Fig. 4.9 (A)) and Western blotting (Fig. 4.9 (B)). Identity of the chimeric and lectin-conjugated PapMV proteins was confirmed by Western blot detection with an α-His monoclonal antibody, as described in 3.3.13. The results obtained were similar to those described in section 4.8.1. However, due to the MagReSyn® NTA purification strategy aimed to specifically purify Histidine-tagged proteins, the purity and yield of the chimeric PapMV proteins was much higher than in the density gradient fractions. This enabled us to visualise the PapMV proteins on the SDS-PAGE gel (Fig. 4 .9 (A)). A protein band, approximately 20kDa in size, was observed in lane 1 of Fig. 4 .9 (A) and was confirmed to contain a His-tag via Western blotting (Fig. 4 .9 (B); lane 1). This confirmed the identity of the ST-PapMV protein in lane 1, even though it was smaller than the expected size of 27kDa, due to possible protein cleavage/truncation. The 45kDa band visualised in lane 2 of the PAGE gel (Fig. 4 .9 (A)) was also confirmed to contain a His-tag via Western blotting (Fig. 4 .9 (B)), although the

protein was much larger than the expected 37kDa molecular weight of the chimeric SC-PapMV protein. This may be due to unexpected post-translational modifications. As previously when the SC-PapMV protein was co-expressed with the PCL-ST in plant cell (lanes 5-6 of Fig. 4.7 (b)), no SC-PapMV CP band was visualised in lane 3 either on the SDS-Page gel (Fig. 4 .9 (A)) or on the Western blot membrane (Fig. 4 .9 (B)). This indicated that the PCL-ST protein interferes with SC-PapMV protein folding and VLP assembly and may instead result in protein aggregation. However, when the SC-PapMV protein is co-expressed with the ST-PCL, a faint protein band of approximately 45kDa was detected via the anti-His antibody in lane 4 (Fig. 4 .9 (B)). This band was not observed previously on our Western blot result (Fig. 4.7 (b), lanes 9-10) likely due to its suboptimal expression. This indicates that co-expression of SC-PapMV with ST-PCL still enables PapMV VLP assembly although it is less optimal. Also, no PapMV VLP conjugation with PCL occurs as the size of detected band in lane 4 is approximately the same size of the 45kDa SC-PapMV protein band in lane 2. These results indicate that the location of the ST element, either on the N-terminal or the C-terminal of the PCL, plays a significant role in the ability of the SC-PapMV protein to fold correctly and assemble into VLPs.

The presence of a 20kDa protein band, and absence of a 65kDa protein band in lane 6 of the Western blot (Fig. 4.9 (B)), confirmed previous results indicating VLP assembly of the ST-PapMV protein but no conjugation of the VLP to the co-expressed SC-PCL protein (Fig. 4.7 (b), lanes 11-12). However, when the ST-PapMV protein was co-expressed with the PCL protein containing the SC on its C-terminal (PCL-SC), multiple high molecular weight protein bands were observed on the Western blot membrane (Fig. 4 .9 (B), lane 5). One of the faint bands is 65kDa in size, the expected size of the ST-PapMV-PCL-SC conjugate with the higher bands most likely being multimers of this protein and the lower bands being truncated proteins. There is also a sizable 20kDa protein band in lane 5 consisting most likely of the ST-PapMV protein that was not conjugated. None of the protein bands were observed in Lane 7 of the Western blot where a sample of non-infiltrated plant leaf lysate was loaded, indicating that there was no non-specific binding of the α-His monoclonal antibody to the plant host proteins. Next, we wanted to determine whether the Chimeric PapMV proteins that were purified by means of the MagResyn® NTA beads assembled into VLPs and TEM analysis was conducted.

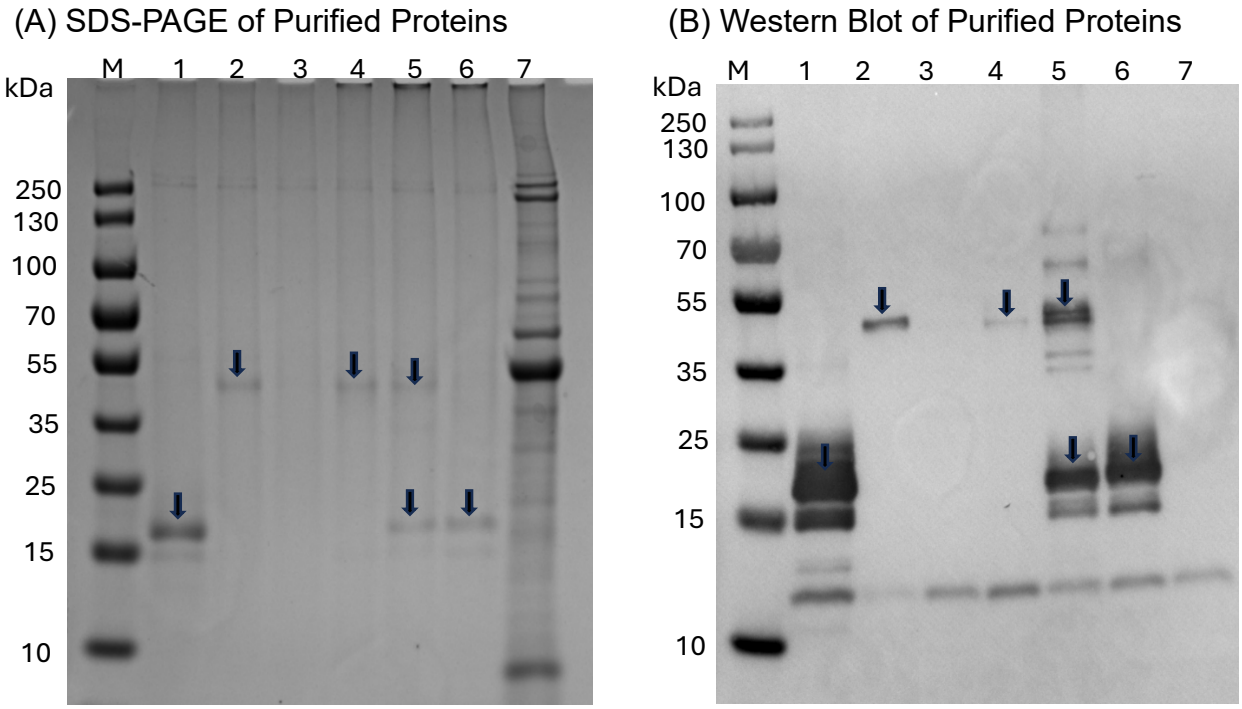

Figure 4. 9. Chimeric PapMV and lectin-conjugated PapMV proteins purified with MagReSyn® NTA beads and analysed with SDS-PAGE (A) and Western Blotting (B). Eluants containing proteins ST-PapMV (27kDa); SC-PapMV (37.6kDa); SC-PapMV-PCL-ST (65.3kDa); SC-PapMV-ST-PCL (65.2kDa); ST-PapMV-PCL-SC (64.9kDa) and ST-PapMV-SC-PCL (65kDa) were loaded in lanes 1-6, respectively. Lane 7 contained uninfiltrated plant cell lysate as a negative control. The first lane in each gel designated 'M' contains the PageRuler Prestained Protein ladder (Thermo Fisher Scientific) and the relevant band sizes are indicated in base pairs (kDa). The α-His-HRP monoclonal (Sigma-Aldrich) was used to detect the chimeric and lectin-conjugated PapMV proteins on the Western blot membrane. The black arrows indicate the position of the chimeric and lectin-conjugated PapMV proteins.

4.10.3 TEM of the MagResyn-purified VLPs

To visualize the His-tag purified particles using MagResyn® NTA beads, samples of the elutions were adsorbed onto carbon grids, stained with uranyl acetate and viewed under the Transmission electron microscope. Tubular structures resembling PapMV VLPs were observed in all the construct samples, although in limited numbers (Fig. 4.10 (A)-(F)). The tubules observed were short in length, ranging between 166 nm and 632.98 nm, and in diameter, from 14.19 nm to 19.87 nm. This indicates that PapMV VLPs retain their tubular structure when purified using the MagResyn® NTA beads. The purified proteins of

construct samples (A),(B), (C), (D) and (F) in Fig. 4.10 showed a slight reduction in tubule length and diameter compared to the iodixanol gradient fractions in Fig. 4.8 (A-F). However, construct (E) in Fig. 4.10 showed a substantial decrease in tubule diameter, reducing from approximately 23.43 nm in iodixanol gradient fractions (Fig. 4.8 (E)) to 15.55 nm after MagResyn bead purification, while also appearing shorter in length. Although, the SDS-PAGE gel and immunotblot results indicated low expression of the and SC-PapMV-ST-PCL (Fig. 4.9 a and b Lane 4) proteins, a few tubular structures resembling morphology of PapMV tubules were observed under the microscope.

(A)

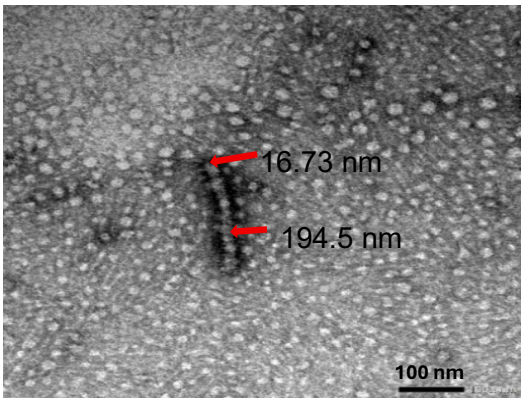

(B)

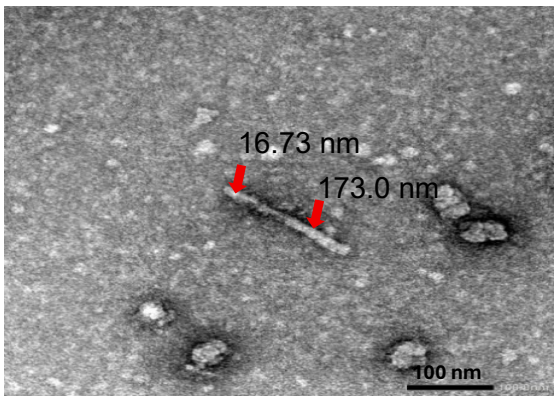

(C)

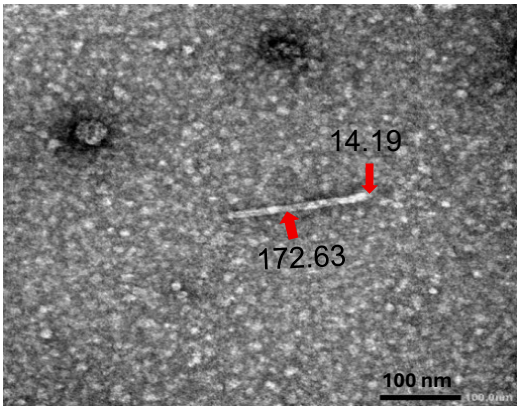

(D)

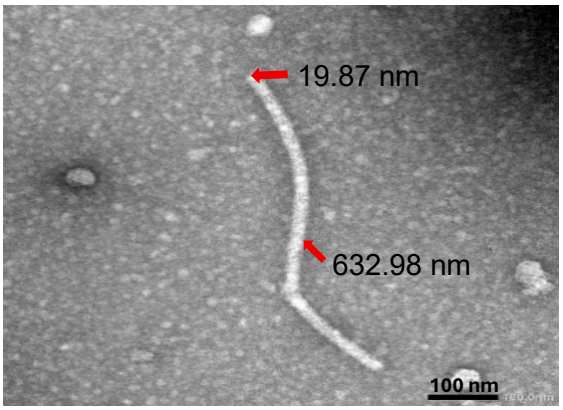

(E)

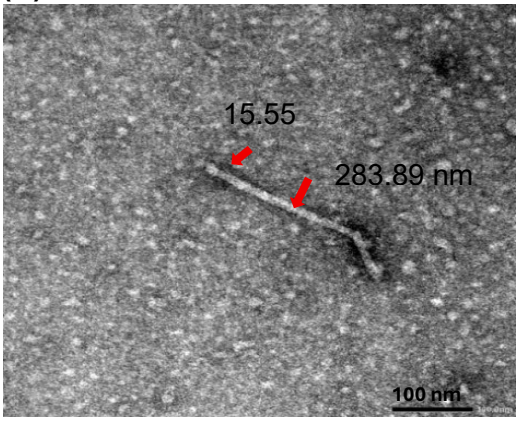

(F)

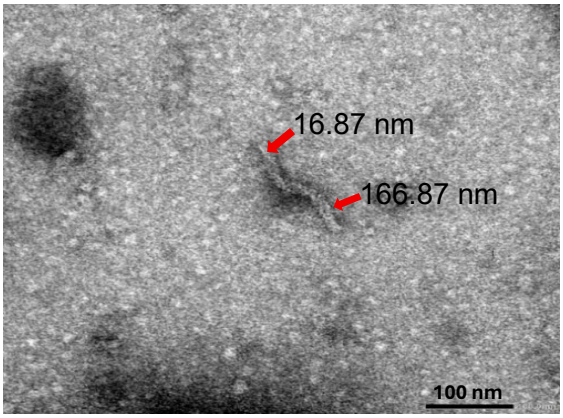

Figure 4. 10. Transmission electron microscope (TEM) images of MagReSyn® NTA purified chimeric and lectin-conjugated PapMV VLPs. (A) ST-PapMV, (B) SC-PapMV, (C) SC-PapMV-PCL-ST, (D) SC-PapMV-ST-PCL, (E) ST-PapMV-PCL-SC and (F) ST-PapMV-SC-PCL VLPs. Particles were visualized with a JEM-2100 transmission electron microscope (JEOL). The red arrows indicate diameter and length of the VLPs in nm. Scale bar is 100nm.

4.11. Quantification of the purified chimeric and lectin-conjugated PapMV VLPs

4.11.1 BCA quantification

The concentrations of density gradient purified proteins produced from single and co-expressed agroinfiltrated constructs were determined using BCA Assay Kit (Thermo Fisher Scientific). This quantification was mandatory to enable accurate normalization of protein for cell culture experiments. Two batches of purified VLPS were quantified with BCA assay kit. Bovine serum albumin standard curves were generated and these standard curves demonstrated a linear relationship between absorbance and protein concentrations, allowing interpolation of purified VLP concentrations. Absorbance was measured at 562 nm wavelength with a spectrophotometer. The plotted standard curves in Fig. 4.11 and 4.12 were used to calculate the protein quantities of the samples by using their regression equations. Different purified protein concentrations were yielded, approximating 83.1 µg/mL, 66.1 µg/mL, 36.8 µg/mL, 97.4 µg/mL, 70.9 µg/mL and 65.5 µg/mL (first batch in Table 4.3) and 74 µg/mL, 47 µg/mL, 82 µg/mL, 87 µg/mL, 61 µg/mL and 79 µg/mL (second batch in Table 4.4) between all expressed and co-expressed constructs, respectively. This protein yield concentrations post-purification suggests a moderate to low yield according to literature (Jung *et al*., 2025; Prado *et al*., 2019).

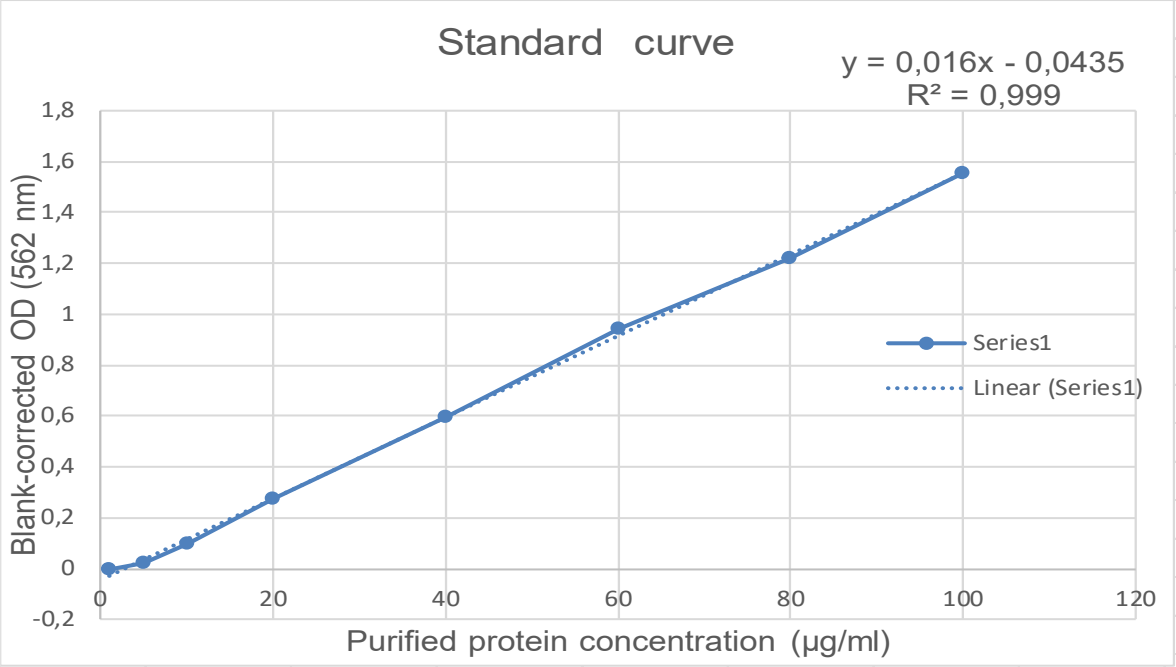

Figure 4. 11. Standard curve for bicinchoninic acid (BCA) assay generated using Bovine serum (BSA) standard of known concentrations (100 µg/mL, 80 µg/mL, 60 µg/mL, 40 µg/mL 20 µg/mL,10 µg/mL, 5 µg/mL and 1 µg/mL). Absorbance was measured at 562 nm optical density and linear regression analysed in Microsoft Excel to generate an equation Y= 0.016× + 0.0435, R^2= 0.999 used for protein concentration calculations. Y-axis indicates Blank-corrected OD (562 nm) and X-axis purified protein concentrations calculations.

Table 4. 3. Protein concentrations of purified PapMV VLPs determined by BCA assay kit – first batch

Types of purified proteins	Sample readings	Sample diluted (µg/mL)	Sample actual concentrations (µg/mL)	Diluted 1:1 with glycerol (µg/mL)
ST-PapMV	0.0895	8.3	166.3	83.1
SC-PapMV	0.062333	6.6	132.3	66.1
SC-PapMV+PCL-ST	0.015333	3.7	73.5	36.8
SC-PapMV+ST-PCL	0.112333	9.7	194.8	97.4
SC-PapMV+PCL-SC	0.07	7.1	141.8	70.9
SC+PapMV+SC-PCL	0.061333	6.6	131.0	65.5

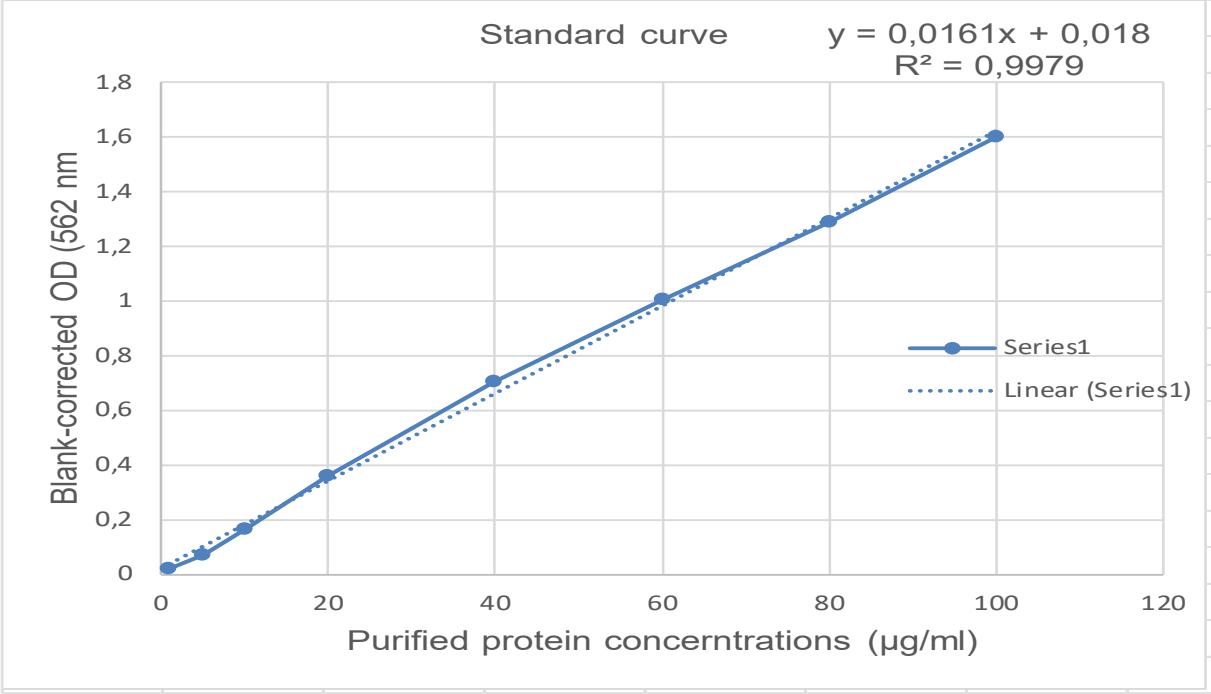

Figure 4. 12. Standard curve for the bicinchoninic acid (BCA) assay generated using Bovine serum albumin (BSA) standards (100 µg/mL, 80 µg/mL, 60 µg/mL, 40 µg/mL, 20 µg/mL, 10 µg/mL, 5 µg/mL and 1 µg/mL). Absorbance was measured at 562 nm optical density and linear regression analysed in Microsoft Excel to generate the equation Y= 0. 0161 X + 0.018, R^2 = 0.09979 used for purified protein concentration calculations. Y-axis indicates Blank-corrected OD (562 nm) and X-axis purified protein concentrations (µg/ml).

Table 4. 4. Protein concentrations of purified PapMV VLPs determined by BCA assay kit–second batch

Types of purified proteins	Sample readings	Sample Diluted (µg/mL)	Sample actual concentrations (µg/mL)	Diluted 1:1 with glycerol (µg/mL)
ST-PapMV	0.13667	7.37	147	74
SC-PapMV	0.09367	5	94	47
SC-PapMV+PCL-ST	0.014967	8	164	82
SC-PapMV+ST-PCL	0.15867	9	175	87
ST-PapMV+PCL-SC	0.117	6	123	61
ST-PapMV+SC-PCL	0.135	7	145	79

4.11.2 Protein quantification via Gel densitometry

The samples of third batch quantified via BCA quantification contained VLPs partially purified through density gradients. Thus there were contaminating plant proteins in the samples that did not give an accurate determination of the VLP quantity. An alternative protein quantification method was thus required and gel densitometry was employed. All purified protein samples were resolved by SDS-PAGE gel in addition to BSA standards of known concentrations from 100 µg/mL, 250 µg/mL, 500 µg/mL, 750 µg/mL, 1000 µg/mL, 1500 µg/mL and 2000 µg/mL. Following Coomassie brilliant blue staining and destaining of the gels, protein bands of the expected molecular weight were visualized using the ChemiDoc MP imager reader (Bio-Rad). By comparing the intensity of the PapMV proteins bands in lanes 1-6 of Figs 4.13 (A) and 4.13 (B) to the intensity of the BSA standard protein bands in the first 7 lanes of the respective gel, it was possible to estimate the protein quantity of the purified proteins using densitometry application from the ChemiDoc MP system. The protein yield harvested from the leaf mass could then also be quantified as shown in Table 4.5. Gel densitometry allowed construct-specific quantification confirming presence of purified proteins each with an approximately concentration of 0.253 µg/mL which was used for the final cell culture experiment in the study.

(A) Purified protein VLPs quantity -SDS-PAGE gel of first 3 constructs (Bio-Rad)

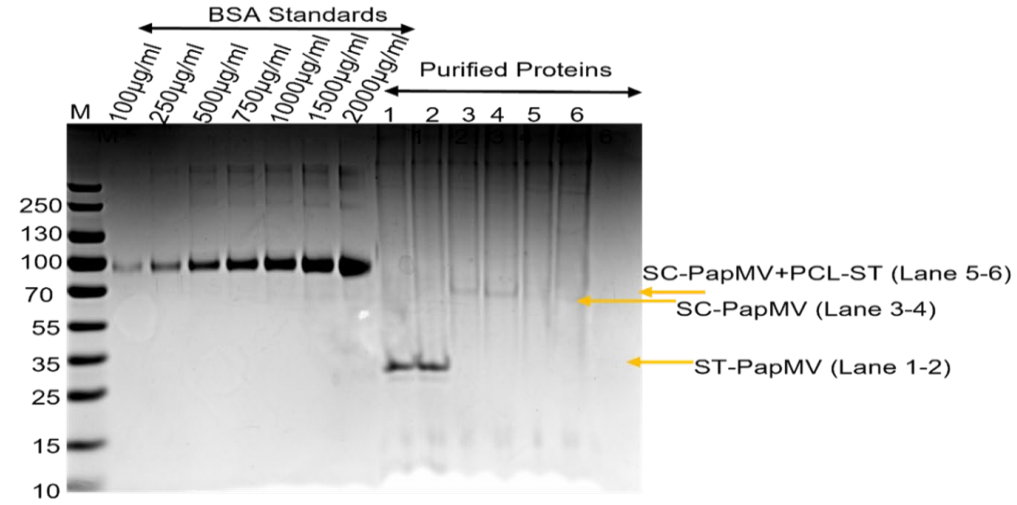

(B) Purified protein VLPs quantity – SDS-Page gel of second 3 constructs

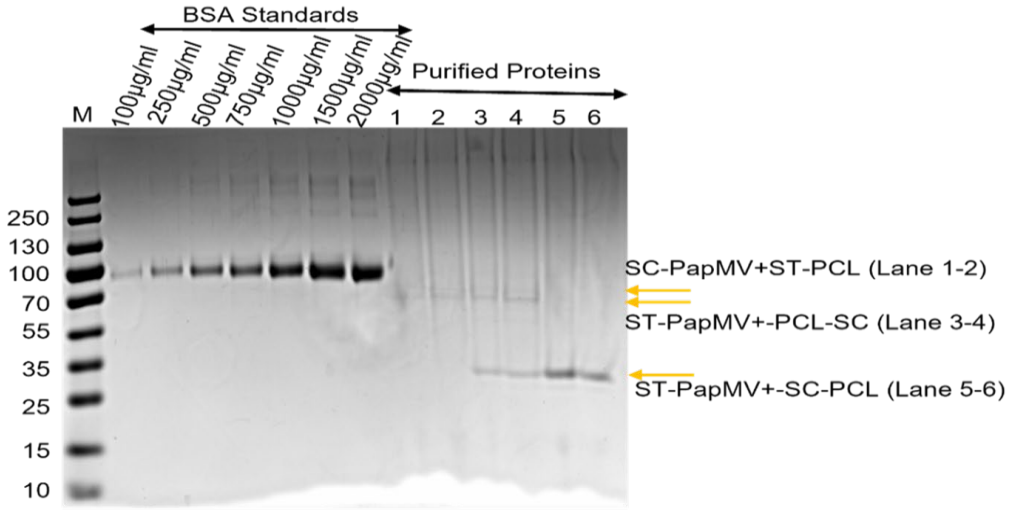

Figure 4. 13. SDS-PAGE gel densitometry analysis of purified PapMV VLP proteins resolved alongside the BSA standards. BSA standards were loaded at volumes of 1µL, 2.5µL, 5µL, 7.5µL, 10µL,15µL and 20µL from second to seventh lanes of the gels (A and B) and respectively. The first Lane of the gels marked "M" indicate molecular weight marker (PageRuler, Prestained Protein Ladder, Thermo Fisher Scientific). (A) Lanes 1-6 indicate purified protein band sizes of ST-PapMV (27kDA Lanes 1-2), SC-PapMV (65kDA Lane 3-4) not as expected, SC-PapMV+PCL-SC faint or no band but expected was (65.3 kDa lanes 5-6). (B) Lanes 1-6 indicate purified protein band sizes of SC-PapMV+ST-PCL (65.2kDa Lane 1-2), ST-PapMV+PCL-SC (64.9kDa) and ST-PapMV+SC-PCL (27kDa, Lanes 5-6) expected being 65kDa. Band intensities of BSA standards were compared to purified protein to estimate protein concentrations (µg/mL).

Table 4. 5. A total purified VLP protein in mg recovered from g of *N. benthamiana* plant leaf tissue and equated to mg/kg leaf biomass.

Types of purified protein	Leaf mass harvested (g)	Total purified protein harvested (mg)	Protein yield (mg/kg leaf biomass)
ST-PapMV	7.9	± 0.066	± 8.37
SC-PapMV	6.2	± 0.042	± 6.82
SC-PapMV+PCL-ST	11.9	± 0.074	± 6.20
SC-PapMV+ST-PCL	9.7	± 0.079	± 8.12
ST-PapMV+PCL-SC	10.4	± 0.055	± 5.32
ST-PapMV+SC-PCL	6.8	± 0.065	± 9.60

4.12. *In vitro* binding of lectin-conjugated PapMV VLPs to breast (HER2+) cancer cells

In order to investigate the ability of the lectin-conjugated PapMV VLPs to bind to target cancer cells, *in vitro* binding experiments were conducted with HER2+ cancer cells to assess VLP binding to carbohydrate moieties on the surface of these cancer cells. Breast cancer cells (AU565) were seeded according to protocols previously published (Gross *et al*., 2023). Binding of the chimeric PapMV VLPs and lectin (PCL)-conjugated PapMV VLPs to target cells were assessed by means of an α-His fluorescent antibody-conjugate that bound to the 6X His tag on the C-terminal of the PapMV core protein. Both non-conjugated PapMV VLPs, as well as PapMV VLPs conjugated to PCL lectin, were used in this experiment to determine whether the conjugated PCL lectin enabled VLP binding to the target cancer cells. The protocol followed was as described in section 3.4. Cancer cells were fixed with paraformaldehyde (PFA) to preserve their morphology and immobilize surface structures.

Following incubation of the conjugated and unconjugated VLPs with the cancer cells, wash steps were performed to remove any unbound VLPs before an anti-His antibody, conjugated to a fluorophore, was added to the wells as shown in Table 3.4. Following a second round of wash steps, level of emitted fluorescence was used as a measure of the degree of PapMV VLP binding to the target cancer cells. Fluorescence readings from the wells of the 24-well plate were measured using a Hidex plate reader at an emission

wavelength of 535 nm (Fig. 4 .14) using GFP assay settings. Fluorescence emitted by the Alexa Fluor 488 fluorophore, bound to the anti-His antibody, was visualised using the Cytation™3 cell imaging multi-mode reader (Biotex) (Fig. 4.15). Each protein was tested in triplicate at a concentration of 0.253 µg/mL in a final volume of 200 µL. This VLP protein concentration amount of 0.2 µg per 1×10^5 cells was appropriate amount according to literature (Mùller *et al*., 1995; Volpers *et al*., 1995) .

Chimeric ST-PapMV and SC-PapMV VLPs, without conjugated PCL lectin, served as controls to assess if binding observed was indeed due to the PCL moiety and not due to non-specific VLP interaction with the cancer cells. The fluorescence readings emitted from the wells containing the PapMV VLPs, with or without conjugated PCL, were very similar to the fluorescence readings emitted from the negative control wells (Fig. 4 .14), indicating no significant differences between expressed VLPs constructs and the control. All the experiments were conducted using three independent replicates (n=3) per construct under identical conditions. One-way ANOVA confirmed that $F = 0.639$ and $P = 0.718$ (*P- value > 0.05*). Therefore, no statistically significant difference was observed (*P > 0.05*) indicating that lectin conjugation did not enhance binding under the tested conditions. There was a lack of anti-His antibody binding to the 6X His tag on the C-terminal of the PapMV CP protein. This led us to conclude that the lectin-conjugated PapMV VLPs did not bind to the surface glycans on the target cancer cells and were thus not present to be detected via the anti-His antibody. Any weak fluorescence signals detected in the wells are hypothesized to be due to non-specific binding of the anti-His antibody conjugate to the cancer cells.

Fluorescence visualised in the wells using a Cytation™3 cell imaging multi-mode reader (Biotex) (Fig. 4 .15) also did not yield higher fluorescence emissions in the wells containing lectin-conjugated PapMV VLPs compared to the negative control wells. The DAPI-stained nuclei and the bright-field microscopy confirmed the presence of intact HER2+ breast cancer cells in the wells being investigated for 535 nm emission. Although we were successful in conjugating a PCL lectin to PapMV VLPs in this study, the ST-PapMV-PCL-SC VLPs were unable to bind to the target cancer cells. It is not clear whether the ST-PapMV-PCL-SC VLPs were not able to bind the target cells due to the inability of the conjugated PCL molecule to bind to the cell surface carbohydrate moieties or perhaps the VLP protein concentration with which the cells were treated (0.253 µg/mL) was too low. Although other protein binding studies have used greater protein

concentrations including 25 µg/mL (Mei *et al*., 1996) and 0.1 µg/mL (Volpers *et al*., 1995; Mùller et al., 1995), we hypothesized that 0.253 µg/mL should be adequate for our experiment. We were not able to obtain enough protein to increase the concentrations with which we treated the cancer cells due to very low plant expression levels. These results emphasize the need of optimising construct design to obtain high protein yields, stable conjugation and successful binding to the target cells.

Figure 4. 14. Fluorescence intensity (RFU) readings measured using a Hidex plate reader. Each constructs fluorescence was measured in triplicate at an emission wavelength of at 535 nm. The clustered column chart illustrates the fluorescence intensity of constructs, SC-PapMV, ST-PapMV, SC-PapMV-PCL-ST, ST-PapMV-PCL-SC, SC-PapMV-ST-PCL and ST-PapMV-SC-PCL tested in three independent replicates (n=3 each construct). Negative control wells contained cells that were incubated with or without anti-His Alexa Fluor 488 conjugated antibody. The addition of glycerol into the control wells to a final concentration of 50% was replicative (n=3) of the 50% glycerol content in the PapMV VLP treated wells.

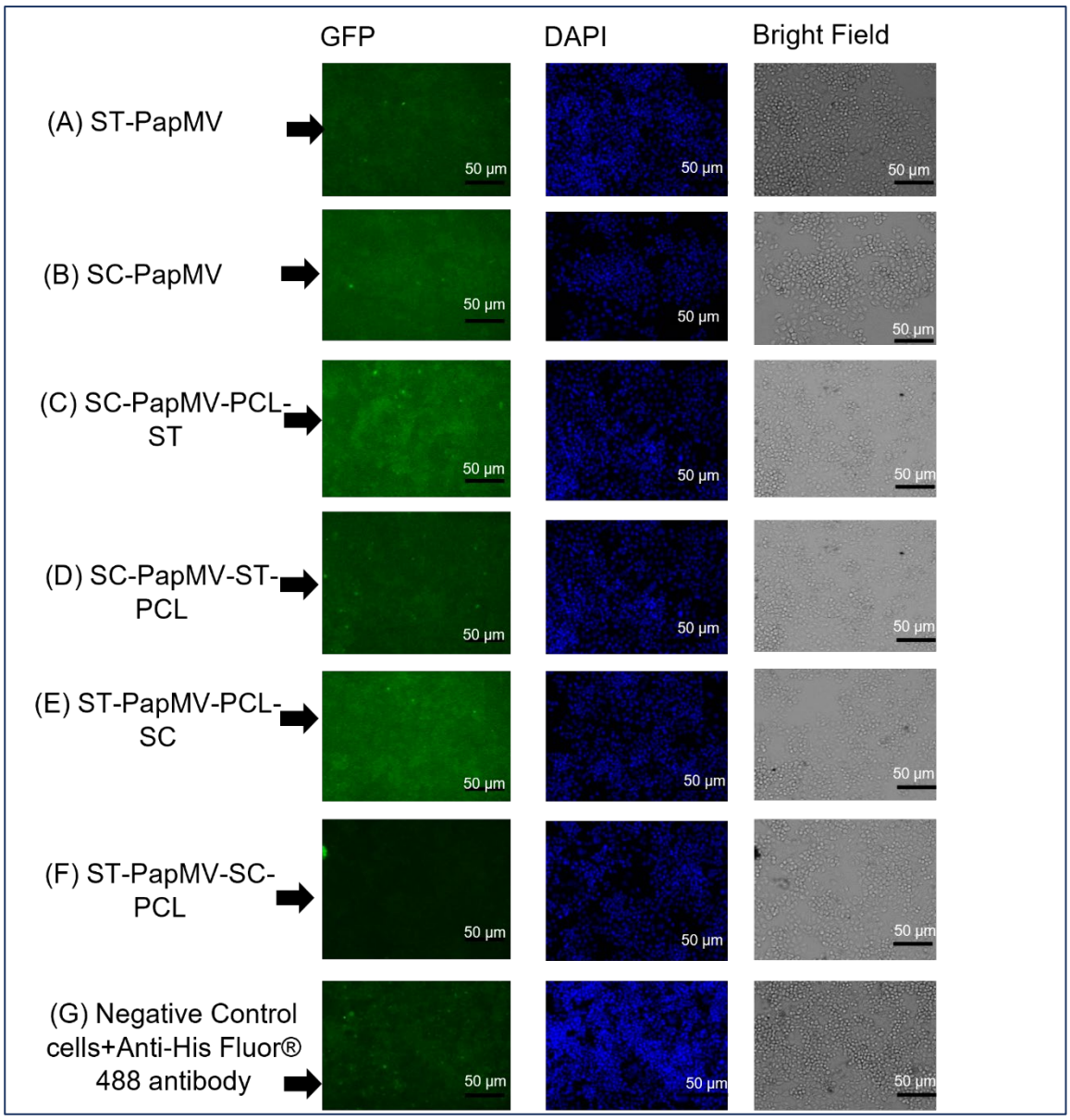

Figure 4. 15. Images of the PapMV treated and untreated HER2+ breast cancer cells obtained using the Cytation™3 cell imaging multi-mode reader (Biotex). Cells were treated with ST-PapMV (a), SC-PapMV (b), SC-PapMV-PCL-ST (c), SC-PapMV-ST-PCL (d), ST-PapMV-PCL-SC (e), ST-PapMV-SC-PCL (f). HER2+ cells untreated with PapMV VLP but incubated with Anti-His Flour® 488 antibody was the designated negative control (g). The different channels of the Cytation 3 cell imaging multi-mode reader (Biotek) that used were GFP (green fluorescence emitted by the Anti-His Flor® 488 antibody), DAPI (nucleic acid-stained blue) and Bright-field (Cell morphology). Scale bar was 50µm.

CHAPTER 5: DISCUSSION

Research in cancer biotherapy against malignant cells with plant-expressed virus-like particles is a promising strategy in the realm of oncology. This study aimed to develop and characterize engineered plant-expressed PapMV VLPs, conjugated to PCL lectins using the SpyTag/SpyCatcher technology for potential cancer-targeting applications. Critical findings are discussed in this chapter.

5.1 Design of the chimeric PapMV CP and PCL lectin proteins containing SpyTag/SpyCatcher elements

Lectins were chosen as targeting ligands because they can selectively bind to glycosylated molecules that are abnormally expressed on cancer cell membranes (Singh *et al*., 2024). Aberrant glycosylation is characterised by malignant transformation, and many tumor cells overexpress carbohydrate moieties including fucose and mannose residues (Thomas *et al*., 2021). The PCL lectins were used as targeting ligands because they have a high affinity to tumor-associated glycans which are often overexpressed on cancer cells surface (Mazalovska and Kouokam, 2020). According to Gurav *et al*. (2024), surface glycans provide a relevant biological mechanism for cancer cells identification and uptake. It was hypothesized that conjugating lectins to PapMV VLPs nanoparticles would improve the targeting ability of the VLPs with the lectins preferentially recognising and binding to cancer cells displaying these surface glycans. The SpyTag/SpyCatcher conjugation technique (Cai *et al*., 2025), was selected to covalently link PCL ligands to the external surface of the VLPs while preserving particle stability.

The SpyTag/SpyCatcher technology offers several benefits, including irreversible covalent bond formation, high conjugation efficiency, VLPs stability and lectin functional activity (Armbruster *et al*., 2025). In contrast genetic insertion can disrupt protein folding, expression yields and VLP assembly (Thrane *et al*., 2016), and chemical ligation reduces the targeting ligand and results in heterogeneous products (Giesler *et al*., 2020). With *N. benthamiana* plants DXT/FX as a host and pEAQ-HT as a transient expression vector, we wanted to evaluate the ability of the engineered PapMV CP proteins to assemble into virus-like particles (VLPs) and investigate the ability of the lectin-conjugated VLPs to target cancer cells in *in vitro* binding assays. This allowed us to address the research questions described in chapter 1: i) Is it possible to transiently express and assemble

lectin-conjugated PapMV VLPs in *Nicotiana benthamiana* plant? and ii) Are the plant-expressed, lectin-conjugated PapMV VLPs capable of binding target HER2+ breast cancer cells *in vitro*?

In order to accomplish this, Dr Daria Rutkowska designed the chimeric PapMV CP and PCL lectins constructs containing the SpyTag/SpyCatcher elements (personal communication). The covalent interaction between the SpyTag (ST) and SpyCatcher (SC) peptide elements would enable covalent ligation of the PCL lectin to the PapMV CP protein and presentation of PCL on the surface of self-assembled PapMV VLPs. Papaya mosaic virus CP is the main viral structural protein. The SpyTag or SpyCatcher sequences were placed at the N-terminal end of CP to produce ST-PapMV and SC-PapMV (Fig.4.1 (1-2)), because placing it at the C-terminus might have interfered with protein folding and VLP assembly according to previous reports (Laliberté-Gagné *et al*., 2021; Rioux, Majeau, *et al.,* 2012). The ST and SC elements were placed either at the N-terminal or the C-terminal of the PCL lectin as it was unknown which location would enable correct protein folding and solubility of the chimeric lectin protein. This was essential if the lectin was to be covalently linked to the surface of PapMV VLPs. Therefore, PCL-ST, ST-PCL, PCL-SC and SC-PCL constructs were designed.

5.2 Gene cloning into pEAQ-HT plant expression

One of the objectives in this study was to determine whether co-expression of the chimeric PapMV CP and PCL lectins in *N. benthamiana* dXT/FX plants would result in conjugation of the lectin protein to the surface of self-assembled PapMV VLPs. To achieve this, the DNA constructs encoding the chimeric PapMV CP (ST-PapMV and SC-PapMV) and chimeric PCL lectin (PCL-ST, ST-PCL, PCL-SC and SC-PCL) proteins were successfully cloned into the pEAQ expression vector. The cloning strategy employed for the study used the highly efficient transient pEAQ-HT expression vector system, previously reported to yield high levels of recombinant protein expression in plants (Peyret and Lomonossoff, 2015; Sainsbury *et al*., 2009). All DNA constructs were stably cloned and maintained in the pEAQ-HT vector. The efficiency of transformation obtained in the present study is comparable to that reported by Amrofell *et al*. (2023), suggesting that antibiotic of choice is a crucial factor for plasmid recovery of positive colonies. This stability enabled VLP assembly and functionalization.

5.3 Agroinfiltration of *Nicotiana benthamiana* plants and protein purification

Chimeric PapMV CP is known to self-assemble into rod-shaped nanoparticles (Laliberté-Gagné *et al*., 2021). Following agroinfiltration and harvesting of *N. benthamiana* DXT/FT plant leaves, crude cellular extracts were subjected to ultracentrifugation through 60-20% iodixanol density gradients. For example, de Mello *et al*. (2023) used iodixanol gradient ultracentrifugation to isolate and concentrate Zika VLPs expressed in insect cell according to their buoyant density. A study by van Zyl and Hitzeroth (2016) reported the importance of protein purification with iodixanol gradients as a highly analytical scale for plant-derived VLPs purity, which indicates effective separation of VLPs based on buoyant density. Importantly, iodixanol purification allows separation of particles based on density, making it appropriate for assessing VLPs assembly in plants (Dennis *et al*., 2018).

5.4 Detection of plant-expressed protein in density gradient fractions

In this study, protein expression levels of single-expressed ST-PapMV and SC-PapMV and co-expressed ST-PapMV+PCL-SC, ST-PapMV+SC-PCL, SC-PapMV+PCL-ST and SC-PapMV+ST-PCL proteins were assessed through SDS-PAGE gel and Western blot analyses. SDS-PAGE gel technique is known to provide high resolution, sensitivity and reproducibility in protein analysis (Nowakowski *et al*., 2014). We expected to see band sizes corresponding to those described in section 4.8.1 for the constructs ST-PapMV, SC-PapMV, SC-PapMV+PCL ST, ST-PapMV+PCL-SC, SC-PapMV+ST-PCL and ST-PapMV+SC-PCL respectively, when detecting protein expression in fractions 9 and 10 for each sample on SDS-PAGE.

5.4.1 SDS-PAGE and Western blotting

As only faint or no bands were visualized on the SDS-PAGE gels, Western blot analysis was performed with an anti-His antibody to confirm the presence of PapMV protein. An anti-His antibody was employed to detect chimeric PapMV VLPs CP, by specifically binding to the polyhistidine tag located at the C-terminal region using an established approach used for confirming expression and purification of the His-tagged proteins (Loughran *et al*., 2023). For example, Tan *et al*. (2023) used an anti-His antibody to confirm the purity of the C-terminal His-tagged turnip yellow mosaic (TYMV) VLP following a novel nickel ion affinity purification which omitted the IMAC column. Here, although the anti-His antibody bound to protein bands within the 20%-35% iodixanol fractions indicating PapMV particle assembly, there were deviations from the expected

band sizes. Protein of the single-expressed constructs migrated at approximately 20kDa (ST-PapMV) and 45kDa (SC-PapMV), while in lanes containing co-expressed constructs, bands were observed at 44kDa (ST-PapMV+PCL-SC), 19kDa (ST-PapMV+SC-PCL) and no band for proteins SC-PapMV+PCL-ST and SC-PapMV+ST-PCL.

The unusual migration patterns seen in band sizes are most likely caused by protein dimerization or incomplete denaturing, a very common factor for plant-expressed proteins fused with SpyTag/SpyCatcher, resulting in higher molecular weight on SDS-PAGE gel (Rath *et al*., 2008). Another deviation may occur when lectin conjugation physically blocks or interferes with PapMV CP protein interaction required for VLP assembly. The statement is supported by the study by Thérien *et al*. (2017) who reported that PapMV coat proteins can tolerate some C-terminal fusions, although long modifications might inhibit nanoparticles formation and stability. These findings indicate that the visualized molecular weights of the expressed proteins are usually affected not only by the length of their primary sequence but also by their structural and biochemical properties. Regardless of the discrepancies that occurred, the results indicated that only SC-PapMV VLP was conjugated with the PCL-ST lectin (Fig. 4.7 (b) Lane 5-6), likely attributable to construct design and tag position.

This covalent interaction is facilitated by the SpyTag/SpyCatcher sequences conjugated to the PapMV and PCL sequences. Interestingly this covalent bond does not occur when the chimeric ST-PapMV protein is co-expressed with the chimeric SC-PCL where the SpyCatcher sequence is conjugated on the N-terminal of the lectin protein. This indicates the importance of whether the SpyCatcher/SpyTag sequences are conjugated to the N-terminal or the C-terminal of a target protein. In this study we were unable to determine whether the SC-PapMV chimeric protein was able to covalently bond with the ST-PCL protein. This is because the size of the SC-PapMV protein was not the expected 37.6kDa but approximately 45kDa in size, very similar to the size of the conjugated SC-PapMV-ST-PCL protein.

5.5 MagResyn® NTA beads purification

Protein purification is a vital step in the isolation of a desired protein from complex biological mixtures, allowing for structural and functional characterization necessary for therapeutic development (Singh *et al*., 2023). MagReSyn® NTA affinity has been utilized by Carter and Outten (2021) to purify polyhistidine-tagged proteins, providing specificity,

binding efficacy and mild elution conditions to maintain protein functionality. The His-tag purification protocol utilized via MagResyn® NTA beads selectively isolated C-terminal His-tagged PapMV VLPs from *N. benthamiana* DXT/FT plant lysates achieving >90% purify and improved protein yield. Therefore, it was necessary to clarify the lysate and enrich His-tagged proteins via MagReSyn® NTA affinity purification. MagReSyn® NTA affinity purifications allowed for the His-tagged recombinant proteins to be effectively captured and eluted in soluble form. These purification techniques yielded higher and more pure recombinant proteins, as indicated by findings on SDS-PAGE gels. The target band intensity was higher and fewer contaminating bands were present following MagReSyn® NTA affinity purification than in the protein samples obtained using the Iodixanol density purification protocol. The results confirmed the previous SDS-PAGE and aDcovalent bond occurring between the chimeric ST-PapMV protein and the chimeric PCL-SC protein when these proteins are co-expressed in *N. benthamiana* DXT/FT plant cells.

5.6 TEM of the MagResyn® NTA beads-purified VLPs

Transmission electron microscopy revealed assembled VLPs in both single PapMV and co-expressed PapMV-PCL samples. The rod-shaped VLPs measured approximately 14-25 nm diameter and 170 nm - 633 nm in length, consistent with the typical morphology of PapMV VLPs reported by other studies (Rioux *et al*., 2014). This further indicates expression and proper self-assembly of the chimeric PapMV CP in the *N. benthamiana* DXT/FT. Co-expression of the PCL lectin and PapMV CP resulted in VLP assembly and VLP conjugation to PCL lectins highlighting how resilient plant expression systems are in producing morphologically intact VLPs (Rioux, Babin, *et al*., 2012). Previous study reported that co-expression of biomolecules with VLPs can impact their structural uniformity and assembly (Balke and Zeltins, 2020). In the present study there was no effect.

Shorter average particle length ranging between 166.57 to 632.9 nm was measured in some constructs after MagReSyn® NTA purification compared to the iodixanol gradients fractions described in section 4.8.2. It is possible that the presence of glycerol used to stabilise purified protein may have contributed to the reduced filament length, an effect previously reported for filamentous viral nanoparticles (García-Anaya *et al*., 2025). However, particle diameters of conjugated PapMV VLPs showed a slight increase compared to unconjugated PapMV VLPs likely due to the attachment of lectins on the

particle surface. This includes constructs SC-PapMV-ST-PCL and ST-PapMV-SC-PCL. The findings also showed a few assembled VLPs in SC-PapMV-PCL-ST co-expressed construct which the proteins was too low to be detected on SDS-Page gel and Western blot analysis. Nevertheless, the presence of intact VLPs demonstrated that plant-expression system can enable conjugation of the PCL lectin to PapMV VLPs. The null hypothesis was rejected because the experimental results showed the presence of lectin-conjugation, expression and assembly of VLPs. The SpyTag/SpyCatcher elements did not abolish chimeric protein production, correct folding and VLP assembly in plant cells.

5.7 Quantification of the chimeric and lectin-conjugated PapMV VLPs

Purified protein quantification is very important for downstream applications for comparative analysis of construct expression and *in vitro* assays. In this study, two complementary methods were used to quantify chimeric PapMV VLP and lectin-conjugated PapMV VLP proteins. These methods included the BCA assay and SDS-PAGE gel densitometry.

5.7.1 BCA quantification

Initially, BCA assay was used to quantify total purified protein concentrations in preparation for cell culture experiment. The first (Table 4.4 and Fig. 4.11) and second (Table 4.5 and Fig. 4.12) colorimetric assays yielded successful recovery of the final protein concentrations for the constructs ST-PapMV, SC-PapMV, SC-PapMV+PCL-ST, SC-PapMV+ST-PCL, ST-PapMV+PCL-SC and ST-PapMV+SC-PCL, respectively. Both BSA standards curves indicated high linearity of R^2 = 0.99 and R^2 = 0.9979, suggesting technically sound results. Several studies reported different protein concentration yield from *N. benthamiana* plant expression, including 210-500 µg/mL GFP (Jung *et al*., 2025) and 100-150 µg/mL α-AIC3 (Prado *et al*., 2019). These findings showed that protein concentration (Table 4.3-4.4) represents moderate to low yield for *N. benthamiana* transient expression.

During the third batch of protein quantification, which was final experiment before *in vitro* assay, unusual intense purple colour was observed. This result was caused by the 1:1 dilution of glycerol added to purified protein samples before the BCA quantification. Glycerol was added to the purified proteins solution as a cryoprotectant before storage, preventing protein aggregation and denaturation while preserving their stability for subsequent *in vitro* assays. Other researchers reported that glycerol interferes with BCA

reactions by producing background colour which results in unreliable absorbance readings (Löptien *et al*., 2024). We were unable to quantitate the final protein batch. Therefore, an alternative quantification method had to be employed, which was SDS-PAGE gel to address this matter.

5.7.2 Protein quantification via Gel densitometry

By using gel densitometry, BSA standards of known concentrations was compared to the band intensity of purified proteins of interest. This method confirmed the presence of bands corresponding to sizes of the MagResyn NTA beads purified proteins obtained in earlier experiments. The molecular sizes of these protein bands were estimated using the PageRuler Prestained Protein Ladder. It was clear that gel densitometry was less affected by glycerol and a protein concentration estimate of 0.253 µg/mL was obtained for the final experiment. The protein concentrations was low because gel densiometry quantified only targeted bands compared to BCA assay, which measures total protein including host proteins and fragments. Several studies reported different amounts of VLPs concentration used for binding experiments, including 25µg/mL of HPV6b L1 VLPs (Mei et al., 1996), 0.1µg/mL of HPV Type-33 VLPs (Volpers et al., 1995) and 0.1µg/mL of BPV VLPs (Mùller et al., 1995). Based on these findings, 0.253µg/mL of VLPs used in the present study was appropriate amount.

5.8 In vitro binding of lectin-conjugated PapMV VLPs to breast cancer cells

The subsequent phase of this study focused on functionalization of PCL-conjugated PapMV-VLPs to establish the ability of the VLPs to target HER2+ cancer cells *in vitro*. We wanted to determine whether PCL-conjugated PapMV VLPs bind to the cancer cells through lectin-mediated targeting. The *in vitro* binding experiment provided valuable information on the functional characteristics of the engineered VLPs. Optimization through preliminary testing demonstrated that 1:1000 ratio antibody dilution produced optimal fluorescence intensity signal and background. The use of an anti-His antibody at 1:1000 dilutions has been previously reported and validated in immunofluorescence microscopy and enzyme-linked immunosorbent assay (ELISA). For example, a 1:1000 dilution of the Alexa Fluor 488-conjugated anti-6x His antibody was previously reported by Chi *et al*. (2020) for immunofluorescence detection of His-tagged proteins. Similarly, Goodell *et al*. (2008) employed a His-tag specific monoclonal antibody of 1:1000 dilution to coat ELISA plates, to provide adequate specificity for the detection of His-tagged

antigens. Therefore, these reports informed the selection and utilization of 1:1000 dilution in the presented *in vitro* experimental setup. Fluorescence intensities measured at the wavelength 535 nm during the *in vitro* binding assays showed that there was no significant increase in the fluorescence emitted from the test wells as compared to that emitted from the negative control wells. This indicated a lack of binding not only by the unconjugated PapMV VLPs, which was expected, but also by the ST-PapMV-PCL-SC VLPs previously shown to be covalently conjugated. Based on these findings, the null hypothesis could not be rejected because of no detectable binding of proteins to targeted cancer cells. These findings suggest that the folding of the chimeric PCL lectins may not have allowed for conjugation to the PapMV VLPs or if conjugation occurred, as in the case of ST-PapMV-PCL-SC, the orientation of PCL lectin did not allow for interaction with the cancer cell target.

5.9 Limitations and challenges

Despite this study achieving significant milestones, several limitations and challenges must also be acknowledged, including low protein yield and a lack of VLP binding to the target cancer cells. As outlined in the literature review, plant viral nanoparticles (PVNPs) are non-infectious virus-based nanostructures used in biotherapeutic applications (Donaldson *et al*., 2018). Some researchers demonstrated that spatial presentation of functional design or motifs on PVNPs is a crucial factor for efficient receptor-mediated binding (Cheng *et al*., 2023; Ly et al., 2024; Nkanga and Steinmetz, 2021; Yildiz *et al*., 2011). Consequently, it may be necessary to optimize the targeting molecule or linker design to improve the exposure of the PCL lectin while maintaining PapMV capsid assembly. These results highlight the complex balance between structural stability and functional targeting when engineering plant-derived viral nanoparticles for cancer biotherapy applications.

CHAPTER 6: SUMMARY AND CONCLUSIONS

This study explored the potential of using plant-expressed PapMV VLPs conjugated to PCL lectins as a biotherapeutic agent capable of targeting cancer cells. The main objectives and their results are summarized in this chapter:

6.1 Transient co-expression of chimeric PapMV coat protein (CP) and Polygonatum cyrtonema lectin (PCL) gene sequences in *Nicotiana benthamiana* plants and assessment of chimeric protein expression, VLP assembly and lectin-VLP conjugation.

By using the pEAQ-HT expression vector system in *N. benthamiana* plants, the study aimed to produce structurally stable lectin-conjugated VLPs that bind to cancer cells, thereby providing a plant-derived cancer biotherapy foundation. The subsequent ligation or loading of therapeutic agents into these VLPs would then enable targeted delivery to cancer cells and the formation of a biotherapy against cancer. The study showed chimeric PapMV CP proteins containing SpyTag/SpyCatcher elements successfully assembled into VLPs as confirmed by TEM analysis. When co-expressed with the chimeric PCL-SC lectin, one of the chimeric PapMV proteins, ST-PapMV, successfully assembled and conjugated to the lectin.

6.2 Investigation of the binding capability of the plant-expressed, lectin-conjugated PapMV VLPs to HER2+ breast cancer cells *in vitro*.

A HER2+ breast cancer cell line was used as the target. Protocols utilized in this study could be employed using different types of cancer cell lines, both in humans and animals, due to the aberrant glycosylation patterns present in all cancer cells. *In vitro* binding assays demonstrated no significant fluorescence intensity emitted by the test samples. These findings indicate that functional targeting to cancer cells through lectin-conjugated VLPs was not achieved.

6.3 Protein quantification via gel densitometry

The quantitative gel densitometry indicated low protein yields with consistent recombinant protein expression across replicates with no significant variation among constructs. TEM further confirmed successful assembly, revealing uniform well-structured VLPs, even at low protein yields. The fluorescence in vitro binding assays did not show any detectable binding of the fluorophore-conjugated antibodies to His-tagged VLPs. This resulted in a

p-value > 0.05 when compared to control variables. Ultimately, it confirms no statistically significant differences in HER2+ cancer cells.

6.4 General conclusion, recommendations and future perspectives

Despite the lack of binding of the PapMV VLPs to target cancer cells, the findings establish several key significant advancements in plant-derived cancer nanobiotechnology. The successful expression and conjugation of the PCL lectin to the surface of assembled chimeric PapMV VLPs in *N. benthamiana* plants further illustrates the flexibility of molecular farming system for producing complex nanoparticle structures (Peralta-Cuevas *et al*., 2025; Vo and Trinh, 2025). These results indicate that with optimal construct design, high expression yields of lectin-conjugated VLPs may be produced in *N. benthamiana* plants for optimal binding to cancer target cells.

Additional importance of this research also contributes to current efforts in the development of plant-based nanocarrier cancer therapy. Theoretically, incorporation of tumor-targeting ligands, including lectins, could enhance selective accumulation in the tumor tissues due to specific binding, thereby minimizing off-target effects (Morales-Cruz *et al*., 2019). Although functional binding was not achieved with the lectin-conjugated PapMV VLPs, the platform allows further optimization and ligand engineering. Consequently, this study bridges basic plant molecular biology to applied cancer nanomedicine.

Future research should address the limitations through construct optimization and a comprehensive functional assay to further validate plant-expressed VLPs for therapeutic use. This study demonstrated the possibility of targeting cancer therapy by decorating chimeric PapMV VLPs with PCL lectins using SpyTag/SpyCatcher technology. This forms a foundation for future plant-derived biotherapeutic development.

REFERENCES

Akash, S. (2021). An overview of advanced treatment of Cancer Where are we today? *International Journal of Multidisciplinary Research and Explorer*, *1*(3), 20–25 https://doi-ds.org/doilink/06.2021-22765836/IJMRE

Al Meslamani, A. Z. (2023). The future of precision medicine in oncology. *In Expert Review of Precision Medicine and Drug Development*, *8*(1), 43–47. https://doi.org/10.1080/23808993.2023.2292988

Amrofell, M. B., Rengarajan, S., Vo, S. T., Ramirez Tovar, E. S., LoBello, L., Dantas, G., & Moon, T. S. (2023). Engineering E. coli strains using antibiotic-resistance-gene-free plasmids. *Cell Reports Methods*, *3*(12). https://doi.org/10.1016/j.crmeth.2023.100669

An, J., Liu, J. Z., Wu, C. F., Li, J., Dai, L., Van Damme, E., Balzarini, J., De Clercq, E., Chen, F., & Bao, J. K. (2006). Anti-HIV I/II activity and molecular cloning of a novel mannose/sialic acid-binding lectin from rhizome of Polygonatum cyrtonema Hua. *Acta Biochimica et Biophysica Sinica*, *38*(2), 70–78. https://doi.org/10.1111/j.1745-7270.2006.00140.x

Anand, U., Dey, A., Chandel, A. K. S., Sanyal, R., Mishra, A., Pandey, D. K., De Falco, V., Upadhyay, A., Kandimalla, R., Chaudhary, A., Dhanjal, J. K., Dewanjee, S., Vallamkondu, J., & Pérez de la Lastra, J. M. (2023). Cancer chemotherapy and beyond: Current status, drug candidates, associated risks and progress in targeted therapeutics. *In Genes and* Diseases, *10*(4), 1367–1401. https://doi.org/10.1016/j.gendis.2022.02.007

Armbruster, A., Hörner, M., Wagner, H. J., Fink-Straube, C., & Weber, W. (2025). Genetically encoded SpyTag enables modular AAV retargeting via SpyCatcher-fused ligands for targeted gene delivery. *ACS Synthetic Biology*. https://doi.org/10.1101/2025.08.22.671696

Arora, U., Tyagi, P., Swaminathan, S., & Khanna, N. (2012). Chimeric Hepatitis B core antigen virus-like particles displaying the envelope domain III of dengue virus type 2. *Journal of Nanobiotechnology*, *10*(1), 30. https://doi.org/10.1186/1477-3155-10-30

Babin, C., Majeau, N., & Leclerc, D. (2013). Engineering of papaya mosaic virus (PapMV) nanoparticles with a CTL epitope derived from influenza NP. *Journal of Nanobiotechnology*, *11*(1), 10. https://doi.org/10.1186/1477-3155-11-10

Bachmann, M. F., & Jennings, G. T. (2010). Vaccine delivery: A matter of size, geometry, kinetics and molecular patterns. *In Nature Reviews Immunology*, *10*(11), 787–796. https://doi.org/10.1038/nri2868

Bachmann, M. F., van Damme, P., Lienert, F., & Schwarz, T. F. (2025). Virus-like particles: a versatile and effective vaccine platform. *Expert Review of Vaccines*, *24*(1), 444–456. https://doi.org/10.1080/14760584.2025.2508517

Balke, I., & Zeltins, A. (2020). Recent advances in the use of plant virus-like particles as vaccines. *Viruses*, *12*(3), 270. https://doi.org/10.3390/v12030270

Bamogo, P. K. A., Brugidou, C., Sérémé, D., Tiendrébéogo, F., Djigma, F. W., Simpore, J., & Lacombe, S. (2019). Virus-based pharmaceutical production in plants: An opportunity to reduce health problems in Africa. *Virology Journal*, *16*(1), 167. https://doi.org/10.1186/s12985-019-1263-0

Baskar, R., Dai, J., Wenlong, N., Yeo, R., & Yeoh, K. W. (2014). Biological response of cancer cells to radiation treatment. *Frontiers in Molecular Biosciences*, *1*, 24. https://doi.org/10.3389/fmolb.2014.00024

Beatty, P. H., & Lewis, J. D. (2019). Cowpea mosaic virus nanoparticles for cancer imaging and therapy. *Advanced Drug Delivery Review,145*, 130–144. https://doi.org/10.1016/j.addr.2019.04.005

Bhinder, B., Gilvary, C., Madhukar, N. S., & Elemento, O. (2021). Artificial intelligence in cancer research and precision medicine. *Cancer Discovery*, *11*(4), 900–915. https://doi.org/10.1158/2159-8290.CD-21-0090

Bray, F., Laversanne, M., Sung, H., Ferlay, J., Siegel, R. L., Soerjomataram, I., & Jemal, A. (2024). Global cancer statistics 2022: GLOBOCAN estimates of incidence and mortality worldwide for 36 cancers in 185 countries. *CA: A Cancer Journal for Clinicians*, *74*(3), 229–263. https://doi.org/10.3322/caac.21834

Bruder, M. R., & Aucoin, M. G. (2023). Evaluation of Virus-Free Manufacture of Recombinant Proteins Using CRISPR-Mediated Gene Disruption in Baculovirus-

Infected Insect Cells. *Vaccines*, *11*(2), 225. https://doi.org/10.3390/vaccines11020225

Brune, K. D., Buldun, C. M., Li, Y., Taylor, I. J., Brod, F., Biswas, S., & Howarth, M. (2017). Dual Plug-and-Display Synthetic Assembly Using Orthogonal Reactive Proteins for Twin Antigen Immunization. *Bioconjugate Chemistry*, *28*(5), 1544–1551. https://doi.org/10.1021/acs.bioconjchem.7b00174

Brune, K. D., Leneghan, D. B., Brian, I. J., Ishizuka, A. S., Bachmann, M. F., Draper, S. J., Biswas, S., & Howarth, M. (2016). Plug-and-Display: decoration of Virus-Like Particles via isopeptide bonds for modular immunization. *Scientific Reports*, *6*(1), 19234. https://doi.org/10.1038/srep19234

Cai, M. meng, Ni, Z. fu, Sun, Z. ke, Li, X. long, Wang, Z. hao, Zhang, M., & Li, C. wei. (2025). Research Progress Based on SpyTag/SpyCatcher Self-Assembling Peptides and Their Applications in the Food Field. In *Food Bioengineering*, *4*(3), 279–291. https://doi.org/10.1002/fbe2.70023

Calvillo-Rodríguez, K. M., Lorenzo-Anota, H. Y., Rodríguez-Padilla, C., Martínez-Torres, A. C., & Scott-Algara, D. (2023). Immunotherapies inducing immunogenic cell death in cancer: insight of the innate immune system. *Frontiers in Immunology*,*14*, 1294434. https://doi.org/10.3389/fimmu.2023.1294434

Cañizares, M. C., Nicholson, L., & Lomonossoff, G. P. (2005). Use of viral vectors for vaccine production in plants. In *Immunology and Cell Biology*, *83*(3), 263–270. https://doi.org/10.1111/j.1440-1711.2005.01339.x

Carignan, D., Thérien, A., Rioux, G., Paquet, G., Gagné, M. È. L., Bolduc, M., Savard, P., & Leclerc, D. (2015). Engineering of the PapMV vaccine platform with a shortened M2e peptide leads to an effective one dose influenza vaccine. *Vaccine*, *33*(51), 7245–7253. https://doi.org/10.1016/J.VACCINE.2015.10.123

Carter, T. D., & Outten, F. W. (2021). Ni-NTA Affinity Chromatography to Characterize Protein–Protein Interactions During Fe-S Cluster Biogenesis. *Methods in Molecular Biology*, 2353, 125–136. https://doi.org/10.1007/978-1-0716-1605-5_7

Chen, Q., & Lai, H. (2013). Plant-derived virus-like particles as vaccines. *Human Vaccines and Immunotherapeutics*, *9*(1), 26–49. https://doi.org/10.4161/hv.22218

Cheng, X., Xie, Q., & Sun, Y. (2023). Advances in nanomaterial-based targeted drug delivery systems. *Frontiers in Bioengineering and Biotechnology*, *11*, 1177151. https://doi.org/10.3389/fbioe.2023.1177151

Chi, X., Liu, X., Wang, C., Zhang, X., Li, X., Hou, J., Ren, L., Jin, Q., Wang, J., & Yang, W. (2020). Humanized single domain antibodies neutralize SARS-CoV-2 by targeting the spike receptor binding domain. *Nature Communications*, *11*(1), 4528. https://doi.org/10.1038/s41467-020-18387-8

Chiu, M. L., Goulet, D. R., Teplyakov, A., & Gilliland, G. L. (209). Antibody Structure and Function : The Basics for Engineering Therapeutics. *Antibodies (Basel, Switzerland)*, *8*(4), 55. https://doi.org/10.3390/antib8040055

Chung, Y. H., Cai, H., & Steinmetz, N. F. (2020). Viral nanoparticles for drug delivery, imaging, immunotherapy, and theranostic applications. *Advanced Drug Delivery Reviews*, *156*, 214–235. https://doi.org/10.1016/j.addr.2020.06.024

Cordeiro, D., Alves, A., Ferraz, R., Casimiro, B., Canhoto, J., & Correia, S. (2023). An Efficient Agrobacterium-Mediated Genetic Transformation Method for Solanum betaceum Cav. Embryogenic Callus. *Plants*, *12*(5), 1202. https://doi.org/10.3390/plants12051202

Czapar, A. E., Zheng, Y. R., Riddell, I. A., Shukla, S., Awuah, S. G., Lippard, S. J., & Steinmetz, N. F. (2016). Tobacco Mosaic Virus Delivery of Phenanthriplatin for Cancer therapy. *ACS Nano*, *10*(4), 4119–4126. https://doi.org/10.1021/acsnano.5b07360

Dai, S., Wang, H., & Deng, F. (2018). Minireview Open Access Advances and challenges in enveloped virus-like particle (VLP)-based vaccines. *Journal of Immunological Sciences*, *2*(2), 36–41.

Damen, M. P. F., van Rheenen, J., & Scheele, C. L. G. J. (2021). Targeting dormant tumor cells to prevent cancer recurrence. *FEBS Journal*, *288*(21), 6286–6303. https://doi.org/10.1111/febs.15626

D'Aoust, M. A., Couture, M. M. J., Charland, N., Trépanier, S., Landry, N., Ors, F., & Vézina, L. P. (2010). The production of hemagglutinin-based virus-like particles in plants: A rapid, efficient and safe response to pandemic influenza. *Plant*

Biotechnology Journal, *8*(5), 607–619. https://doi.org/10.1111/j.1467-7652.2009.00496.x

de Mello, R. G., Bernardino, T. C., Guardalini, L. G. O., Astray, R. M., Antoniazzi, M. M., Jared, S. G. S., Núñez, E. G. F., & Jorge, S. A. C. (2023). Zika virus-like particles (VLPs) produced in insect cells. *Frontiers in Pharmacology*, *14*, 1181566. https://doi.org/10.3389/fphar.2023.1181566

Debela, D. T., Muzazu, S. G. Y., Heraro, K. D., Ndalama, M. T., Mesele, B. W., Haile, D. C., Kitui, S. K., & Manyazewal, T. (2021). New approaches and procedures for cancer treatment: Current perspectives. *SAGE Open Medicine*, *9*, 20500312121103343 66. https://doi.org/10.1177/20503121211034366

Dennis, S. J., Meyers, A. E., Guthrie, A. J., Hitzeroth, I. I., & Rybicki, E. P. (2018). Immunogenicity of plant-produced African horse sickness virus-like particles: implications for a novel vaccine. *Plant Biotechnology Journal*, *16*(2), 442–450. https://doi.org/10.1111/pbi.12783

Desai, I., Thakur, S., & Pagariya, P. (2024). Current advances in immunotherapy for cancer. *Oral Oncology Reports*, *12*, 100652. https://doi.org/10.1016/j.oor.2024.100652

Donaldson, B., Lateef, Z., Walker, G. F., Young, S. L., & Ward, V. K. (2018). Virus-like particle vaccines: immunology and formulation for clinical translation. *Expert Review of Vaccines*, *17*(9), 833–849. https://doi.org/10.1080/14760584.2018.1516552

Fischer, R., Stoger, E., Schillberg, S., Christou, P., & Twyman, R. M. (2004). Plant-based production of biopharmaceuticals. *Current Opinion in Plant Biology*, *7*(2), 152–158. https://doi.org/10.1016/J.PBI.2004.01.007

Flynn, N. H., & Ramsey, J. D. (2015). Virus-like particles in gene, vaccine and therapeutic delivery. *Nanoparticles for Biotherapeutic Delivery,1*, 38–48. https://doi.org/10.4155/fseb2013.14.62

Formoso, R., Vighi, I. L., Galli, V., & Pinto, L. da S. (2022). Plant viral vectors: an strategy for transient expression of recombinant proteins in plants. *Conjecturas*, *22*(2), 107–121. https://doi.org/10.53660/conj-633-515

Fox, J. L. (2012). First plant-made biologic approved. *Nature Biotechnology*, *30*(6), 472–472. https://doi.org/10.1038/nbt0612-472

Fu, L. L., Zhou, C. C., Yao, S., Yu, J. Y., Liu, B., & Bao, J. K. (2011). Plant lectins: Targeting programmed cell death pathways as antitumor agents. *International Journal of Biochemistry and Cell Biology*, *43*(10), 1442–1449. https://doi.org/10.1016/j.biocel.2011.07.004

Fuenmayor, J., Gòdia, F., & Cervera, L. (2017). Production of virus-like particles for vaccines. *New Biotechnology*, *39*, 174–180. https://doi.org/10.1016/j.nbt.2017.07.010

García-Anaya, M. C., Sepúlveda, D. R., Zamudio-Flores, P. B., & Acosta-Muñiz, C. H. (2025). Effect of the glycerol content on the A511 bacteriophage release in films made with whey protein isolated. *Journal of Food Engineering*, *388*, 112388. https://doi.org/10.1016/j.jfoodeng.2024.112388

Garg, P., Pareek, S., Kulkarni, P., Horne, D., Salgia, R., & Singhal, S. S. (2024). Next-Generation Immunotherapy: Advancing Clinical Applications in Cancer Treatment. *Journal of Clinical Medicine*, *13*(21), 6537. https://doi.org/10.3390/jcm13216537

Gavas, S., Quazi, S., & Karpiński, T. M. (2021). Nanoparticles for Cancer Therapy: Current Progress and Challenges. *Nanoscale Research Letters*, *16*(1), 173. https://doi.org/10.1186/s11671-021-03628-6

Ghosh, K., Tarapdar, S., Duggal, M., Tyagi, S., Kumar, V., & Gupta, A. (2020). Overview on virus-like particles from plants used as vaccine antigen. *International Journal of Current Research and Review*,*12*(21), 05–09. https://doi.org/10.31782/ijcrr.2020.sp55

Giesler, R. J., Erickson, P. W., & Kay, M.S. (2020). Enhancing native chemical ligation for challenging chemical protein syntheses. *Current Opinion in Chemical Biology, 58*, 37–44. https://doi.org/10.1016/j.cbpa.2020.04.003

Goodell, V., McNeel, D., & Disis, M. L. (2008). His-tag ELISA for the detection of humoral tumor-specific immunity. *BMC Immunology*, *9*(1), 23. https://doi.org/10.1186/1471-2172-9-23

Goodin, M. M., Zaitlin, D., Naidu, R. A., & Lommel, S. A. (2008). Nicotiana benthamiana: Its History and Future as a Model for Plant-Pathogen Interactions. *Molecular plant-microbe interactionsI*, *21*(8), 1015–1026. https://doi.org/10.1094/MPMI

Grace, S., Goodness, N., Chigozie Malachy, U., Onyinye Ifeyinwa Onyekachi, Chukwunwejim Chidimma Ruth, Ijeoma Ngozi Ebenebe, Chinenye, H. N., & Angus, N. O. (2024). Agrobacterium tumefaciens: Biology and application in genetic engineering. *GSC Advanced Research and Reviews*, *20*(1), 389–398. https://doi.org/10.30574/gscarr.2024.20.1.0272

Grinzato, A., Kandiah, E., Lico, C., Betti, C., Baschieri, S., & Zanotti, G. (2020). Anatomic structure of potato virus X, the prototype of the *Alphaflexiviridae* family. *Nature Chemical Biology, 16*(5), 564-569. https://doi.org/10.1038/s41589-020-0502-4

Gross, S. M., Mohammadi, F., Sanchez-Aguila, C., Zhan, P. J., Liby, T. A., Dane, M. A., Meyer, A. S., & Heiser, L. M. (2023). Analysis and modeling of cancer drug responses using cell cycle phase-specific rate effects. *Nature Communications*, *14*(1), 3450. https://doi.org/10.1038/s41467-023-39122-z

Grosser, R., Cherkassky, L., Chintala, N., & Adusumilli, P. S. (2019). Combination Immunotherapy with CAR T Cells and Checkpoint Blockade for the Treatment of Solid Tumors. *Cancer Cell*, *36*(5), 471–482. Cell Press. https://doi.org/10.1016/j.ccell.2019.09.006

Gurav, M. J., Manasa, J., Sanji, A. S., Megalamani, P. H., & Chachadi, V. B. (2024). Lectin-glycan interactions: a comprehensive cataloguing of cancer-associated glycans for biorecognition and bio-alteration: a review. *Glycoconjugate Journal*, *41*(4), 301–322). https://doi.org/10.1007/s10719-024-10161-y

Hanselmann, R. G., & Welter, C. (2022). Origin of Cancer: Cell work is the Key to Understanding Cancer Initiation and Progression. *Frontiers in Cell and Developmental Biology*, *10*, 787995. https://doi.org/10.3389/fcell.2022.787995

Hatlem, D., Trunk, T., Linke, D., & Leo, J. C. (2019). Catching a SPY: Using the SpyCatcher-SpyTag and related systems for labeling and localizing bacterial proteins. *International Journal of Molecular Sciences*, *20*(9), 2129. https://doi.org/10.3390/ijms20092129

Hatlem, D., Trunk, T., Linke, D., & Leo, J. C. (2022). SpyCatcher-SpyTag System. *SpyCatcher-SpyTag System | Encyclopedia*. https://encyclopedia.pub/entry29949

He, J., Zeng, X., Wang, C., Wang, E., & Li, Y. (2024). Antibody–drug conjugates in cancer therapy: mechanisms and clinical studies. *Med Comm*, *5*(8), 671. https://doi.org/10.1002/mco2.671

Hefferon, K. L. (2012). Plant virus expression vectors set the stage as production platforms for biopharmaceutical proteins. *Virology*, *433*(1), 1–6. https://doi.org/10.1016/J.VIROL.2012.06.012

Hemmati, F., Hemmati-Dinarvand, M., Karimzade, M., Rutkowska, D., Eskandari, M. H., Khanizadeh, S., & Afsharifar, A. (2022). Plant-derived VLP: a worthy platform to produce vaccine against SARS-CoV-2. *Biotechnology Letters*, *44*(1), 45–57. https://doi.org/10.1007/s10529-021-03211-0

Ho, W. L., Hsu, W. M., Huang, M. C., Kadomatsu, K., & Nakagawara, A. (2016). Protein glycosylation in cancers and its potential therapeutic applications in neuroblastoma. In *Journal of Hematology and Oncology*, *9*(1), 1–15. BioMed Central Ltd. https://doi.org/10.1186/s13045-016-0334-6

Hwang, H.-H., Yu, M., & Lai, E.-M. (2017). Agrobacterium -Mediated Plant Transformation: Biology and Applications. *The Arabidopsis Book*, *15*, e0186. https://doi.org/10.1199/tab.0186

Ioele, G., Chieffallo, M., Occhiuzzi, M. A., De Luca, M., Garofalo, A., Ragno, G., & Grande, F. (2022). Anticancer Drugs: Recent Strategies to Improve Stability Profile, Pharmacokinetic and Pharmacodynamic Properties. *Molecules*, *27*(17), 5436. https://doi.org/10.3390/molecules27175436

Jansing, J., Sack, M., Augustine, S. M., Fischer, R., & Bortesi, L. (2019). CRISPR/Cas9-mediated knockout of six glycosyltransferase genes in Nicotiana benthamiana for the production of recombinant proteins lacking β-1,2-xylose and core α-1,3-fucose. *Plant Biotechnology Journal*, *17*(2), 350–361. https://doi.org/10.1111/pbi.12981

Jin, T., Wang, J., Zhu, X., Xu, Y., Zhou, X., & Yang, L. (2015). A new transient expression system for large-scale production of recombinant proteins in plants based on air-

brushing an Agrobacterium suspension. *Biotechnology Reports*, *6*, 36–40. https://doi.org/10.1016/j.btre.2015.01.004

Joshi, D. C., Sharma, A., Prasad, S., Singh, K., Kumar, M., Sherawat, K., Tuli, H. S., & Gupta, M. (2024). Novel therapeutic agents in clinical trials: emerging approaches in cancer therapy. *Discover Oncology*,*15*(1), 342. https://doi.org/10.1007/s12672-024-01195-7

Jung, C., Choi, H. J., Jo, S. H., Paek, K. H., & Park, J. M. (2025). Engineering PVX vectors harboring heterogeneous VSRs to enhance recombinant protein expression in plants. Scientific Reports, 15, 40330. https://doi.org/10.1038/s41598-025-24470-01

Kanekiyo, M., & Buck, C. B. (2017). Virus-Like Particle and Nanoparticle Vaccines. *Human Vaccines: Emerging Technologies in Design and Development*, 87–98. https://doi.org/10.1016/B978-0-12-802302-0.00003-0

Kaur, M., Manchanda, P., Kalia, A., Ahmed, F. K., Nepovimova, E., Kuca, K., & Abd-Elsalam, K. A. (2021). Agroinfiltration mediated scalable transient gene expression in genome edited crop plants. In *International Journal of Molecular Sciences*, *22*(19), 10882. https://doi.org/10.3390/ijms221910882

Kheirvari, M., Liu, H., & Tumban, E. (2023). Virus-like Particle Vaccines and Platforms for Vaccine Development. *Viruses*, *15*(5), 1109. https://doi.org/10.3390/v15051109

Kim, K. R., Lee, A. S., Kim, S. M., Heo, H. R., & Kim, C. S. (2023). Virus-like nanoparticles as a theranostic platform for cancer. *Frontiers in Bioengineering and Biotechnology*, *10*, 1106767. https://doi.org/10.3389/fbioe.2022.1106767

Kole, C., Chaurasia, A., Hefferon, K. L., & Panigrahi, J. (2024). Applications of Plant Molecular Farming. *Concepts and strategies in plant sciences series*. https://doi/org/10.1007/978-981-97-0176-6

Kolesanova, E. F., Melnikova, M. V., Bolshakova, T. N., Rybalkina, E. Y., & Sivov, I. G. (2019). Bacteriophage MS2 as a tool for targeted delivery in solid tumor chemotherapy. *Acta Naturae*, *11*(2), 98–101. https://doi.org/10.32607/20758251-2019-11-2-98-101

Komane, M. D., Kayoka-Kabongo, P. N., & Rutkowska, D. A. (2025). The Use of Plant Viral Nanoparticles in Cancer Biotherapy-A Review. *Viruses*, *17*(2), 218. https://doi.org/10.3390/v17020218

Koseoglou, E., van der Wolf, J. M., Visser, R. G. F., & Bai, Y. (2022). Susceptibility reversed: modified plant susceptibility genes for resistance to bacteria. *Trends in Plant Science*, 27(1), 69–79. Elsevier https://doi.org/10.1016/j.tplants.2021.07.018

Koury, J., Lucero, M., Cato, C., Chang, L., Geiger, J., Henry, D., Hernandez, J., Hung, F., Kaur, P., Teskey, G., & Tran, A. (2018). Immunotherapies: Exploiting the immune system for cancer treatment. *Journal of Immunology Research*, *2018*(1), 9585614. https://doi.org/10.1155/2018/9585614

Kurosawa, M., Sekine, M., Yamaguchi, M., Kudo, R., Hanley, S. J. B., Hara, M., Adachi, S., Ueda, Y., Miyagi, E., Ikeda, S., Yagi, A., & Enomoto, T. (2022). Long-Term Effects of Human Papillomavirus Vaccination in Clinical Trials and Real-World Data: A Systematic Review. *Vaccines*,*10*(2), 256. https://doi.org/10.3390/vaccines10020256

Kushnir, N., Streatfield, S. J., & Yusibov, V. (2012). Virus-like particles as a highly efficient vaccine platform: Diversity of targets and production systems and advances in clinical development. *Vaccine*,*31*(1), 58–83. https://doi.org/10.1016/j.vaccine.2012.10.083

Labani-Motlagh, A., Ashja-Mahdavi, M., & Loskog, A. (2020). The Tumor Microenvironment: A Milieu Hindering and Obstructing Antitumor Immune Responses. *Frontiers in Immunology*, *11*, 940. https://doi.org/10.3389/fimmu.2020.00940

Laliberté-Gagné, M. E., Bolduc, M., Garneau, C., Olivera-Ugarte, S. M., Savard, P., & Leclerc, D. (2021). Modulation of antigen display on papmv nanoparticles influences its immunogenicity. *Vaccines*, *9*(1), 1–14. https://doi.org/10.3390/vaccines9010033

Landry, N., Ward, B. J., Trépanier, S., Montomoli, E., Le Dargis, M., Lapini, G., & Vézina, L. P. (2010). Preclinical and clinical development of plant-made virus-like particle vaccine against avian H5N1 influenza. *PLoS ONE*, *5*(12), e15559. https://doi.org/10.1371/journal.pone.0015559

Lebel, M. È., Chartrand, K., Tarrab, E., Savard, P., Leclerc, D., & Lamarre, A. (2016). Potentiating Cancer Immunotherapy Using Papaya Mosaic Virus-Derived Nanoparticles. *Nano Letters*, *16*(3), 1826–1832. https://doi.org/10.1021/acs.nanolett.5b04877

Lebel, M. ève, Chartrand, K., Leclerc, D., & Lamarre, A. (2015). Plant viruses as nanoparticle-based vaccines and adjuvants. *Vaccines*, 3(3), 620–637. https://doi.org/10.3390/vaccines3030620

Lee, J., Kang, S., Park, H., Sun, J. G., Kim, E. C., & Shim, G. (2023). Nanoparticles for Lymph Node-Directed Delivery. *Pharmaceutics*, *15*(2), 565. MDPI. https://doi.org/10.3390/pharmaceutics15020565

Lee, W. C., Kopetz, S., Wistuba, I. I., & Zhang, J. (2017). Metastasis of cancer: When and how? In *Annals of Oncology*, *28*(9), 2045–2047. https://doi.org/10.1093/annonc/mdx327

Lindsay, B. J., Bonar, M. M., Costas-Cancelas, I. N., Hunt, K., Makarkov, A. I., Chierzi, S., Krawczyk, C. M., Landry, N., Ward, B. J., & Rouiller, I. (2018). Morphological characterization of a plant-made virus-like particle vaccine bearing influenza virus hemagglutinins by electron microscopy. *Vaccine*, *36*(16), 2147–2154. https://doi.org/10.1016/j.vaccine.2018.02.106

Liu, T., Li, L., Cheng, C., He, B., & Jiang, T. (2022). Emerging prospects of protein/peptide-based nanoassemblies for drug delivery and vaccine development. *Nano Research*,*15*(8), 7267–7285. https://doi.org/10.1007/s12274-022-4385-4

Liu, Z., Luo, Y., Zhou, T. T., & Zhang, W. Z. (2013). Could plant lectins become promising anti-tumour drugs for causing autophagic cell death? *Cell Proliferation*, *46*(5), 509–515. https://doi.org/10.1111/cpr.12054

Lomonossoff, G. P., & D'aoust, M. A. (2016). Plant-produced biopharmaceuticals: A case of technical developments driving clinical deployment. *Science, 353*(6305), 1237-1240 http://science.sciencemag.org/

Lopez, J. S., & Banerji, U. (2017). Combine and conquer: Challenges for targeted therapy combinations in early phase trials. *Nature Reviews Clinical Oncology*, *14*(1), 57–66. https://doi.org/10.1038/nrclinonc.2016.96

López-Sagaseta, J., Malito, E., Rappuoli, R., & Bottomley, M. J. (2016). Self-assembling protein nanoparticles in the design of vaccines. *Computational and Structural Biotechnology Journal*, 14, 58–68. https://doi.org/10.1016/j.csbj.2015.11.001

Löptien, J., Vesting, S., Dobler, S., & Mohammadi, S. (2024). Evaluating the efficacy of protein quantification methods on membrane proteins. *Open Biology, 14*(12), 240082 https://doi.org/10.1101/2024.04.02.587709

Loughran Sinéad T. and Bree, R. T. and W. D. (2023). Poly-histidine-tagged protein purification using immobilized metal affinity chromatography (IMAC). *Protein Chromatography: Methods and Protocols,2699,* 193–223. https://doi.org/10.1007/978-1-0716-3362-5_11

Ludwig, C., & Wagner, R. (2007). Virus-like particles-universal molecular toolboxes. *Current Opinion in Biotechnology*, *18*(6), 537–545. https://doi.org/10.1016/j.copbio.2007.10.013

Ly, P. D., Ly, K. N., Phan, H. L., Nguyen, H. H. T., Duong, V. A., & Nguyen, H. V. (2024). Recent advances in surface decoration of nanoparticles in drug delivery. In *Frontiers in Nanotechnology*,*6*, 1456939. Frontiers Media SA. https://doi.org/10.3389/fnano.2024.1456939

Ma, J. K. C., Drossard, J., Lewis, D., Altmann, F., Boyle, J., Christou, P., Cole, T., Dale, P., van Dolleweerd, C. J., Isitt, V., Katinger, D., Lobedan, M., Mertens, H., Paul, M. J., Rademacher, T., Sack, M., Hundleby, P. A. C., Stiegler, G., Stoger, E., Twyman, T. M., Vcelar, B., & Fischer, R. (2015). Regulatory approval and a first-in-human phase I clinical trial of a monoclonal antibody produced in transgenic tobacco plants. *Plant Biotechnology Journal*, *13*(8), 1106–1120. https://doi.org/10.1111/pbi.12416

Makarkov, A. I., Golizeh, M., Ruiz-Lancheros, E., Gopal, A. A., Costas-Cancelas, I. N., Chierzi, S., Pillet, S., Charland, N., Landry, N., Rouiller, I., Wiseman, P. W., Ndao, M., & Ward, B. J. (2019). Plant-derived virus-like particle vaccines drive cross-presentation of influenza A hemagglutinin peptides by human monocyte-derived macrophages. *Npj Vaccines*, *4*(1), 17. https://doi.org/10.1038/s41541-019-0111-y

Mardanova, E. S., Vasyagin, E. A., & Ravin, N. V. (2024). Virus-like Particles Produced in Plants: A Promising Platform for Recombinant Vaccine Development. *Plants*,*13*(24), 3564. https://doi.org/10.3390/plants13243564

Mattiuzzi, C., & Lippi, G. (2019). Current cancer epidemiology. *Journal of Epidemiology and Global Health*, *9*(4), 217–222. https://doi.org/10.2991/jegh.k.191008.001

Mazalovska, M., & Kouokam, J. C. (2020). Plant-derived lectins as potential cancer therapeutics and diagnostic tools. BioMed Research International, 2020(1). https://doi.org/10.1155/2020/1631394

Mc Neil, V., & Lee, S. W. (2025). Advancing Cancer Treatment: A Review of Immune Checkpoint Inhibitors and Combination Strategies. *Cancers*,*17*(9), 1408. https://doi.org/10.3390/cancers17091408

Meghana, P., Jayasri, M. A. I., & Suthindhiran, K. (2025). VLP (Virus-Like Particles) Vaccines - Current Knowledge and Future Directions. *Brazilian Archives of Biology and Technology*, *68,* e25240942. https://doi.org/10.1590/1678-4324-2025240942

Mei, Y. Q., Wen Peng, S., Hengst, K., Evander, M., Park, D. S., Zhou, J., & Frazer, I. H. (1996). Epithelial Cells Display Separate Receptors for Papillomavirus VLPs and for Soluble L1 Capsid Protein. *Virology, 216*(1), 35–45.

Mejía-Méndez, J. L., Vazquez-Duhalt, R., Hernández, L. R., Sánchez-Arreola, E., & Bach, H. (2022). Virus-like Particles: Fundamentals and Biomedical Applications. *International Journal of Molecular Sciences*,*23*(15), 8579. https://doi.org/10.3390/ijms23158579

Mohsen, M. O., & Bachmann, M. F. (2022). Virus-like particle vaccinology, from bench to bedside. *Cellular and Molecular Immunology*, *19*(9), 993–1011. https://doi.org/10.1038/s41423-022-00897-8

Mohsen, M. O., Speiser, D. E., Knuth, A., & Bachmann, M. F. (2020). Virus-like particles for vaccination against cancer. *Wiley Interdisciplinary Reviews- Nanomedicine and Nanobiotechnology*,*12*(1), e1579. https://doi.org/10.1002/wnan.1579

Morales-Cruz, M., Delgado, Y., Castillo, B., Figueroa, C. M., Molina, A. M., Torres, A., Milián, M., & Griebenow, K. (2019). Smart targeting to improve cancer therapeutics. *Drug Design, Development and Therapy*, *13*, 3753–3772. Dove Medical Press Ltd. https://doi.org/10.2147/DDDT.S219489

Mùller, M., Gissmann, L., Cristiano, R. J., Sun, X.-Y., Frazer, I. H., Jenson, A. B., Alonso, A., Zentgraf, H., & Zhou, J. (1995). Papillomavirus capsid binding and uptake by cells

from different tissues and species. *Journal of Virology, 69*(2), 948–954. https://doi.org/10.1128/JVI.69.2.948-954.1995

Mukherjee, A. G., Wanjari, U. R., Namachivayam, A., Murali, R., Prabakaran, D. S., Ganesan, R., Renu, K., Dey, A., Vellingiri, B., Ramanathan, G., Doss C, G. P., & Gopalakrishnan, A. V. (2022). Role of immune cells and receptors in cancer treatment: an immunotherapeutic approach. *Vaccines*, *10*(9), 1493. https://doi.org/10.3390/vaccines10091493

Naimi, A., Mohammed, R. N., Raji, A., Chupradit, S., Yumashev, A. V., Suksatan, W., Shalaby, M. N., Thangavelu, L., Kamrava, S., Shomali, N., Sohrabi, A. D., Adili, A., Noroozi-Aghideh, A., & Razeghian, E. (2022). Tumor immunotherapies by immune checkpoint inhibitors (ICIs); the pros and cons. *Cell Communication and Signaling*, *20*(1), 44. https://doi.org/10.1186/s12964-022-00854-y

National Cancer Institute. (2019). Immunotherapy to treat cancer. https://www.cancer.gov/about-cancer/treatment/types/immunotherapy. [Accessed on 13 February 2026].

National Cancer Institute. (2021). What Is Cancer? https://www.cancer.gov/about-cancer/understanding/what-is-cancer. [Accessed on 09 September 2023].

Ning, W., Yan, S., Song, Y., Xu, H., Zhang, J., & Wang, X. (2024). Virus-like particle: a nano-platform that delivers cancer antigens to elicit an anti-tumor immune response. *Frontiers in Immunology*, *15*, 1504124. https://doi.org/10.3389/fimmu.2024.1504124

Nkanga, C. I., & Steinmetz, N. F. (2021). The pharmacology of plant virus nanoparticles. *Virology*, *556*, 39–61. https://doi.org/10.1016/J.VIROL.2021.01.012

Nonaka, S., Someya, T., Kadota, Y., Nakamura, K., & Ezura, H. (2019). Super-Agrobacterium ver. 4: improving the transformation frequencies and genetic engineering possibilities for crop plants. *Frontiers in Plant Science*, *10*, 1204. https://doi.org/10.3389/fpls.2019.01204

Nooraei, S., Bahrulolum, H., Hoseini, Z. S., Katalani, C., Hajizade, A., Easton, A. J., & Ahmadian, G. (2021). Virus-like particles: preparation, immunogenicity and their roles as nanovaccines and drug nanocarriers. *Journal of Nanobiotechnology*, *19*(1), 59. https://doi.org/10.1186/s12951-021-00806-7

Nosaki, S., Hoshikawa, K., Ezura, H., & Miura, K. (2021). Transient protein expression systems in plants and their applications. *Plant Biotechnology*,38(3), 297–304). https://doi.org/10.5511/plantbiotechnology.21.0610a

Nowakowski, A. B., Wobig, W. J., & Petering, D. H. (2014). Native SDS-PAGE: High resolution electrophoretic separation of proteins with retention of native properties including bound metal ions. *Metallomics*, *6*(5), 1068–1078. https://doi.org/10.1039/c4mt00033a

Omotoso, O., Teibo, J. O., Atiba, F. A., Oladimeji, T., Paimo, O. K., Ataya, F. S., Batiha, G. E. S., & Alexiou, A. (2023). Addressing cancer care inequities in sub-Saharan Africa: current challenges and proposed solutions. *International Journal for Equity in Health*, *22*(1). https://doi.org/10.1186/s12939-023-01962-y

Palatty, P. L., Sacheendran, D., & Jayachandran, M. (2025). Human Papilloma Virus Vaccines. *Confronting HPV - Insights and Solutions*,*6*, 77. https://doi.org/10.5772/intechopen.1004419

Parodi, A., Molinaro, R., Sushnitha, M., Evangelopoulos, M., Martinez, J. O., Arrighetti, N., Corbo, C., & Tasciotti, E. (2017). Bio-inspired engineering of cell- and virus-like nanoparticles for drug delivery. *Biomaterials*, *147*, 155–168. https://doi.org/10.1016/j.biomaterials.2017.09.020

Paul, S., Mukherjee, S., & Banerjee, P. (2023). Recent advancement in nanomaterial-encapsulated drug delivery vehicles for combating cancer, COVID-19, and HIV-like chronic diseases. *Materials Advances*, *4*(9), 2042–2061. https://doi.org/10.1039/d2ma01075e

Peralta-Cuevas, E., Garcia-Atutxa, I., Huerta-Saquero, A., & Villanueva-Flores, F. (2025). The role of plant virus-like particles in advanced drug delivery and vaccine development: structural attributes and application potential. *Viruses*, *17*(2), 148. https://doi.org/10.3390/v17020148

Pessione, E. (2020). The Russian doll model: how bacteria shape successful and sustainable inter-kingdom relationships. *Frontiers in Microbiology*, *11*, 573759. https://doi.org/10.3389/fmicb.2020.573759

Peterson, C., Denlinger, N., & Yang, Y. (2022). Recent advances and challenges in cancer immunotherapy. *Cancers*, *14*(16), 3972. https://doi.org/10.3390/cancers14163972

Peyret, H., & Lomonossoff, G. P. (2015). When plant virology met Agrobacterium: the rise of the deconstructed clones. *Plant Biotechnology Journal*,*13*(8), 1121–1135. https://doi.org/10.1111/pbi.12412

Pillet, S., Aubin, É., Trépanier, S., Bussière, D., Dargis, M., Poulin, J. F., Yassine-Diab, B., Ward, B. J., & Landry, N. (2016). A plant-derived quadrivalent virus like particle influenza vaccine induces cross-reactive antibody and T cell response in healthy adults. *Clinical Immunology*, *168*, 72–87. https://doi.org/10.1016/j.clim.2016.03.008

Pillet, S., Couillard, J., Trépanier, S., Poulin, J. F., Yassine-Diab, B., Guy, B., Ward, B. J., & Landry, N. (2019). Immunogenicity and safety of a quadrivalent plant-derived virus like particle influenza vaccine candidate—Two randomized Phase II clinical trials in 18 to 49 and 50 years old adults. *PLoS ONE*, *14*(6), e0216533. https://doi.org/10.1371/journal.pone.0216533

Pinho, S. S., & Reis, C. A. (2015). Glycosylation in cancer: mechanisms and clinical implications. *Nature Reviews Cancer*, *5*(9), 540–555. https://doi.org/10.1038/nrc3982

Prado, G. S., Bamogo, P. K. A., de Abreu, J. A. C., Gillet, F. X., Dos Santos, V. O., Silva, M. C. M., Brizard, J. P., Bemquerer, M.P., Bangratz, M., Brugidou, C., Sérémé, D., Grossi-de-Sa, M. F., & Lacombe, S. (2019). *Nicotiana benthamiana* is a suitable transient expression of an active inhibitor of cotton boll weevil α-amylase. *BMC Biotechnology*, *19*(1), 15. https://doi.org/10.1186/s12896-019-0507-9

Pucci, C., Martinelli, C., & Ciofani, G. (2019). Innovative approaches for cancer treatment: current perspectives and new challenges. *ecancermedicalscience*,*13*, 961. https://doi.org/10.3332/ecancer.2019.961

Qian, C., Liu, X., Xu, Q., Wang, Z., Chen, J., Li, T., Zheng, Q., Yu, H., Gu, Y., Li, S., & Xia, N. (2020). Recent progress on the versatility of virus-like particles. *Vaccines*, *8*(1), 139. https://doi.org/10.3390/vaccines8010139

Rahman, M. M., Behl, T., Islam, M. R., Alam, M. N., Islam, M. M., Albarrati, A., Albratty, M., Meraya, A. M., & Bungau, S. G. (2022). Emerging management approach for the adverse events of immunotherapy of cancer. *Molecules*, 27(12), 3798. https://doi.org/10.3390/molecules27123798

Rath, A., Glibowicka, M., Nadeau, V. G., Chen, G., & Deber, C. M. (2008). Detergent binding explains anomalous SDS-PAGE migration of membrane proteins. *Proceedings of the National Academy of Sciences*, *106*(6), 1760–1765.

Raza, S. A. (2025). Emerging trends in global cancer epidemiology. *Cancers*, *17*(9), 1483. https://doi.org/10.3390/cancers17091483

Reddington, S. C., & Howarth, M. (2015). Secrets of a covalent interaction for biomaterials and biotechnology: SpyTag and SpyCatcher. *Current Opinion in Chemical Biology*, *29*,94–99. https://doi.org/10.1016/j.cbpa.2015.10.002

Rioux, G., Babin, C., Majeau, N., & Leclerc, D. (2012). Engineering of papaya mosaic virus (papmv) nanoparticles through fusion of the ha11 peptide to several putative surface-exposed sites. *PLoS ONE*, *7*(2), e31925. https://doi.org/10.1371/journal.pone.0031925

Rioux, G., Majeau, N., & Leclerc, D. (2012). Mapping the surface-exposed regions of papaya mosaic virus nanoparticles. *FEBS Journal*, *279*(11), 2004–2011. https://doi.org/10.1111/j.1742-4658.2012.08583.x

Rioux, G., Mathieu, C., Russell, A., Bolduc, M., Laliberté-Gagné, M. E., Savard, P., & Leclerc, D. (2014). PapMV nanoparticles improve mucosal immune responses to the trivalent inactivated flu vaccine. *Journal of Nanobiotechnology*, *12*(1),19. https://doi.org/10.1186/1477-3155-12-19

Röder, J., Dickmeis, C., & Commandeur, U. (2019). Small, smaller, nano: new applications for potato virus X in nanotechnology. *Frontiers in Plant Science*, *10*, 158. https://doi.org/10.3389/fpls.2019.00158

Sainsbury, F., Thuenemann, E. C., & Lomonossoff, G. P. (2009). PEAQ: Versatile expression vectors for easy and quick transient expression of heterologous proteins in plants. *Plant Biotechnology Journal*, *7*(7), 682–693. https://doi.org/10.1111/j.1467-7652.2009.00434.x

Sakai, C., Hosokawa, K., Watanabe, T., Suzuki, Y., Nakano, T., Ueda, K., & Fujimuro, M. (2021). Human hepatitis B virus-derived virus-like particle as a drug and DNA delivery carrier. *Biochemical and Biophysical Research Communications*, *581*, 103–109. https://doi.org/10.1016/J.BBRC.2021.10.009

Sáez-LIorens, X., deAntonio, R., López-Medina, E., López, P., Masuda, T., Mendelman, P. M., Sherwood, J., Baehner, F., & Borkowski, A. (2025). Safety and immunogenicity of bivalent norovirus vaccine candidate in infants from 6 weeks to 5 months of age: A phase 2. Randomized, double-blind trial. *Human Vaccines & Immunotherapeutics*, *21*(1). https://doi.org/10.1080/21645515.2020.2450878

Schoene, C., Bennett, S. P., & Howarth, M. (2016). SpyRings Declassified: A blueprint for using isopeptide-mediated cyclization to enhance Enzyme thermal resilience. *Methods in Enzymology*, *580*, 149–167. https://doi.org/10.1016/BS.MIE.2016.05.004

Schütz, A., Bernhard, F., Berrow, N., Buyel, J. F., Ferreira-da-Silva, F., Haustraete, J., van den Heuvel, J., Hoffmann, J. E., de Marco, A., Peleg, Y., Suppmann, S., Unger, T., Vanhoucke, M., Witt, S., & Remans, K. (2023). A concise guide to choosing suitable gene expression systems for recombinant protein production. *STAR Protocols*, *4*(4), 102572. https://doi.org/10.1016/J.XPRO.2023.102572

Shahgolzari Mehdi, & Fiering Steven. (2022). Emerging potential of plant virus nanoparticles (PVNPs) in anticancer immunotherapies. *Journal of Cancer Immunology*, *4*(1), 22. https://doi.org/10.33696/cancerimmunol.4.061

Shoeb, E., Badar, U., Venkataraman, S., & Hefferon, K. (2021). Frontiers in bioengineering and biotechnology: Plant nanoparticles for anti-cancer therapy. *Vaccines*, 9(8), 830. https://doi.org/10.3390/vaccines9080830

Singh, A., Kumar, K., Chaudhary, D. P., Kumar, N., & Pandey, D. (2023). Protein purification: basic principles and techniques. *Basic Biotechniques for Bioprocess and Bioentrepreneurship*, 165–171. https://doi.org/10.1016/B978-0-12-816109-8.00009-X

Singh, K., Agrawal, L., Gupta, R., Singh, D., Kathpalia, M., & Kaur, N. (2024). Lectins as a promising therapeutic agent for breast cancer: a review. *Breast Disease*, *43*(1), 193–211. https://doi.org/10.3233/BD-230047

Spice, A. J., Aw, R., Bracewell, D. G., & Polizzi, K. M. (2020). Synthesis and assembly of hepatitis B virus-like Particles in a Pichia pastoris cell-free System. *Frontiers in Bioengineering and Biotechnology*, *8*, 72. https://doi.org/10.3389/fbioe.2020.00072

Spriestersbach, A., Kubicek, J., Schäfer, F., Block, H., & Maertens, B. (2015). Purification of His-tagged proteins. *Methods in Enzymology*, *559*, 1–15. https://doi.org/10.1016/bs.mie.2014.11.003

Sun, D., Liang, H., Mu, Q., Chu, C., Liu, G., & Liu, C. (2025). Virus-inspired biogenic delivery system for advancing cancer therapy. *Biomedical Technology*, *9*, 100069. https://doi.org/10.1016/J.BMT.2025.100069

Sun, Y., Yu, X., Wang, X., Yuan, K., Wang, G., Hu, L., Zhang, G., Pei, W., Wang, L., Sun, C., & Yang, P. (2023). Bispecific antibodies in cancer therapy: Target selection and regulatory requirements. *Acta Pharmaceutica Sinica B*, *13*(9), 3583–3597. https://doi.org/10.1016/j.apsb.2023.05.023

Taghizadeh, M. S., Niazi, A., & Afsharifar, A. (2024). Virus-like particles (VLPs): a promising platform for combating against Newcastle disease virus. *Vaccine-X*, *16*, 100440. https://doi.org/10.1016/j.jvacx.2024.100440

Tan, F. H., Ng, J. F., Mohamed Alitheen, N. B., Muhamad, A., Yong, C. Y., & Lee, K. W. (2023). A simple and high efficiency purification of His-tagged turnip yellow mosaic virus-like particle (TYMV-VLP) by nickel ion affinity precipitation. *Journal of Virological Methods*, *319*, 114771. https://doi.org/10.1016/j.jviromet.2023.114771

Tan, M. (2021). Norovirus vaccines: Current clinical development and challenges. *Pathogens*, *10*(12), 1641. https://doi.org/10.3390/pathogens10121641

Tariq, H., Batool, S., Asif, S., Ali, M., & Abbasi, B. H. (2022). Virus-like particles: revolutionary platforms for developing vaccines against emerging infectious diseases. *Frontiers in Microbiology*, *12*. https://doi.org/10.3389/fmicb.2021.790121

Thérien, A., Bédard, M., Carignan, D., Rioux, G., Gauthier-Landry, L., Laliberté-Gagné, M. È., Bolduc, M., Savard, P., & Leclerc, D. (2017). A versatile papaya mosaic virus (PapMV) vaccine platform based on sortase-mediated antigen coupling. *Journal of Nanobiotechnology*, *15*(1), 54. https://doi.org/10.1186/s12951-017-0289-y

Thomas, D., Rathinavel, A. K., & Radhakrishnan, P. (2021). Altered glycosylation in cancer: a promising target for biomarkers and therapeutics. *Biochimica et Biophysica Acta - Reviews on Cancer*, *1875* (1). https://doi.org/10.1016/j.bbcan.2020.188464

Thompson, C. M., Petiot, E., Lennaertz, A., Henry, O., & Kamen, A. A. (2013). Analytical technologies for influenza virus-like particle candidate vaccines: challenges and emerging approaches. *Virology Journal, 10*(1), 141. http://www.virologyj.com/content/10/1/141

Thong, Q. X., Biabanikhankahdani, R., Ho, K. L., Alitheen, N. B., & Tan, W. S. (2019). Thermally-responsive virus-like particle for targeted delivery of cancer drug. *Scientific Reports*, *9*(1), 3945. https://doi.org/10.1038/s41598-019-40388-x

Thrane, S., Janitzek, C. M., Matondo, S., Resende, M., Gustavsson, T., Jongh, W. A., Clemmensen, S., Roeffen, W., Vegte-Bolmer, M., Gemert, G. J., Sauerwein, R., Schiller, J. T., Nielsen, M. A., Theander, T. G., Salanti, A., & Sander, A. F. (2016). Bacterial superglue enables easy development of efficient virus-like particle-based vaccines. *Journal of Nanobiotechnology*, *14*(1), 30. https://doi.org/10.1186/s12951-016-0181-1

Tsaneva, M., & Van Damme, E. J. M. (2020). 130 years of Plant Lectin Research. *Glycoconjugate Journal*, *37* (5), 533-551. https://doi.org/10.1007/s10719-020-09942-y/Published

Tuccillo, F. M., De Laurentiis, A., Palmieri, C., Fiume, G., Bonelli, P., Borrelli, A., Tassone, P., Scala, I., Buonaguro, F. M., Quinto, I., & Scala, G. (2014). Aberrant glycosylation as biomarker for cancer: Focus on CD43. *BioMed Research International*, *2014*(1), 13. https://doi.org/10.1155/2014/742831

Vaccarella, S., Lortet-Tiulent, J., Saracci, R. (2019). Reducing social inequalities in cancer: evidence and priorities for research. *International Agency for Research on Cancer, 168*. https://ww.ncbi.nlm.nih.gov/books/NBK566181/

van Zyl A. R. & Hitzeroth, I. I. (2016). Purification of virus-like particles (VLPs) from plants. *Vaccine Design-Methods and Protocols-Vaccines for Veterinary Diseases, 2*, 569–579. https://doi.org/10.1007/978-1-4939-3389-1_37

Verchot, J. (2022). Potato virus X: A global potato-infecting virus and type member of the Potexvirus genus. *Molecular Plant Pathology*, *23*(3), 315–320. https://doi.org/10.1111/mpp.13163

Verdaguer, N., Ferrero, D., & Murthy, M. R. N. (2014). Viruses and viral proteins. *IUCrJ*, *1*, 492–504. https://doi.org/10.1107/S205225251402003X

Vo, D. K., & Trinh, K. T. L. (2025). Molecular farming for immunization: current advances and future prospects in plant-produced vaccines. *Vaccines*, *13*(2), 191. https://doi.org/10.3390/vaccines13020191

Volpers, C., Unckell, F., Schirmacher, P., Streeck, R. E., & Sapp, M. (1995). Binding and internalization of human papillomavirus type 33 virus-like particles by eukaryotic cells. *Journal of Virology,* 69(6), 3258–3264. https://journals.asm.org/journal/jvi

Wang, J., Li, Y., & Nie, G. (2021). Multifunctional biomolecule nanostructures for cancer therapy. *Nature Reviews Materials*, *6*(9), 766–783. https://doi.org/10.1038/s41578-021-00315-x

Wang, R., Hu, B., Pan, Z., Mo, C., Zhao, X., Liu, G., Hou, P., Cui, Q., Xu, Z., Wang, W., Yu, Z., Zhao, L., He, M., Wang, Y., Fu, C., Wei, M., & Yu, L. (2025). Antibody–Drug Conjugates (ADCs): current and future biopharmaceuticals. *Journal of Hematology and Oncology*, *18*(1), 51. https://doi.org/10.1186/s13045-025-01704-3

Wang, S. ya, Yu, Q. jia, Bao, J. ku, & Liu, B. (2011). Polygonatum cyrtonema lectin, a potential antineoplastic drug targeting programmed cell death pathways. *Biochemical and Biophysical Research Communications*, *406*(4), 497–500). https://doi.org/10.1016/j.bbrc.2011.02.049

Wang, Y., Cong, Q. Q., Lan, Y. F., Geng, C., Li, Xian Dao, Liang, Y. C., Yang, Z. Y., Zhu, X. P., & Li, Xiang Dong. (2014). Development of new potato virus X-based vectors for gene over-expression and gene silencing assay. *Virus Research*, *191*(1), 62–69. https://doi.org/10.1016/J.VIRUSRES.2014.07.018

Wang, Yian, Yan, Q., Fan, C., Mo, Y., Wang, Yumin, Li, X., Liao, Q., Guo, C., Li, G., Zeng, Z., Xiong, W., & Huang, H. (2023). Overview and countermeasures of cancer burden in China. *Science China Life Sciences*, *66*(11), 2515–2526). https://doi.org/10.1007/s11427-022-2240-6

Ward, B. J., Gobeil, P., Séguin, A., Atkins, J., Boulay, I., Charbonneau, P. Y., Couture, M., D'Aoust, M. A., Dhaliwall, J., Finkle, C., Hager, K., Mahmood, A., Makarkov, A., Cheng, M. P., Pillet, S., Schimke, P., St-Martin, S., Trépanier, S., & Landry, N. (2021). *Nature Medicine*, *27*(6), 1071–1078. https://doi.org/10.1038/s41591-021-01370-1

Wu, L., & Bao, J. K. (2013). Anti-tumor and anti-viral activities of Galanthus nivalis agglutinin (GNA)-related lectins. *Glycoconjugate Journal*, *30*(3), 269–279. https://doi.org/10.1007/s10719-012-9440-z

Yajaman, D. R., Oh, Y., Trevino, J. G., & Harrell, J. C. (2025). Advancing antibody–drug conjugates: precision oncology approaches for breast and pancreatic cancers. *Cancers*, 17(11), 1792. https://doi.org/10.3390/cancers17111792

Yan, S., Na, J., Liu, X., & Wu, P. (2024). Different Targeting Ligands-Mediated Drug Delivery Systems for Tumor Therapy. *Pharmaceutics*, *16*(2), 248. https://doi.org/103390/pharmaceutics16020248

Yang, S., Wang, T., Bohon, J., Gagné, M. È. L., Bolduc, M., Leclerc, D., & Li, H. (2012). Crystal Structure of the Coat Protein of the Flexible Filamentous Papaya Mosaic Virus. *Journal of Molecular Biology*, *422*(2), 263–273. https://doi.org/10.1016/J.JMB.2012.05.032

Yang, Z., Chi, Y., Bao, J., Zhao, X., Zhang, J., & Wang, L. (2022). Virus-like particles for TEM regulation and antitumor therapy. *Journal of Functional Biomaterials*, *13*(4), 304. https://doi.org/10.3390/jfb13040304

Yildiz, I., Shukla, S., & Steinmetz, N. F. (2011). Applications of viral nanoparticles in medicine. *Current Opinion in Biotechnology*, *22*(6), 901–908. https://doi.org/10.1016/j.copbio.2011.04.020

Zahmanova, G., Aljabali, A. A. A., Takova, K., Minkov, G., Tambuwala, M. M., Minkov, I., & Lomonossoff, G. P. (2023). Green Biologics: Harnessing the Power of Plants to Produce Pharmaceuticals. *International journal of molecular sciences*, *24*(24), 17575. https://doi.org/10.3390/ijms242417575

Zakeri, B., Fierer, J. O., Celik, E., Chittock, E. C., Schwarz-Linek, U., Moy, V. T., & Howarth, M. (2012). Peptide tag forming a rapid covalent bond to a protein, through

engineering a bacterial adhesin. *Proceedings of the National Academy of Science*, *109*(12), e690–e697. https://doi.org/10.1073/pnas.1115485109/-/DCSupplemental

Zanganeh, S., Doroudian, M., Nowzari, Z. R., Nasirmoghadas, P., Nahand, J. S., Sepehrpour, S., & Moghoofei, M. (2023). Viral nanoparticles-mediated delivery of therapeutic cargo. *Advanced Therapeutics*, *6*(10). https://doi.org/10.1002/adtp.202300082

Zeltins, A. (2013). Construction and characterization of virus-like particles: a review. *Molecular Biotechnology*, *53*(1), 92–107. https://doi.org/10.1007/s12033-012-9598-4

Zhao, Z., Simms, A., & Steinmetz, N. F. (2022). Cisplatin-loaded tobacco mosaic virus for ovarian cancer treatment. *Biomacromolecules*, *23*(10), 4379–4387. https://doi.org/10.1021/acs.biomac.2c00831

APPENDICES

Appendix 1: Ethics approval letter from the UNISA College of Agriculture and Environmental Sciences Research Ethics Committee.

UNISA university of south africa

College of Agriculture and Environmental Sciences_Health REC

NHREC Registration # : REC-170616-051
Ref #: 2024/CAES_HREC/3343
Name: Ms Mamorake Donty Komane
Student #: 56749988

Date: 27/06/2024

Dear: Ms Mamorake Donty Komane

Decision: Ethics Approval from 26/04/2024 to 30/06/2027

Researcher: Ms Mamorake Donty Komane
56749988@mylife.unisa.ac.za 0810390258

Supervisor: Dr Prudence Ngalula Kayoka kabonpnk@unisa.ac.za

Co-Supervisor: Dr Daria Rutkowska DRutkowska@csir.co.za

Cancer Biotherapy: targeting cancer cells with a plant-expressed, virus-like particle

Qualification: MSc Agriculture

Thank you for the application for research ethics clearance by the College of Agriculture and Environmental Sciences_Health REC for the above mentioned research study. Ethics approval is granted for three years, **subject to submission of yearly progress reports. Failure to submit the progress report will lead to withdrawal of the ethics clearance until the report is submitted.**

Due date for progress report: 30 June 2025

The **medium risk application** was **reviewed** by College of Agriculture and Environmental Sciences_Health REC on 06 June 2024, and the required clarifications approved on 26 June 2024 in compliance with the Unisa Policy on Research Ethics and the Standard Operating Procedure on Research Ethics Risk Assessment.

The proposed research may now commence with the provisions that:

1. The researcher(s) will ensure that the research project adheres to the values and principles expressed in the UNISA Policy on Research Ethics.
2. Any adverse circumstance arising in the undertaking of the research project that is relevant to the ethicality of the study should be communicated in writing to the College of Agriculture and Environmental Sciences_Health REC.
3. The researcher(s) will conduct the study according to the methods and procedures set out in the approved application.
4. Any changes that can affect the study-related risks for the research participants, particularly in terms of assurances made with regards to the protection of participants' privacy and the confidentiality of the data, should be reported to the Committee in writing, accompanied by a progress report.

Page 1 of 2

5. The researcher will ensure that the research project adheres to any applicable national legislation, professional codes of conduct, institutional guidelines and scientific standards relevant to the specific field of study. Adherence to the following South African legislation is important, if applicable: Protection of Personal Information Act, no 4 of 2013; Children's act no 38 of 2005 and the National Health Act, no 61 of 2003.

6. Only de-identified research data may be used for secondary research purposes in future on condition that the research objectives are similar to those of the original research. Secondary use of identifiable human research data requires additional ethics clearance.

7. No field work activities may continue after the expiry date (30 June 2025). Submission of a completed research ethics progress report will constitute an application for renewal, for Ethics Research Committee approval.

Additional Conditions

1. Disclosure of data to third parties is prohibited without explicit consent from Unisa.
2. De-identified data must be safely stored on password protected PCs.
3. Care should be taken by the researcher when publishing the results to protect the confidentiality and privacy of the university.
4. Adherence to the National Statement on Ethical Research and Publication practices, principle 7 referring to Social awareness, must be ensured: "Researchers and institutions must be sensitive to the potential impact of their research on society, marginal groups or individuals, and must consider these when weighing the benefits of the research against any harmful effects, with a view to minimising or avoiding the latter where possible." Unisa will not be liable for any failure to comply with this principle.

Note

The reference number 2024/CAES_HREC/3343 should be clearly indicated on all forms of communication with the intended research participants, as well as with the Committee.

Kind regards,

Prof MA Antwi
Chair of College of Agriculture and Environmental Sciences_Health REC
E-mail: antwima@unisa.ac.za

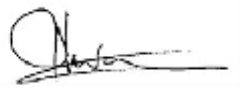

Prof M Ntwasa
Executive Dean / By delegation from the Executive Dean of College of Agriculture and Environmental Sciences_Health REC
E-mail: ntwasmm@unisa.ac.za

Appendix 2: Ethical approval from the CSIR Research Ethics Committee.

CSIR Research Ethics Committee
PO Box 395 Pretoria 0001 South Africa
Tel: +27 12 841 4060
Fax: +27 12 841 2476
Email: RandDEthics@csir.co.za

Review report

17 May 2024

Dear: **Dr Daria Rutkowska**

RE: **Targeting a plant viral nanoparticle to Leiomyosarcoma cancer cells for drug delivery. (CSIR REC Ref: 470/2024).**

Thank you for responding to the CSIR REC's review report dated April 25, 2024. Your responses were reviewed electronically by the CSIR REC. The responses were found to be in order. The CSIR REC recommended approval of the study with the following provisos.

- The CSIR REC unconditionally approves that the PI proceed with the work on Milestone 1, objective 1 till Milestone 3, objective 7.
- However, while the PI indicated that an import permit will be applied for once funding and ethics approval for the project is obtained, the CSIR REC wish to bring to the PI's attention that the import permit is a prerequisite for ethics approval specifically related to LMS cell line (objectives 9 and 10) hence the importation of LSM cell lines cannot be approved until such time when the PI furnishes the CSIR REC with the relevant import permit.

We wish you all the best with your research project.

Kind regards,
Dr Teedzai Chitura
CSIR REC Chair

Appendix 3: First page of published review article for this study.

viruses

MDPI

Systematic Review

The Use of Plant Viral Nanoparticles in Cancer Biotherapy—A Review

Mamorake Donty Komane [1], Prudence Ngalula Kayoka-Kabongo [1] and Daria Anna Rutkowska [2,*]

[1] Department of Agriculture and Animal Health, College of Agriculture and Environmental Sciences, University of South Africa, Science Campus, Private Bag X6 Florida 1710, Pretoria 0002, South Africa; 56749988@mylife.unisa.ac.za (M.D.K.); kabonpnk@unisa.ac.za (P.N.K.-K.)
[2] Advanced Agriculture and Food Cluster, Council for Scientific and Industrial Research, P.O. Box 395, Pretoria 0001, South Africa
* Correspondence: drutkowska@csir.co.za

Abstract: Cancer is a major global health problem that poses significant challenges. Conventional cancer therapies often have severe side effects, necessitating the development of novel therapeutic approaches that are more effective and less toxic. The utilization of plant viral nanoparticles is one of the more promising strategies for cancer biotherapy. Plant viral nanoparticles exhibit advantageous properties, including safety, high stability, rapid production and scalability, biocompatibility and biodegradability, structural uniformity, inherent immunogenicity, ease of modification and high update efficacy as well as lower cost implications, making them attractive vehicles for health applications. Various studies have demonstrated the efficacy of plant viral nanoparticles in targeted therapeutic drug/molecule delivery, tumor imaging and immunotherapy, highlighting their potential as a versatile platform for cancer biotherapy. The drawbacks of plant viral nanoparticles include their perceived ability to induce a hypersensitive/allergic immune response, non-well-defined regulatory approval processes as well as the reluctance of pharmaceutical companies to adapt their manufacturing processes to facilitate plant-based expression. This review discusses applications of plant virus-derived nanoparticles in cancer therapeutics and prospects for translating these findings into clinical practice.

Keywords: plant viral nanoparticles; cancer biotherapy; drug delivery; virus-like particles; cancer vaccines; tumor targeting; cancer immunotherapy; targeted delivery; imaging agents; plant viruses

Academic Editor: Olga V. Morozova

Received: 18 December 2024
Revised: 24 January 2025
Accepted: 29 January 2025
Published: 1 February 2025

Citation: Komane, M.D.; Kayoka-Kabongo, P.N.; Rutkowska, D.A. The Use of Plant Viral Nanoparticles in Cancer Biotherapy—A Review. *Viruses* 2025, *17*, 218. https://doi.org/10.3390/v17020218

1. Introduction

Cancer remains a significant global health problem, accounting for approximately 19.96 million cases in 2022 [1], despite advancements in conventional treatments, such as chemotherapy, surgery and radiation [2]. These treatments frequently have limitations, such as nonspecific targeting, severe side effects and drug resistance [3]. Thus, there is a need for innovative therapeutic approaches that can combat these challenges. Nanotechnology has opened a new platform in cancer biotherapy, with nanoparticles that allow for targeted drug delivery, enhanced therapeutic efficacy and reduced systemic toxicity [4]. Viral nanoparticles (VNPs) are virus-based nanoparticles that may be bacteriophages or plant or mammalian viruses, among others, and may be infectious or non-infectious [5]. Plant virus-based nanoparticles are among the different types of nanoparticles explored for cancer therapy and have gained popularity due to their biocompatibility, low toxicity as well as reduced ecological impact [5]. Plant viral nanoparticles (PVNPs) are naturally

Source: (Komane *et al*., 2025)